ENGINEERING PRINT® NANOPARTICLE SUBUNIT VACCINE TO INDUCE ANTITUMOR IMMUNE RESPONSE

Chintan H. Kapadia

A dissertation submitted to the faculty of the University of North Carolina at Chapel Hill in partial fulfillment of the requirements for the degree of Doctor of Philosophy in the Division of Molecular Pharmaceutics in the UNC Eshelman School of Pharmacy

Chapel Hill
2016

Approved By:

Andrew Wang

Chris Luft

Jason Whitmire

Joseph M. DeSimone

Leaf Huang

Michael Jay

ABSTRACT

Chintan H. Kapadia: Engineering PRINT® Nanoparticle Subunit Vaccine to Induce Antitumor Immune Response
(Under the Directions of Joseph M. DeSimone)

Educating our immune system via vaccination is an attractive approach to combat cancer. Tumor-specific cytotoxic T cells (CTLs) such as $CD8^+$ effector T cells play a critical role in tumor control. However, vaccination aimed at eliciting a potent $CD8^+$ T cell response with tumor-associated peptide antigens, are typically ineffective due to poor immunogenicity. Nanoparticle delivery of antigens and adjuvants can enhance their uptake by antigen presenting cells (APCs) and facilitate their intracellular delivery to induce antigen specific $CD8^+$ cells. PRINT® (Particle Replication in Non-Wetting Template) is a unique platform to fabricate nano and microparticles with exquisite control over size, shape, and surface chemistry. The goal of this study is to design a PRINT® nanoparticle based subunit vaccine for the intracellular delivery of antigenic peptides and adjuvants to induce potent CTLs response. The aims of project include, i) formulation design of nanoparticle subunit vaccine, and induction of ii) in vitro and in vivo immune response.

Under the first aim of this study we have engineered a reduction sensitive PRINT® hydrogel based subunit vaccine for intracellular delivery of antigenic peptide SIINFEKL (ovalbumin-derived CTL epitope [OVA257-264 –SIINFEKL]) and an immunostimulatory adjuvant, CpG ODNs (TLR9 agonist). SIINFEKL and CpG ODN were conjugated to PRINT® hydrogel via disulfide linkages. These NPs were successfully internalized and processed by BMDCs, resulting in BMDC maturation, subsequent cross-presentation of antigenic peptide, and induction of potent antigen-specific T cells in mice. Under the second aim of this study we further demonstrated induction of SIINFEKL specific IFN-γ producing $CD8^+$ T cells as well as

antitumor protective immune response in EG7 tumor mouse model by delivering sustained release formulations of CSIINFEKL and CpG ODN via PRINT® hydrogel NPs. Taken together, this study provides a highly effective approach, i) to induce potent CTLs response by reduction sensitive NP subunit vaccine and, ii) to induce antitumor immunity by tuning the release of antigenic peptide by changing the conjugation chemistry.

To my parents and my sister,

Without your support this journey wouldn't have been possible.

ACKNOWLEDGEMENTS

I would like to thank my advisor, Joseph M DeSimone, for his mentorship and support throughout my education and research training at UNC Chapel Hill. He enabled me to mentor other students and to collaborate with others, he pushed me to publish manuscripts, and encouraged me to attend scientific conferences. Thank you so much for believing in me and providing me this wonderful opportunity.

I would like to thank Chris Luft for scientific discussion, suggestions, and providing an encouraging lab environment. I would like to thank my Cancer Vaccine Team in lab, Shaomin Tian and Jillian Perry. Thank you Shaomin for the scientific input in this project, teaching me all the in vitro and in vivo work, and conducting FACS experiments. Jillian encouraged me to work hard, kept me in line, and helped me without hesitation whenever she could. I would also like to thank Jillian for providing excellent mentorship and scientific input in my project. I am thankful for Chris, Jillian, and Shaomin for editing, reviewing, and positively critiquing my manuscripts, poster or ppt presentation.

I am very much thankful to my committee members, Leaf Huang, Michael Jay, Jason Whitmire, and Andrew Wang for providing experimental advice and scientific discussion. I would like to thank UNC Biological Biomedical Science Program (BBSP) for accepting me and all the faculties of Division of Molecular Pharmaceutics (MOPH) for providing me great educational and research experience. I would also like to thank David Sailor one the brightest chemistry undergrad student that I have mentored, for proving his help in this project. I would also like to thank each and every members of DeSimone lab to make life in lab more enjoyable.

I would like to thank, Amar Kumbhar from teaching me SEM. I would like to thank Charlene Santos and Alain Valdivian for the animal injections and tumor measurement. I am

grateful to Dr. Wanda Bodnar from UNC Biomarker Mass Spectrometry Facility for helping me conducting Mass-Spectrometry analysis.

I would also like to acknowledge my funding support, the Carolina Center for Cancer Nanotechnology Excellence (U54CA151652) and the University Cancer Research Fund. Without their support none of this work would have been possible.

I would also like to thank my 'Triangle Family', Nithya, Giridhar, Nishant, Dylan, Kevin, UNC Cricket Club and UNC Hindu Yuva Group for the wonderful time during my stay at UNC. My special thanks goes to Nithya Srinivas, a true friend and well-wisher of mine, for her support during past two years. Thank you for all the fun, laughter, arguments, late night talks, and your philosophy lessons.

Finally, I would like thank my Family! My mom and dad for teaching me lesions of hard-work, dedication, patience, and perseverance. Thank you guys for supporting me in this journey. Special thanks to my sister, a true believer and well-wisher of mine, for supporting me through this journey. I would also like to thank my grandparents from both sides. Without your blessings this wouldn't have been possible.

TABLE OF CONTENTS

LIST OF FIGURES ..... **xii**

LIST OF TABLES ..... **xv**

LIST OF ABBREVIATIONS ..... **xvi**

Chapter 1: Cancer Vaccine- A Type of Immunotherapy **1**

1.1. Introduction to tumor immunobiology 1

1.1.1. Innate/ adaptive immunity 1

1.1.2. Cross talk between tumor cells and immune system 1

1.2. Immune cells and mediators in tumors 3

1.3. Cancer vaccine- A type of immunotherapy 8

1.3.1. Types of cancer vaccines 9

1.3.1.1. Cell-based vaccines 9

1.3.1.1.1. Tumor cell based vaccine 9

1.3.1.1.2. Dendritic cell based vaccine 10

1.3.1.1.3. T cell based vaccine 11

1.3.1.2. Genetic vaccine 11

1.3.1.3. Protein and peptide based vaccine 12

1.4. Challenges in the development of cancer vaccine 13

1.5. References 15

Chapter 2: Delivery of Cancer Vaccine using Nanoparticles **19**

2.1. Introduction 19

2.2. Particle design parameters for local

delivery to immune cells 20

2.3. Delivery of subunit vaccine via particulate carriers..... 23
2.4. Targeting DCs via nanoparticulate vaccine 24
2.5. PRINT (Particle Replication in Non-wetting template)
- a platform for delivery of subunit vaccine.....25
2.6. References..... 29
Chapter 3: Reduction Sensitive PEG Hydrogels for
Co-delivery of Antigen and Adjuvant to Induce Potent CTL.....32
3.1 Introduction 32
3.2. Materials and methods 35
3.2.1. Materials.....35
3.2.2. Methods 36
3.2.2.1. PRINT nanoparticle fabrication..... 36
3.2.2.2. Thermogravimetric analysis 37
3.2.2.3. Scanning electron microscopy.....37
3.2.2.4. Dynamic light scattering..... 37
3.2.2.5. Conjugation of linker to NPs.....37
3.2.2.6. Conjugation of CSIINFEKL to NPs..... 38
3.2.2.7. Reduction and purification of C6 S-S C6 CpG 1826 38
3.2.2.8. Conjugation of thiol-CpG 1826 to NPs 39
3.2.2.9. Co-conjugation of CSIINFEKL and
CpG ODN to NPs..... 39
3.2.2.10. Peptide evaluation via HPLC 40
3.2.2.11. Animals.....41
3.2.2.12. Preparation of single cell culture from
mouse spleens.....41
3.2.2.13. Preparation of BMDCs 41

3.2.2.14. Antigen presentation assay in BMDCs 42
3.2.2.15. In vitro T cell proliferation assay 42
3.2.2.16 BMDC maturation assay 42
3.2.2.17. Immunization study 42
3.2.2.18. ELISPOT assay 43
3.2.2.19. In vivo CTL assay 43
3.3. Results 45
3.3.1 Conjugation of CSIINFEKL and CpG to NPs 45
3.3.2 In vitro antigen presentation in BMDCs by sub-unit vaccine 48
3.3.3 In vitro proliferation of OT-I T cells in BMDCs treated with sub-unit vaccine 52
3.3.4 Maturation of BMDCs by CpG ODN conjugated PEG hydrogel 53
3.3.5. Induction of IFN-γ producing SIINFEKL specific CD8+ T cells in mice 55
3.3.6. In vivo CTL response in mice after immunization with SIINFEKL and CpG co-conjugated NPs 57
3.4. Discussion 58
3.5. Conclusion 60
3.6. References 62
Chapter 4: Induction of Antitumor Protective Immune Response by Sustained Release Delivery of Antigen and Adjuvant 67
4.1 Introduction 67
4.2. Materials and methods 70
4.2.1. Materials 70
4.2.2. Methods 70
4.2.2.1. PRINT nanoparticle fabrication 70

4.2.2.2. Thermogravimetric analysis 71
4.2.2.3. Scanning electron microscopy 71
4.2.2.4. Dynamic light scattering 71
4.2.2.5. Conjugation of linker to NPs 71
4.2.2.6. Conjugation of CSIINFEKL to linker modified NP 71
4.2.2.7. Reduction and purification of
C6 S-S C6 CpG 1826 71
4.2.2.8. Conjugation of thiol-CpG 1826 to NPs 71
4.2.2.9. Co-conjugation of CSIINFEKL and
CpG ODN to NPs 72
4.2.2.10. Release of peptide 72
4.2.2.11. Peptide evaluation via HPLC 72
4.2.2.12. Liquid chromatography-Mass spectrometry (LC-MS) 72
4.2.2.13. Animals 73
4.2.2.14. Preparation of splenocytes and WBCs 73
4.2.2.15. Preparation of BMDCs 74
4.2.2.16. Antigen presentation assay in BMDCs 74
4.2.2.17. BMDC maturation assay 74
4.2.2.18. Immunization study 74
4.2.2.19. ELISPOT assay 74
4.2.2.20. Tumor challenge study 74
4.3. Results 76
4.3.1. Conjugation of CSIINFEKL and CpG to NPs 76
4.3.2. Release of antigenic peptide from NPs in intracellular
Reductive environment (10 mM GSH) 78
4.3.3. Cross-presentation of CSIINFEKL in BMDCs 80

4.3.4. Maturation of BMDCs by particulate conjugated CpG ODN 82
4.3.5. In vitro release of IL-6 by BMDCs treated with NP conjugated CpG 84
4.3.6. In vivo induction of antigen specific IFN-γ producing CD8+ T cells 85
4.3.7. Protection against tumor growth- EG7 mice tumor model 87
4.4. Discussion 89
4.5. Conclusion 91
4.6. References 92
Chapter-5: Future Directions and Summary 95
5.1. Future directions 95
5.2. Summary 99
5.3. References 102
APPENDIX 105

LIST OF FIGURES

Figure 1.1 The three phases of cancer immune editing....2

Figure 1.2 Immunosuppressive regulators in tumor microenvironment....4

Figure 1.3 Immunotherapeutic strategies for cancer....7

Figure 2.1 Effects of particulate size on tissue, cell and intracellular targets after entry into interstitial tissue....21

Figure 2.2 PRINT®- fabrication process....26

Figure 3.1 Conjugation of cleavable linkers and cysteine labelled SIINFEKL to PEG hydrogels....45

Figure 3.2 Representative SEM image of 80x320 nm PRINT subunit peptide vaccine....48

Figure 3.3 Enhanced antigen presentation by NP-peptide in BMDCs....50

Figure 3.4 T cell proliferation assay....52

Figure 3.5 Up-regulation of maturation markers by NP-CpG on BMDCs....54

Figure 3.6 Evaluation of IFN-γ producing CD8+ T cells: separate vs co-conjugation of antigen and adjuvant....56

Figure 3.7 Induction of IFN-γ producing SIINFEKL specific CD8+ T cells in spleen....56

Figure 3.8 In vivo CTL response after vaccination with model peptide hydrogel cancer vaccine....57

Figure 4.1 Co-conjugation of CSIINFEKL and CpG ODN to NPs via SPDP....76

Figure 4.2 Co-conjugation of CSIINFEKL and CpG ODN to NPs via SMCC....76

Figure 4.3 SEM image of 80X320 nm PEG hydrogel....77

Figure 4.4 Release of antigenic peptide CSIINFEKL from NPs....78

Figure 4.5 Modified antigen presentation assay in BMDCs 80

Figure 4.6 Up-regulation of maturation markers by NP-CpG on BMDCs.... 83

Figure 4.7 Secretion of IL-6 from BMDCs treated with particulate conjugated CpG 84
Figure 4.8 Induction of IFN-γ producing SIINFEKL specific CD8+ T cells in a) spleen and b) circulating blood..... 86
Figure 4.9 Tumor growth challenge study 87
Figure 4.10 Evaluation of antigen specific IFN-γ producing CD8+ T Cells 88
Figure 5.1 Multivalent display of antigen and TLR4 agonist to an antigen presenting cell (APC) such as a B cell by a malarial sporozoite and a nanoparticle/adjuvant formulation 96

LIST OF TABLES

Table 3.1 Gradient method for HPLC run 40

Table 3.2 Physical Characterization of nanoparticles conjugated to SPDP 46

Table 3.3 Physical Characterization of PEG hydrogel sub-unit vaccine 47

Table 4.1 Gradient method for LC-MS run 73

Table 4.2 Physical Characterization of NPs 77

LIST OF ABBREVIATIONS

μL	microliter, 10^{-6} Liter
μm	micrometer, 10^{-6} meters
2k, 5k	Molecular weight 2000 gm/mole, 5000 gm/mole
Ab	Antibody
ACK	Ammonium-Chloride-Potassium
ACT	Adoptive cell transfer
APCs	Antigen presenting cells
APM	Antigen presentation machinery
ARG 1	Arginase 1
BCA	Bichiconinic Acid
BCR	B-cell receptors
BMDCs	Bone marrow derived dendritic cells
CAR	Chimeric antigen receptor
CD	Cluster differentiation
CEA	Carcinoembryonic antigen
cGMP	Current good manufacturing practice
CLRs	C-lectin type receptors
CpG	5'—C—phosphate—G—3'
CpG ODN	CpG oligonucleotide
CSP	Circumsporozoite protein
CTLA-4	Cytotoxic T-lymphocyte-associated protein 4
CTLs	Cytotoxic T lymphocytes
DCs	Dendritic cells
DISC	Death-inducing signaling complex

dLN	Draining lymph node
DLS	Dynamic light scattering
DMSO	Dimethyl sulfoxide
DNA	Deoxyribonucleic acid
DOPE	Dioleoylphosphatidylethanolamine
DOTAP	1,2-dioleoyl-3-trimethylammonium-propane
DPBS	Dulbecco's phosphate-buffered saline
ECM	Extracellular matrix
ELISA	Enzyme-linked immunosorbant assay
ELISPOT assay	Enzyme-linked immuno spot assay
Fas L	Fas Ligand
Flt-3	Fms-like tyrosine kinase 3
FVAX	Flt-3 ligand expressing tumor cell based vaccine
GLA-SE	Glucopyranosyl lipid adjuvant- stabilized emulsion
GM-CSF	Granulocyte macrophage- colony stimulating factor
GVAX	GM-CSF transduced autologous tumor cell vaccine
h, hrs	Hours
HA	Hemagglutinin
HAI	Hemagglutinin-inhibition
HCV	Hepatitis C virus
HER-2	Receptor tyrosine-protein kinase erbB-2
HIV	Human immune deficiency virus
HLA	Human leukocyte antigen
HLA-DR	Human leukocyte antigen - antigen D related
HPLC	High performance liquid chromatography

HRP	Highly repetitive patterns
ICMV	Inter-bilayer multilamellar vesicles
IDO	Indoleamine 2 3-dioxygenase
IFN-γ	Interferon gamma
IgM	Immunoglobulin M
IL	Interleukin
IMO	Immunomodulatory
IPA	Isopropyl alcohol
LCP	Lipid–calcium–phosphate
LFA1	Lymphocyte function-associated antigen 1
LFA3	Lymphocyte function-associated antigen 3
LNP	Lipid nanoparticles
MDSCs	Myeloid-derived suppressor cells
MHC-I/II	Major histocompatibility complex molecules class I/II
mL	milliliter, 10^{-3} Liter
MMP	Matrix metalloproteinases
MPL-A	Monophosphoryl lipid-A
NDV	New Castle disease virus
NKs	Natural killer cells
NKT	Natural killer T cells
NLRs	NOD like receptors
nm	nanometer, 10^{-9} meters
nM	nanomolar, 10^{-9} Molar
NOD	Nucleotide binding oligomerization domain
NOS 2	Nitricoxide synthase 2

NPs	Nanoparticles
OS	Overall survival
OVA	Ovalbumin
PADRE	pan DR epitope
PAMPs	Pathogen associated molecular patterns
PD-L1/2	Programmed death ligand 1/2
PEG	Poly (ethylene) glycol
PEI	Polyethylene imine
PFPE	Perfluoropolyether
PGE 2	Prostaglanding E2
poly I:C	Polyinosinic:polycytidylic acid
PPS	Pre-particle solution
PRINT	Particle replication in non-wetting template
PRRs	Pathogen recognition receptors
PSA	Prostate-specific antigen
PTFE	Polytetrafluoroethylene
PVA	Poly (vinyl) alcohol
RIG-I	Retinoic acid inducible gene-1
RLRs	RIG-I like receptors
RNA	Ribonucleic Acid
SEM	Scanning electron microscopy
siRNA	Small interfering RNA
STING	Stimulator of interferon gamma genes
T regs	Regulatory T cells
TAA	Tumor associated antigen

TAMs	Tumor associated macrophages
TCR	T cell receptor
TGA	Thermogravimetric analysis
TGF-β	Transforming growth factor β
TIL	Tumor infiltrating lymphocytes
TLRs	Toll like receptors
TME	Tumor microenvironment
TNF-α	Tumor necrosis factor- alpha
Trp-2	Tyrosinase related protein 2
ZP	Zeta potential
α–Gal Cer	Alpha-galactosylceramide

Chapter-1: Cancer Vaccine- A Type of Immunotherapy*

1.1. Introduction to tumor immunobiology

1.1.1 Innate/adaptive immunity

The immune system fights against pathogenic infections via innate and adaptive mechanisms for immediate defense and long-lasting protection. Innate immune cells, such as macrophages, dendritic cells (DCs), natural killer (NK) cells, etc., provide the initial, "first line" of protection by recognizing conserved pathogen-associated molecular patterns (PAMPs) via pattern-recognition receptors (PRRs) [2], including C-type lectin receptors (CLRs), Toll-like receptors (TLRs), nucleotide-binding oligomerization domain (NOD)-like receptors (NLRs), retinoic acid-inducible gene I (RIG-I)-like receptors (RLRs) and cytosolic DNA sensors [3, 4]. Adaptive immunity usually proceeds the innate immune response and requires activation of T and B lymphocytes. This activation requires recognition of specific antigens by T and B cell receptors and, subsequently results in the generation of antigen-specific effector T cells and/or antibody secreting plasma cells. Importantly, adaptive immunity also features production of 'memory' T and B cells that exist in a state of readiness to mount a more rapid attack upon the second encounter of a pathogen. Effective activation of adaptive immunity depends on the sensing of microbes by PRRs expressed on antigen-presenting cells (APCs) in particular DCs [5].

1.1.2 Cross talk between tumor cells and immune system

Growing evidence has shown that the immune system interacts with tumors throughout tumor development, including initiation, progression, invasion, and metastasis. It is also becoming

---

*With Sections Reprinted from [1] 'Journal of Controlled Release', 219 /December 10, Kapadia CH, Perry JL, Tian S, Luft JC, DeSimone JM, **'Nanoparticulate Immunotherapy for cancer'**, 167-180, Copyright (2015), with permission from Elsevier.

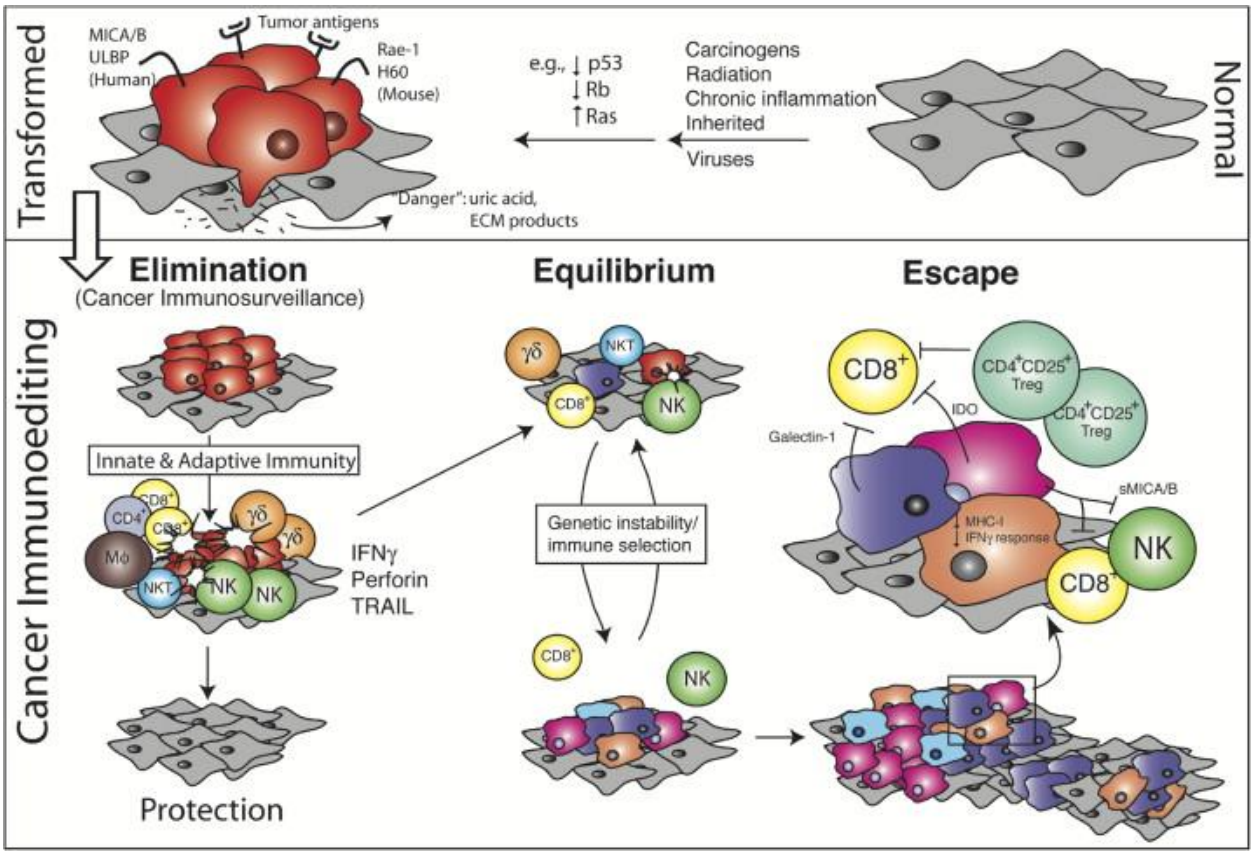

Figure-1.1: The three phases of the cancer immunoediting process
Normal cells (gray) subject to common oncogenic stimuli ultimately undergo transformation and become tumor cells (red) (top). Even at early stages of tumorigenesis, these cells may express distinct tumor-specific markers and generate proinflammatory "danger" signals that initiate the cancer immunoediting process (bottom). In the first phase of elimination, cells and molecules of innate and adaptive immunity, which comprise the cancer immunosurveillance network, may eradicate the developing tumor and protect the host from tumor formation. However, if this process is not successful, the tumor cells may enter the equilibrium phase where they may be either maintained chronically or immunologically sculpted by immune "editors" to produce new populations of tumor variants. These variants may eventually evade the immune system by a variety of mechanisms and become clinically detectable in the escape phase. Figure and caption are reprinted from [9] Immunity, Vol 21, Issue 2, Gavin P. Dunn, Lloyd J. Old, Robert D. Schreiber; The immunobiology of cancer immunosurveillance and immunoediting. 137-148, Copyright (2004), with permission from Elsevier.

clear that the complex cross talk between the immune system and cancer cells can both inhibit and enhance tumor growth, which has become a hallmark of cancer [6]. A cancer immunoediting model (figure 1.1) [7, 8] has been proposed to explain the paradoxical functions of host immunity on cancer, based on the temporal occurrence during tumor progression: an

early elimination phase (elimination of tumor cells by a competent immune system), an equilibrium phase (a balance phase when tumor progression is still controlled by the immune system but sporadic tumor cells that manage to survive immune destruction; immune editing occurs) and an escape phase (when the tumor evades immune surveillance and an immunosuppressive tumor microenvironment is established). Immune editing is believed to be one of the key aspects how tumors evade surveillance and lie dormant in patients for years through “equilibrium" and "senescence" before re-emerging [10].

1.2. Immune cells and mediators in tumors

Elimination of cancer cells via the immune system is mainly mediated by immune effector cells, such as $CD8^+$ cytotoxic T lymphocytes (CTL), natural killer (NK) cells, and natural killer T (NKT) cells. These cells have been found within various types of tumors and studies involving cancer patients revealed that the presence of $CD3^+$ or $CD8^+$ tumor-infiltrating lymphocytes (TILs) were associated with increased overall survival [11]. $CD8^+$ CTL is the major anti-tumor player of adaptive immunity. Recognition and elimination of cancer cells by $CD8^+$ T cells requires two signals: 1) a signal provided by the engagement of tumor antigenic peptide/class I MHC complex on antigen presenting cells, in particular DCs, with antigen-specific T cell receptor (TCR), and 2) stimulatory signals mediated by interactions between accessory molecules (CD80, CD86, LFA3) on APCs and their cognate receptors on CTLs (e.g., CD2, CD28, LFA1) [12]. Activated $CD8^+$ CTLs kill tumor cells by releasing cytotoxic proteins (perforin, granzymes, and granulysin) or engagement of Fas ligand (FasL) on T cells and Fas receptor on target cells, and subsequent recruitment of the death-induced signaling complex (DISC). NK cells are innate immune effector cells that recognize neoplastic cells via non-antigen-specific surface receptors [13] and trigger targeted attack through release of cytotoxic granules and secretion of cytokines and chemokines to promote subsequent adaptive immune responses [14]. NKT cells (also invariant NKT or iNKT cell), another member of innate immune system, express a semi-invariant TCR that recognizes lipid antigens (e.g. α-GalCer) presented by

CD1d (antigen presenting molecules) [15]. Upon activation, NKT cells rapidly elevate production of IFN-γ, which can profoundly modulate innate and adaptive arms of the immune system for tumor rejection. NKT cells may also directly mediate tumor lysis via Fas-FasL engagement or release of perforin [16].

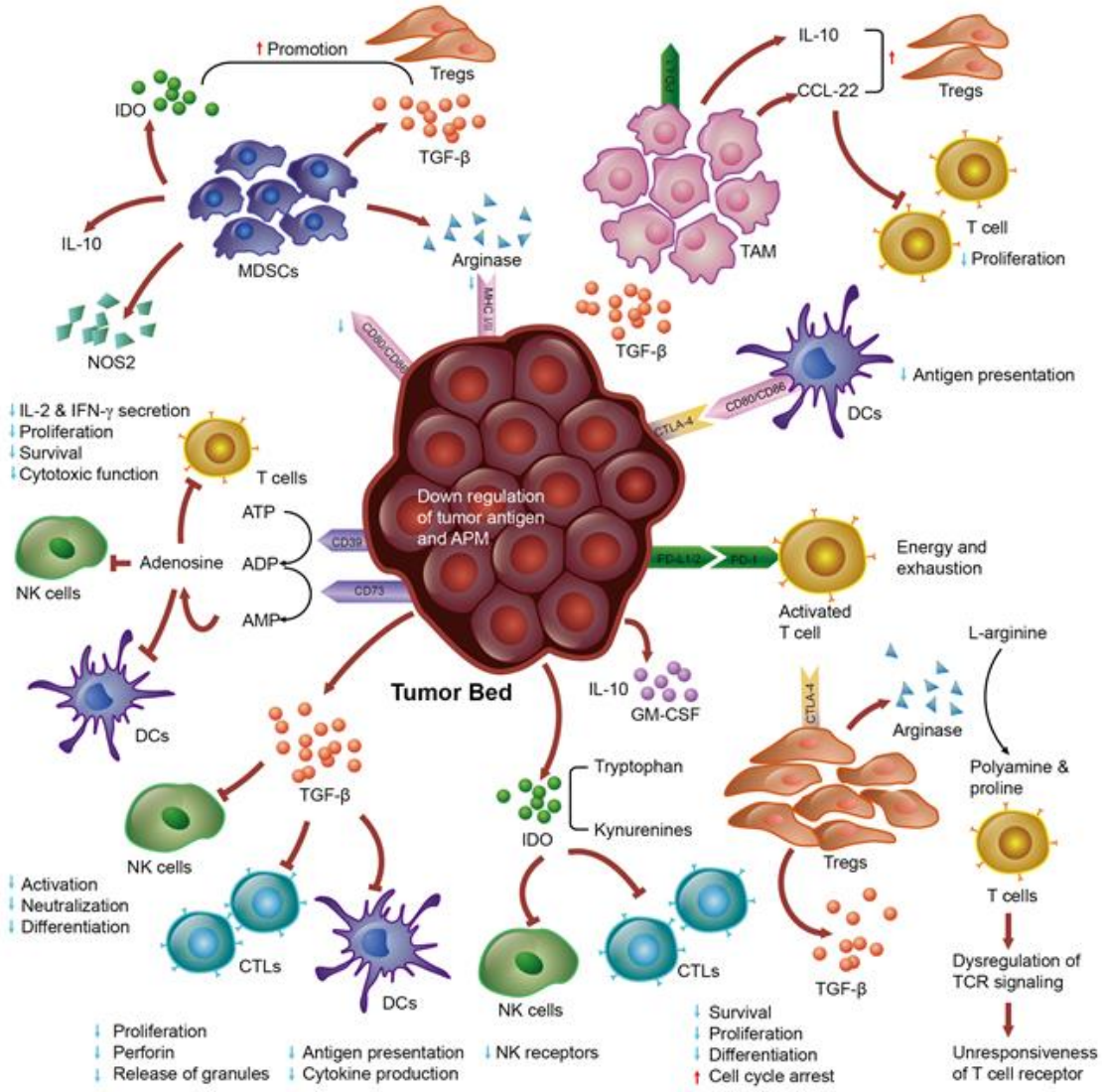

<u>Figure- 1.2:</u> Immunosuppressive regulators in tumor microenvironment.
Tumors escape immune surveillance by various mechanisms that operate in parallel with anti-tumor immunity. Anti-tumor immunity can be suppressed by various cell types including tumor cells, stromal cells and immune cells such as MDSCs, Tregs and TAMs. These immunosuppressive cells secrete numerous soluble mediators such as arginase, prostaglandin E2, TGF-β, IDO, adenosine and NOS2. Arginase and IDO limit T-cell functions by depleting

arginine and consuming tryptophan. TGF-β, IDO and IL-10 suppress the activity of T cells and natural killer cells as well as cause the expansion of Tregs. TGF-β can also suppress or alter activation, maturation and differentiation of DCs, $CD4^+$ and $CD8^+$ T cells. Moreover, due to changes in epigenetic machinery of tumor cells, expression of MHC-I/II molecules, proteins associated with APM and costimulatory molecules (CD80/CD86) is down-regulated which prevents successful antigen presentation and tumor detection. Moreover, tumor cells also express surface molecules such as PD-L1/PD-L2 that engage PD-1 receptor on the surface of activated T cell which cause the anergy and exhaustion of T cells. CTLA-4 receptor on tumor binds to co-stimulatory molecules on APCs and prevent antigen presentation. Collectively, tumors escape immune surveillance via inhibitory mechanisms utilized by all of these cell types.
Reprinted from [1] 'Journal of Controlled Release', 219 /December 10, Kapadia CH, Perry JL, Tian S, Luft JC, DeSimone JM, 'Nanoparticulate Immunotherapy for cancer', 167-180, Copyright (2015), with permission from Elsevier.

In contrast to immune effector cells, $CD25^+$ regulatory T cells (Tregs) and myeloid derived suppressor cells ($CD14^+$ HLA-DR- MDSCs) limit inflammation and immune activation [17] and help to maintain self-tolerance (Figure 1.2) [18]. Tregs have been found at high frequencies in various neoplastic malignancies such as breast, lung, liver, GI tumors, and melanoma contributing to an immune-suppressive tumor microenvironment (TME) [19, 20]. Increased recruitment of Tregs is correlated with reduced survival and increased progression in pancreatic and ovarian carcinomas [21, 22]. MDSCs also down-regulate both innate and adaptive arms of the immune system via a variety of mechanisms, including release of IL-10, activation of Tregs, and sequestration of cysteine needed for T cell protein synthesis and suppress $CD8^+$ T cell function [23]. Analogous to associations between Tregs and outcome, elevated circulating MDSCs correlate with poor prognosis in pancreatic, esophageal, and gastric cancers [24].

Macrophages are divided into two categories based on their functions: classical M1 and alternative M2 macrophages. The M1 macrophage is involved in the inflammatory response, pathogen clearance, and antitumor immunity while M2 macrophages influence an anti-inflammatory response, wound healing, and pro-tumorigenic properties. During tumor progression, large numbers of monocytes are recruited to the tumor site which then differentiate into tumor-associated macrophages (TAMs) [25]. In response to various signals generated from

tumor and stromal cells, TAMs are predominantly polarized toward a M2-like phenotype and subsequently promote tumor growth, angiogenesis, invasion, and metastasis. Clinical studies have suggested that TAM accumulation in tumors correlates with a poor clinical outcome [26]

In addition to immune cells, immune mediator molecules are also an important part of immunoediting process (Figure 1.2). Cytokines such as interferons (IFN), specifically IFN-γ and IFN-α, as well as interleukins (IL) (IL-2, IL-12), and granulocyte macrophage colony-stimulating factor (GM-CSF) etc., have shown anti-tumor capability and act directly on tumors or enhance functions of effector cells. For example, IFN-γ is one of the major anti-cancer immune mediators and is produced by activated Th1 cells (a subset of $CD4^+$ T-helper cells), $CD8^+$ T cells, NK cells and NKT cells. IFN-γ is a potent activator of macrophages, NK cells, neutrophil phagocytic activity, and promotes synthesis of Class I and II MHC molecules that enhance antigen presentation [27]. Genetic deficiencies in IFN-γ (or of its receptor) result in spontaneous tumor development implying that IFN-γ plays a crucial role in immunosurveillance and elimination of neoplastic cells [28]. On the other hand, a range of inflammation mediators [cytokines, chemokines, free radicals, prostaglandins, transcription factors, microRNAs, and enzymes such as, arginase (ARG1), indoleamine 2,3-dioxygenase (IDO), cyclooxygenase and matrix metalloproteinase (MMP), nitric oxide synthase (NOS2)] are released by or reside in cancer cells and immune cells, collectively act to create a favorable microenvironment for the development of tumors. Transforming growth factor β (TGF-β) and IL-10 are the major immune suppressive cytokines secreted by tumor cells, MDSC, and TAMs while several proinflammatory cytokines (IL-1, IL-6, TNF-α) that mediate chronic inflammation in the tumor, significantly contribute to tumorigenesis and progression [29].

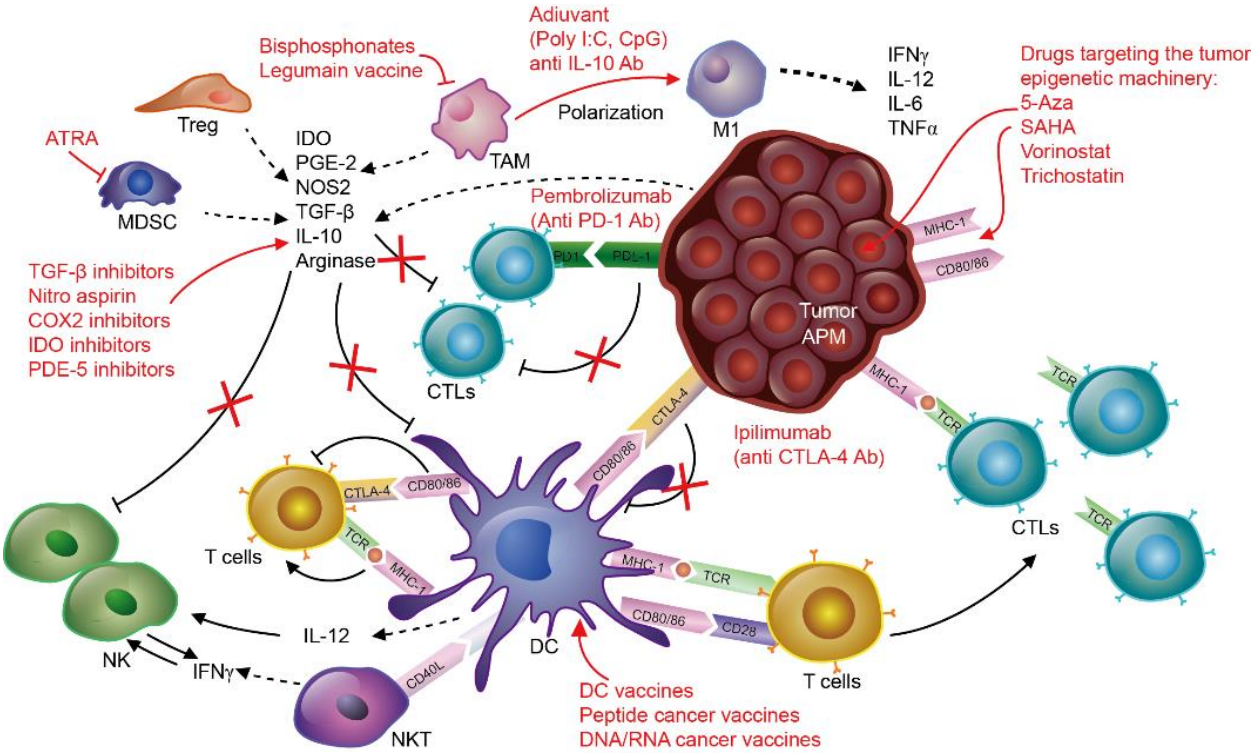

<u>Figure- 1.3:</u> Immunotherapeutic strategies for cancer.
A growing understanding of the complex interplay between tumor cells and immune system have provided pharmacological targeting opportunities for cancer immunotherapy. Antigen expression and presentation of tumor cells can be increased by delivering drugs that manipulate epigenetic machinery (5-Aza, 5AHA, etc.). Tumor antigen specific effector cells can be generated via cell based or subunit vaccines targeting DCs and the delivery of cytokines and growth factors. Blocking of CTLA-4 or PD-1 pathways via antibodies (Anti CTLA-4 or Anti PD-1) can restore T cell exhaustion in TME. Immunosuppression can be reversed by many mechanisms – such as depleting MDSCs (via All-trans-retinoic acid (ATRA), PDE-5 inhibitors and nitroaspirin), depleting Tregs, and TAMs (via bisphosphonates and legumain vaccine) and inhibiting regulatory mediators (via siRNA, antibodies or small molecules inhibitors against TGF-β, IDO, PDE-5 and COX-2). Reprinted from [1] 'Journal of Controlled Release', 219 /December 10, Kapadia CH, Perry JL, Tian S, Luft JC, DeSimone JM, 'Nanoparticulate Immunotherapy for cancer', Pages No.167-180, Copyright (2015), with permission from Elsevier.

Tumor exploit several immunological processes to escape immune surveillance, such as increasing Treg cell functionality, down-regulating expression of tumor-associated antigens, antigen processing machinery (APM) and accessory/co-stimulatory molecules through epigenetic reprogramming and modifying production of immune suppressive mediators. Our growing understanding of the complex interplay between tumor cells and the immune system

has provided pharmacological targeting opportunities for cancer immunotherapy (Figure 1.3). Depending on the approach, immunotherapy could strike more specifically against the tumor, thus lowering the damage to healthy tissue and preventing debilitating side effects that are nearly unavoidable with radiation, chemotherapy, and surgery. Activated and tumor-specific immune cells can invade areas that are difficult/impossible to access surgically, and the immune system may, when appropriately stimulated, target even microscopic disease and disseminated metastases. Further, immunotherapy should provide long-lasting benefits while by-passing issues with multidrug resistance related to chemotherapy and radiation therapy. Also, immunotherapy could more efficiently target cancer cells that are slowly dividing or quiescent - characteristics associated with cancer stem cells. Finally, memory cells elicited by immunotherapy may suppress the re-emergence of cancer. This potential of long-term control or even complete eradication of the cancer is possibly the most promising aspect of immunotherapy since induced anti-tumor responses have sometimes proven durable over many years (at least in a subset of patients).

1.3. Cancer Vaccine- A type of Immunotherapy

Vaccines are one of the major revolutions in the history of modern medicine. Contributions made by vaccines include the almost complete elimination of polio, the eradication of small pox and a decrease by more than 95% of the incidence of diphtheria, tetanus, pertussis, measles, mumps and rubella [30]. Harnessing the power of a patient's own immune system to target, fight, and eradicate cancer cells without destroying the healthy cells is a highly attractive and innovative approach for cancer management. If the immune system is appropriately stimulated by an immunotherapy, activated immune cells can target both macroscopic and microscopic disease [1]. Developing a successful cancer vaccine, involves activation of CTLs with antigens and adjuvants, as well as modulating the immune-evasive tumor microenvironment; both are essential for tailoring anti-tumor immune responses. The aim of most cancer vaccines is to activate and stimulate tumor specific $CD8^+$ T cells employing

either tumor cell-based vaccines, DCs vaccines, T cell vaccines, or peptide/protein-based subunit vaccines [31].

1.3.1 Types of cancer Vaccines

1.3.1.1 Cell-Based Vaccines

1.3.1.1.1. Tumor cell based Vaccines

Tumor cell-based vaccines utilize autologous or allogeneic tumor cells modified with cytokines, such as GM-CSF, or formulated with adjuvants. In autologous tumor cell vaccines, tumor cells are derived from the patient, irradiated and combined with cytokines or adjuvants. An advantage of cell-based vaccine is that these cells contain the entire spectrum of mutated and overly expressed tumor specific protein antigens and present them to patient's immune system [32]. On the other hand, preparation of this type of vaccine requires sufficient numbers of tumor cells which is only possible for certain tumor types and stage which limits its feasibility and utility in clinical settings. GVAX (GM-CSF transduced autologous tumor cell vaccine) has been extensively studied in pre-clinical and clinical trials to recruits DCs [33]. GVAX stimulated the maturation of DCs and when combined with anti-CTL-associated antigen 4 (CTLA-4) antibody promoted the rejection of murine melanoma [34, 35]. Enhanced antitumor efficacy was observed when FVAX (Flt-3 ligand expressing tumor cell based vaccine) or GVAX was combined with anti-CTLA-4 or anti-PD-1 antibody in melanoma or ovarian cancer mouse model [36, 37].

To overcome the limitation of autologous tumor cell vaccine, an allogeneic tumor cell vaccine has been developed which includes two or three human tumor cell lines. Allogeneic tumor cells can be easily modified to express immunostimulatory cytokines and can be produced at a large scale. Canvaxin™ is a combination of three melanoma tumor cell lines, which were selected from 150 tumor cell lines on the basis of their tumor antigen profile. Canvaxin™ contain 20 different melanoma associated and tumor associated antigens from which at least one antigen was found in every melanoma patient studied to date. It has produced striking results in clinical studies for stage II and stage IV melanoma [38]. Algenpantucel-L and

Tergenpantucel-L are others antigen-expressing whole cell vaccines which are reviewed elsewhere [39].

1.3.1.1.2. Dendritic cell based Vaccines

Dendritic cells are professional antigen-presenting cells that play an essential role in generating robust antigen-specific T cell immune responses against cancer. Immunotherapeutic strategies have attempted to utilize the ability of dendritic cells to deliver antigens as a means of therapeutic vaccination in individuals with advanced malignancies [40-42]. In 1995, the first clinical trial was carried out to investigate therapeutic dendritic cell cancer vaccines for the treatment of melanoma [40]. For these studies, DCs were generated *ex vivo* by culturing a patient's own hematopoietic progenitor cells with cytokine combinations, pulsed with tumor antigens, followed by *ex vivo* maturation, and then administered back into the patient to elicit an immune response against the cancer cells carrying the antigens. Sipuleucel-T (Provenge®) was the first DC-based therapeutic cancer vaccine approved in 2010 by the FDA, for the treatment of prostate cancer [43]. As a personalized therapy, DC vaccines are highly labor intensive, requiring skilled technicians to isolate and expand cells from each patient, a process that can take between 4 to 16 weeks, which might not be feasible for patients with highly progressive diseases. Furthermore, storage, transportation, and reconstitution of these cellular vaccines are problematic. These issues combined make these cellular vaccines very expensive [44]. In addition, even though the vaccination resulted in antigen-specific CTL responses at the immunization and metastatic disease sites , no major therapeutic response was demonstrated in many advanced tumors [40]. One hypothesis regarding the lack of response was that immune inhibitory pathways elicited by the TME prevented CTLs from exerting their functions. Therefore, as discussed, inhibiting immune checkpoint receptors CTLA-4 and PD-1 (involved in the negative regulation of CTL function) and modulating immunosuppressive environment may be good companion therapies for DC vaccines.

1.3.1.1.3. T cell based Vaccines

The isolation, stimulation, and reinfusion of patients' T lymphocytes for the treatment of disease, termed adoptive cell transfer (ACT), was initially reported in the 1980's. ACT has been utilized for the stimulation and expansion of potent antigen-specific T cells that can kill cancer cells. The primary challenges in this field are identifying tumor-specific targets and avoiding off-target toxicities. Using this approach a personalized treatment can be achieved based on growing tumor-infiltrating lymphocytes (TIL) *ex vivo* from surgically excised tumor specimens of patients and then adoptively transferring them back into the patient [45]. This treatment is often coupled with IL-2 therapy and has been used on a number of different cancers – renal cell carcinoma, breast cancer, oral squamous cell carcinoma, and non-small cell lung cancer [45, 46]. A similar therapy utilizes genetically modified T cells, which target cancer through a chimeric antigen receptor (CAR). T cells are isolated, modified with T cell signaling domains that are fused with antibody derived targeting domains, and then infused back into patients. This therapy redirects the effector function of T cells towards specific tumor associated antigens (TAAs), without the requirement of antigen processing or presentation. CAR T cell therapy has been successful in treating patients with hematologic malignancies, however it has been less effective in treating solid tumors [47]. Although these therapies have great potential to be efficacious – it is extremely difficult to offer as a widely available therapy since the cell culture process requires extensive manipulation by highly skilled scientists/technicians.

1.3.1.2. Genetic Vaccine

Delivering antigen fragments via viral vectors or plasmid DNA is another method to transfect locally infiltrated APCs in muscles or skin. One major advantage of genetic vaccines is to delivery of multiple antigens in one immunization to stimulate different arms of immunity. Plasmid DNA or viral vectors are shuttle system to deliver them to target cells and to express antigenic proteins. The backbone of bacterial DNA itself acts as a PAMPs and stimulate innate arm of immune system by activating TLRs or other PRRs [48]. Moreover, DNA vaccine can be

combined with TLR agonists. HER-2/neu targeted or CEA targeted DNA vaccine when delivered (via electroporation) with TLR9 agonist IMO (immunomodulatory oligonucleotide) or with TLR7 agonist SM360320 resulted into inhibition of tumor growth in HER-2 positive mammary carcinoma and CEA positive colon carcinoma transgenic mouse model [49, 50]. Furthermore, fusion of $CD4^+$ antigenic fragments with $CD8^+$ antigenic fragments can be easily done to generate helper $CD4^+$ T cells to boost $CD8^+$ T cells response and to create long lasting memory [51]. Viral vectors with less disease causing potential and low intrinsic immunogenicity can be engineered to encode TAA or TAA with immunostimulating molecules. One of such vaccine platform called PROSTVAC is a replication incompetent vaccinia virus vector consist of a construct for prostate specific antigen (PSA) and three immunostimulatory molecules CD80, CD54 and CD58. PROSTVAC® has improved median overall survival (OS) to the control (25.5 months vs 16.1 months) when tested in double-blinded phase II clinical study for castration-resistant prostate cancer [52]. TG4010, ProstAtak™, -V/F-TRICOM™ and Alvax are other viral vector based vaccines which have been reviewed in details elsewhere [39]. Although DNA vaccination platform achieved significant success in mouse and rat models, translation into non-human primates and human remains biggest challenge for this type of vaccine. Perhaps new drug delivery platforms need to be designed for the delivery of plasmid DNA to achieve maximum transfection efficiency to induce more efficient and potent response in clinical trials.

1.3.1.3. Protein and Peptide based Vaccine

Perhaps, the most common vaccine strategy is to deliver MHC-I (HLA) restricted tumor associated antigenic peptides with adjuvants or immunomodulatory cytokines to induce potent CTLs response against tumors. In contrast to cellular vaccines, specific components of subunit vaccines (viral or non-viral-based recombinant antigen proteins, antigenic peptides, formulated with or without adjuvants such as TLR agonists) can be directly administered to the patient, to induce high numbers of antigen-specific effector and memory T cells. These vaccines rely on the patients' endogenous DCs for their uptake and antigen presentation. Components of subunit

vaccines can be readily designed based on recombinant technology and epitope focusing and these vaccines can be easily stored and transported. Peptide based vaccines for cancer have been in clinical trials since 1995 [39, 53]. There have been durable clinical responses in some patients that receive melanoma vaccines, however overall positive clinical response rates were low. In an effort to improve subunit vaccines, researchers have moved away from using short peptides (which have little or no tertiary structure and thus undergo rapid degradation in tissue and serum) to longer peptides [39, 53]. These longer peptides prevent degradation by exopeptidase and provide extra "handles" to proteasome and APM to present with MHC-I. Additionally the longer peptides have the potential to induce memory $CD8^+$ T cells. Currently there are several Phase III clinical trials of subunit cancer vaccines with multiple tumor types, such as peptide-based gp100, IMA901, NeuVax, etc., have been reviewed in detail elsewhere [54].

1.4. Challenges in the development of Cancer Vaccines

As discussed earlier: i) APCs carry the antigen from vaccines, travel to the nearest lymph nodes and cross-present these tumor associated antigens on their surface MHC proteins, ii) in lymph nodes, naïve T cells recognize these antigens via binding of surface TCR to MHC-I/p complexes and in presence of other co-stimulatory signals they proliferate, and iii) as T cells increase in numbers they identify tumor cells, perform their effector functions at tumor site and prevent the spread of tumor by killing tumor cells. All three steps are very critical and important for effectiveness of cancer vaccine to generate potent immune response against tumor.

Inducing high numbers of functional $CD8^+$ T cells against tumor antigens is not a trivial task. Once T cells proliferate, antigen recognition on tumor cells happens in the periphery-away from lymph nodes. $CD8^+$ T cells can recognize antigens on tumor cells as a 'foreign' and proliferate or $CD8^+$ T cells can undergo anergy and deactivation if antigens are recognized as a 'self'. Since tumor antigens are already present in the body, most of them can be recognized as a self-antigens resulting in T cell anergy and deactivation. On the contrary, due to ongoing antitumor immune response in the body, these antigen carrying APCs may be recognized as a

'tumor' and can be eliminated by $CD8^+$ T cells. If high numbers of CTLs are generated against tumor cells, lack of pro-inflammatory cytokines in tumor microenvironment and presence of immunosuppressive regulators can prevent them from performing their effector functions therefore rendering therapeutic vaccination ineffective.

Generally, during bacterial or viral infections, infected cells secrete chemokines and cytokines which attract effector cells to the site of infection. Due to immunosuppressive microenvironment tumor downregulates chemokines which attract effector immune cells. Moreover, immunosuppressive cellular and soluble mediators prevent T cells from carrying out their effector functions resulting in suppression of anti-tumor immune responses. Therefore, induction of high numbers of potent effective CTLs and modulating the immunosuppressive tumor microenvironment are crucial steps for the success of cancer vaccine. Engineering a particulate carrier system to deliver tumor antigens in order to achieve maximum immune response are discussed in chapter-2.

1.5. REFERENCES

[1] Kapadia CH, Perry JL, Tian S, Luft JC, DeSimone JM. Nanoparticulate immunotherapy for cancer. J Control Release. 2015;219:167-80.

[2] Janeway CA. Approaching the Asymptote? Evolution and Revolution in Immunology. Cold Spring Harbor Symposia on Quantitative Biology. 1989;54:1-13.

[3] Kawai T, Akira S. The role of pattern-recognition receptors in innate immunity: update on Toll-like receptors. Nat Immunol. 2010;11:373-84.

[4] Wu J, Chen ZJ. Innate Immune Sensing and Signaling of Cytosolic Nucleic Acids. Annual Review of Immunology. 2014;32:461-88.

[5] Iwasaki A, Medzhitov R. Control of adaptive immunity by the innate immune system. Nat Immunol. 2015;16:343-53.

[6] Hanahan D, Weinberg Robert A. Hallmarks of Cancer: The Next Generation. Cell. 2011;144:646-74.

[7] Dunn GP, Old LJ, Schreiber RD. The Immunobiology of Cancer Immunosurveillance and Immunoediting. Immunity. 2004;21:137-48.

[8] Mittal D, Gubin MM, Schreiber RD, Smyth MJ. New insights into cancer immunoediting and its three component phases;elimination, equilibrium and escape. Current Opinion in Immunology. 2014;27:16-25.

[9] Dunn GP, Old LJ, Schreiber RD. The immunobiology of cancer immunosurveillance and immunoediting. Immunity. 2004;21:137-48.

[10] Vinay DS, Ryan EP, Pawelec G, Talib WH, Stagg J, Elkord E, et al. Immune evasion in cancer: Mechanistic basis and therapeutic strategies. Seminars in Cancer Biology.

[11] Gooden MJM, de Bock GH, Leffers N, Daemen T, Nijman HW. The prognostic influence of tumour-infiltrating lymphocytes in cancer: a systematic review with meta-analysis. Br J Cancer. 2011;105:93-103.

[12] Smith-Garvin JE, Koretzky GA, Jordan MS. T Cell Activation. Annual Review of Immunology. 2009;27:591-619.

[13] Waldhauer I, Steinle A. NK cells and cancer immunosurveillance. Oncogene. 0000;27:5932-43.

[14] Bodduluru LN, Kasala ER, Madhana RMR, Sriram CS. Natural killer cells: The journey from puzzles in biology to treatment of cancer. Cancer Letters. 2015;357:454-67.

[15] Cohen NR, Garg S, Brenner MB. Chapter 1 Antigen Presentation by CD1: Lipids, T Cells, and NKT Cells in Microbial Immunity. In: Frederick WA, editor. Advances in Immunology: Academic Press; 2009. p. 1-94.

[16] Robertson FC, Berzofsky JA, Terabe M. NKT cell networks in the regulation of tumor immunity. Frontiers in Immunology. 2014;5.

[17] Schaue D, Xie MW, Ratikan JA, McBride WH. Regulatory T cells in radiotherapeutic responses. Frontiers in Oncology. 2012;2.

[18] Sakaguchi S. Naturally Arising CD4+ Regulatory T Cells for Immunologic Self-Tolerance and Negative Control of Immune Responses. Annual Review of Immunology. 2004;22:531-62.

[19] Faget J, Biota C, Bachelot T, Gobert M, Treilleux I, Goutagny N, et al. Early Detection of Tumor Cells by Innate Immune Cells Leads to Treg Recruitment through CCL22 Production by Tumor Cells. Cancer Research. 2011;71:6143-52.

[20] Nishikawa H, Sakaguchi S. Regulatory T cells in cancer immunotherapy. Current Opinion in Immunology. 2014;27:1-7.

[21] Curiel TJ, Coukos G, Zou L, Alvarez X, Cheng P, Mottram P, et al. Specific recruitment of regulatory T cells in ovarian carcinoma fosters immune privilege and predicts reduced survival. Nat Med. 2004;10:942-9.

[22] Tang Y, Xu X, Guo S, Zhang C, Tang Y, Tian Y, et al. An Increased Abundance of Tumor-Infiltrating Regulatory T Cells Is Correlated with the Progression and Prognosis of Pancreatic Ductal Adenocarcinoma. Plos One. 2014;9:e91551.

[23] Seung LP, Rowley DA, Dubey P, Schreiber H. Synergy between T-cell immunity and inhibition of paracrine stimulation causes tumor rejection. Proceedings of the National Academy of Sciences of the United States of America. 1995;92:6254-8.

[24] Chen M-F, Kuan F-C, Yen T-C, Lu M-S, Lin P-Y, Chung Y-H, et al. IL-6-stimulated CD11b + CD14 + HLA-DR – myeloid-derived suppressor cells, are associated with progression and poor prognosis in squamous cell carcinoma of the esophagus2014.

[25] Chanmee T, Ontong P, Konno K, Itano N. Tumor-Associated Macrophages as Major Players in the Tumor Microenvironment. Cancers. 2014;6:1670-90.

[26] Zhang Y, Cheng S, Zhang M, Zhen L, Pang D, Zhang Q, et al. High-Infiltration of Tumor-Associated Macrophages Predicts Unfavorable Clinical Outcome for Node-Negative Breast Cancer. Plos One. 2013;8:e76147.

[27] Schroder K, Hertzog PJ, Ravasi T, Hume DA. Interferon-γ: an overview of signals, mechanisms and functions. Journal of Leukocyte Biology. 2004;75:163-89.

[28] Kaplan DH, Shankaran V, Dighe AS, Stockert E, Aguet M, Old LJ, et al. Demonstration of an interferon γ-dependent tumor surveillance system in immunocompetent mice. Proceedings of the National Academy of Sciences. 1998;95:7556-61.

[29] Fernandes J, Cobucci R, Jatobá C, de Medeiros Fernandes T, de Azevedo J, de Araújo J. The Role of the Mediators of Inflammation in Cancer Development. Pathol Oncol Res. 2015:1-8.

[30] Rappuoli R, Mandl CW, Black S, De Gregorio E. Vaccines for the twenty-first century society. Nat Rev Immunol. 2011;11:865-72.

[31] Butterfield LH. Cancer vaccines. BMJ. 2015;350:h988.

[32] Guo C, Manjili MH, Subjeck JR, Sarkar D, Fisher PB, Wang XY. Therapeutic cancer vaccines: past, present, and future. Adv Cancer Res. 2013;119:421-75.

[33] Dranoff G. GM-CSF-based cancer vaccines. Immunol Rev. 2002;188:147-54.

[34] van Elsas A, Hurwitz AA, Allison JP. Combination immunotherapy of B16 melanoma using anti-cytotoxic T lymphocyte-associated antigen 4 (CTLA-4) and granulocyte/macrophage colony-stimulating factor (GM-CSF)-producing vaccines induces rejection of subcutaneous and metastatic tumors accompanied by autoimmune depigmentation. J Exp Med. 1999;190:355-66.

[35] Quezada SA, Peggs KS, Curran MA, Allison JP. CTLA4 blockade and GM-CSF combination immunotherapy alters the intratumor balance of effector and regulatory T cells. J Clin Invest. 2006;116:1935-45.

[36] Curran MA, Montalvo W, Yagita H, Allison JP. PD-1 and CTLA-4 combination blockade expands infiltrating T cells and reduces regulatory T and myeloid cells within B16 melanoma tumors. Proc Natl Acad Sci U S A. 2010;107:4275-80.

[37] Duraiswamy J, Freeman GJ, Coukos G. Therapeutic PD-1 pathway blockade augments with other modalities of immunotherapy T-cell function to prevent immune decline in ovarian cancer. Cancer Res. 2013;73:6900-12.

[38] Hsueh EC, Morton DL. Antigen-based immunotherapy of melanoma: Canvaxin therapeutic polyvalent cancer vaccine. Semin Cancer Biol. 2003;13:401-7.

[39] Slingluff CL. The Present and Future of Peptide Vaccines for Cancer: Single or Multiple, Long or Short, Alone or in Combination? Cancer journal (Sudbury, Mass). 2011;17:343-50.

[40] Anguille S, Smits EL, Lion E, van Tendeloo VF, Berneman ZN. Clinical use of dendritic cells for cancer therapy. The Lancet Oncology.15:e257-e67.

[41] Palucka K, Banchereau J. Cancer immunotherapy via dendritic cells. Nat Rev Cancer. 2012;12:265-77.

[42] Mantia-Smaldone G, Chu C. A Review of Dendritic Cell Therapy for Cancer: Progress and Challenges. BioDrugs. 2013;27:453-68.

[43] Schlom J, Arlen PM, Gulley JL. Cancer vaccines: moving beyond current paradigms. Clin Cancer Res. 2007;13:3776-82.

[44] Yee C. Adoptive T cell therapy: Addressing challenges in cancer immunotherapy. J Transl Med. 2005;3:17.

[45] Kalos M, June Carl H. Adoptive T Cell Transfer for Cancer Immunotherapy in the Era of Synthetic Biology. Immunity. 2013;39:49-60.

[46] Maus MV, Fraietta JA, Levine BL, Kalos M, Zhao Y, June CH. Adoptive Immunotherapy for Cancer or Viruses. Annual Review of Immunology. 2014;32:189-225.

[47] Curran KJ, Brentjens RJ. Chimeric antigen receptor T cells for cancer immunotherapy. J Clin Oncol. 2015;33:1703-6.

[48] Spies B, Hochrein H, Vabulas M, Huster K, Busch DH, Schmitz F, et al. Vaccination with plasmid DNA activates dendritic cells via Toll-like receptor 9 (TLR9) but functions in TLR9-deficient mice. J Immunol. 2003;171:5908-12.

[49] Dharmapuri S, Aurisicchio L, Neuner P, Verdirame M, Ciliberto G, La Monica N. An oral TLR7 agonist is a potent adjuvant of DNA vaccination in transgenic mouse tumor models. Cancer Gene Ther. 2009;16:462-72.

[50] Aurisicchio L, Peruzzi D, Conforti A, Dharmapuri S, Biondo A, Giampaoli S, et al. Treatment of mammary carcinomas in HER-2 transgenic mice through combination of genetic vaccine and an agonist of Toll-like receptor 9. Clin Cancer Res. 2009;15:1575-84.

[51] Maecker HT, Umetsu DT, DeKruyff RH, Levy S. Cytotoxic T cell responses to DNA vaccination: dependence on antigen presentation via class II MHC. J Immunol. 1998;161:6532-6.

[52] Kantoff PW, Schuetz TJ, Blumenstein BA, Glode LM, et al. Overall survival analysis of a phase II randomized controlled trial of a Poxviral-based PSA-targeted immunotherapy in metastatic castration-resistant prostate cancer. J Clin Oncol. 2010;28:1099-105.

[53] Yamada A, Sasada T, Noguchi M, Itoh K. Next-generation peptide vaccines for advanced cancer. Cancer Science. 2013;104:15-21.

[54] Nguyen T, Urban J, Kalinski P. Therapeutic cancer vaccines and combination immunotherapies involving vaccination. ImmunoTargets & Therapy. 2014;3.

Chapter-2: Delivery of Cancer Vaccine using Nanoparticles*

2.1. Introduction

The key advantages of using nanoparticulate carriers are improved solubility and bioavailability of the cargo. They can be loaded with a variety of cargos such as siRNA, peptides, proteins, and small molecule therapeutics. Importantly, by associating the cargo with a nanoparticulate carrier, the cargo can be protected from degradation, which can increase its half-life, enhancing potential efficacy. Furthermore, these systems can be modified for targeted site-specific delivery, mitigating systemic toxicity issues. To date, there are 45 nanoparticulate formulations approved for clinical use including liposomes for cancer therapeutics and diagnostic agents, polymer-protein conjugates of IFN-α, GM-CSF and anti-TNF-α monocloncal antibodies for tumor therapy, and virosomes for flu vaccines [2].

There are a multitude of methods for fabricating nanoparticles (NPs) – varying from formation of micelles [3], liposomes [4], emulsions [5], or through a template/particle molding techniques [6, 7]. Using these techniques, NPs can be composed of an assortment of different materials, with varying sizes, shapes, and chemical and surface properties. Possessing the manufacturing platforms to control and design nanoparticles possessing specific parameters allows investigators the unique ability to match optimized NPs to the specific delivery requirements. For example, the design parameters for the delivery of immunotherapy agents that require systemic (intravenous) delivery and accumulation and release at the tumor site, will differ from those that require local delivery to tissue resident APC's or to draining lymph nodes. Design parameters for delivery of subunit vaccine are outlined below.

*With Sections Reprinted from [1] 'Journal of Controlled Release', 219 /December 10, Kapadia CH, Perry JL, Tian S, Luft JC, DeSimone JM, **'Nanoparticulate Immunotherapy for cancer'**, 167-180, Copyright (2015), with permission from Elsevier.

2.2. Particle design parameters for local delivery to immune cells

The development of nanoparticles to target immune cells is a newer field, however much work has gone into designing particles to deliver cargo to tissue resident APC's or drain and trigger activation of immune cells residing in lymph node, as required for vaccine administrations. For these applications particles are administered subcutaneously, intradermally, intramuscularly, intraperitoneally, etc. Since the adaptive immune response is mainly initiated in secondary lymphoid organs, transport of nanoparticulate vaccine to the draining lymph node (dLN) is an important factor in designing these nanocarriers. As shown in figure-2.1, the size of nanoparticulate carrier plays an important role in shaping an immune response; it not only influences cellular uptake and intracellular trafficking, but also affects lymphatic trafficking. NPs from 5 nm to 100 nm in size, transport via convective force and diffuse deeper into the extracellular matrix and are able to travel to dLNs by afferent lymphatic vesicles. Particles greater than 500 nm remains trapped in extracellular matrixes [8]. These larger particles can potentially be taken up by resident APCs and then trafficked to the dLNs [9]. Once they reach the dLNs, retention of NPs is also dependent on their size. Larger particles will be taken up by subcapsular macrophages whereas smaller particles can directly access T cell region and can be taken up by immature DCs residing within LNs [8]. Moreover, in the dLNs, smaller nanoparticles can target larger numbers of immature DCs, B cells and T cells [10]. Reddy et al. have shown higher lymphatic drainage and lymph node retention of 20 nm and 45 nm polypropylene disulfide (PPS) NPs as compared to 100 nm NPs after intradermal injections. Retention of smaller sized particles was seen up to 5 days [11]. Mueller et al., have also shown the importance of particle size for targeting LNs and generating a better humoral response. In comparing non-draining 1 ×1 μm cylindrical particles, to rapidly draining 80 × 180 nm rod-shaped particles, smaller particles were able to sustain prolonged antigen presentation to APCs and elicited a stronger humoral response than the non-draining 1 × 1 μm NPs [12]. Furthermore, Fifis et al. also demonstrated the significance of size in generating anti-tumor immune response

utilizing 40 nm and 100 nm ovalbumin coated particles. The 40 nm particles were able to drain to LNs and localized with residing DCs to a higher extent than 100 nm particles, and were able to induce prophylactic as well therapeutic immunization responses against the tumor. These studies indicate that targeting immature DCs residing LNs is a successful strategy to elicit antigen specific immune response [13]. This concept is further supported by positive results

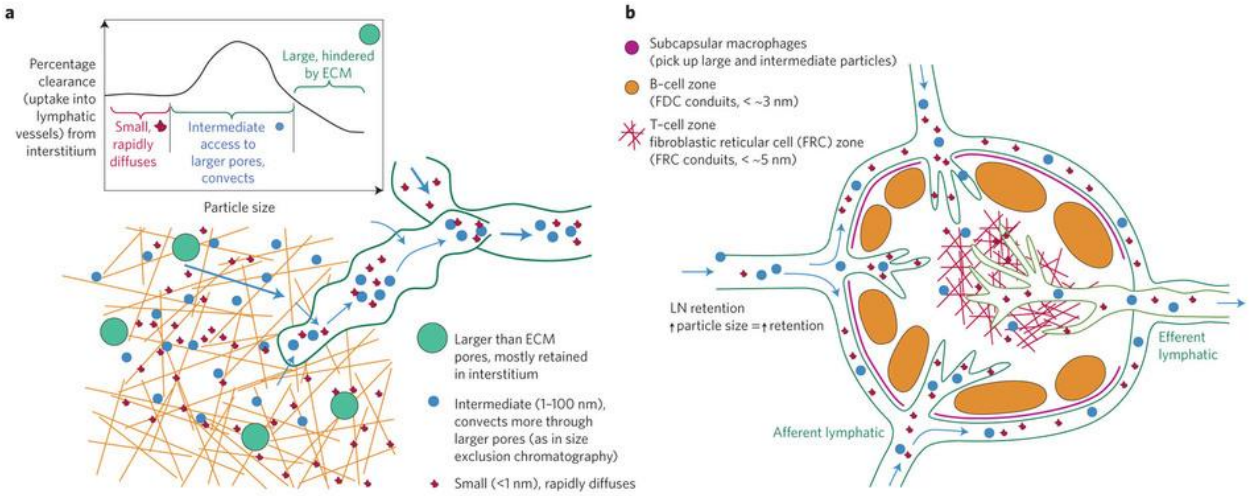

Figure-2.1: Effects of particulate size on tissue, cell and intracellular targets after entry into interstitial tissue.

a, After injection into the interstitium (that is, intramuscular, intradermal or subcutaneous injection, for instance), particles (whose definition here includes molecules) will disperse and convect with interstitial flow, driven by transient pressure gradients that arise from the injection as well as the natural small pressure gradient between blood and lymphatic capillaries. Very small particles (red), whose diffusion velocity is greater than convective velocity, can readily diffuse and will rapidly dilute in local concentration, which limits the effective lymphatic concentration. Larger, intermediate-sized (blue) particles have smaller diffusion speeds and furthermore are transported within the more permeable regions of the extracellular matrix (as in size-exclusion chromatography). Their transport is thus governed more by convection, and they are more efficiently directed into the lymphatic vessels. As size increases, however, steric hindrance becomes limiting, and particles that are too large (over about 500 nm, although this depends on tissue, level of hydration and experimental conditions) remain mostly trapped in the interstitial space. b, Once inside the lymphatic vessel, lymph node (LN) retention positively correlates with particle size. Larger (or opsonized) particles are readily taken up by subcapsular macrophages, whereas intermediate-sized particles can directly access the T-cell zone and associated dendritic cells. The B-cell zone conduits, however, which are formed by follicular dendritic cells (FDC), restrict access to particles under about 3 nm. Figure and caption are reprinted by permission from Macmillan Publishers Ltd: [NATURE MATERIALS] [8], copyright (2013).

from human clinical trials utilizing 40 nm ISOMATRIX particle which induced potent $CD8^+$ T cell [14].

Particle surface charge can also affect lymphatic drainage and lymphatic retention. The extracellular matrix (ECM) is made up of collagen fibers and negatively charged proteins (glycosaminoglycans), therefore positively charged (cationic) particles remain trapped at the injection site and possibly phagocytosed by APCs and then trafficked to the LNs [15]. In contrast, particles that are negatively charged and neutral/surface pacified with PEG have limited interaction with the ECM, which facilitate their traffic to dLN either through enhanced trafficking in lymphatic vesicles or through internalization by migratory DCs [16]. Furthermore, surface ligand coatings are highly important in determining the outcome of particles. APCs and B cells are able to recognize pathogens by their surfaces, which are densely covered with proteins, lipids and polysaccharides. By mimicking these highly repetitive patterns (HRP) of biomolecules on the surface of particulate carriers, we can enhance multivalent antigen presentation and induce more a robust and potent immune response. In multivalent ligand vaccines, increasing the valency of ligands on NPs increases avidity and apparent binding, which influences cell surface receptor clustering for signal transduction [15]. More specifically, 15-20 hapten molecules that are spaced 5-10 nm apart (similar to the average spacing of viral coat proteins) is an ideal special arrangement to efficiently activate B cell receptors [17]. Highly repetitive patterns of antigen/adjuvants on nanoparticulate carriers allow efficient binding of natural IgM antibodies through high-avidity interactions, leading to recruitment and activation of complement component 1q (C1q) and the classical pathway of the complement cascade [17]. Furthermore, hydrophilic nanoparticle surfaces such as polyhydroxylated (-OH) pluronic-coated NPs, can activate alternative pathways of complement activation [18]. Therefore changing chemical groups on particle surface (by changing chemistry of polymer or linkers) may allow us to manipulate their capacity to trigger the complement activation cascade and opsonization profile [19].

2.3. Delivery of subunit vaccine via particulate carriers

Subunit vaccines offer a safer and more specific approach to generate immunity, by administering specific components of pathogenic organisms (e.g. bacterial coat proteins, peptides, carbohydrates or lipids) to stimulate the immune system. In the soluble form these biomolecules suffer from poor immunogenicity as well as short *in vivo* half-lives that limit their ability to reach target cells. This necessitates design of nanoparticle carriers to deliver subunit vaccines that target APCs and specific cellular compartments. Specifically, cytosolic delivery of exogenous antigen into MHC class I presentation pathway of APCs is required to induce potent CTLs response. Lipid–calcium–phosphate (LCP) nanoparticles represent a new class of intracellular delivery systems for sending cell membrane impermeable antigens to cytosol to induce CTLs response in cancer immunotherapy. Xu et al. have co-encapsulated Trp-2 (tyrosinase related protein-2, melanoma associated antigen) peptide and CpG ODN in mannose decorated LCP nanoparticles which resulted in higher cargo deposition to LNs and superior inhibition of tumor growth in both B16F10 melanoma subcutaneous and lung metastasis models [20]. Interestingly, Vasievich et al. reported that a cancer vaccine with Trp-2 peptide and a cationic lipid (R)-DOTAP (1, 2-dioleoyl-3-trimethylammonium-propane) formulated into nanocomplexes was able to elicit high population of functionally active tumor-infiltrating lymphocytes and break the T cell tolerance in tumor in a murine melanoma model, achieving significantly delayed tumor growth [21].

Since cancerous cells can escape immune surveillance via multiple mechanisms, utilizing a single epitope peptide restricted to MHC-I might not be sufficient to generate efficient anti-tumor immune response. Nanoparticulate delivery systems offer the opportunity to deliver multiple epitope peptide vaccines to a single cell. Tan et al., have shown that combinational delivery of multiple NPs carrying different tumor-associated antigen (TAA) peptides generated a better anti-tumor response than NPs loaded with single peptide epitope. Specifically, delivery of PLGA emulsion carrying TAA peptides Trp-2, gp100, and immunosuppressive retroviral protein

epitope p15E had significantly better tumor regression and survival in B16F10 murine melanoma model as compared to PLGA emulsion loaded with only a single TAA peptide [22].

Moreover, particulate carriers can provide sustained release of antigens to induce more potent cellular responses and immune memory. PLGA is a commonly used biodegradable polymer in nanoparticle synthesis, with physicochemical properties readily tunable to achieve various degradation profiles and cargo release kinetics. Liposomes are another commonly used particulate carrier, in which cargo release is achieved after disruption of lipid bi-layer. In comparing release kinetics, liposomes typically release their cargo at a faster rate than the PLGA nanoparticles. In comparing these release kinetics, it was found that a prolonged and sustained release from PLGA NPs resulted in persistent antibody titers, stronger cellular responses and higher frequency of effector T cells as compare to liposomal formulation [23].

2.4. Targeting DCs via nanoparticulate vaccine

Dendritic cells are the major class of APCs. Targeting DCs via antibodies against their cell surface receptor such as DC205, CD40 or CD11c, for delivery of subunit vaccine components can increase the efficiency of cross-presentation and induce more potent $CD8^+$ T cells. Cruz et al. have evaluated the efficiency of these different targeting strategies to activate DCs and elicit a potent $CD8^+$ T cell response. Model antigen protein ovalbumin (OVA), TLR3 ligand Poly I:C and TLR7/8 ligand R848 were encapsulated in PLGA NPs decorated with different antibodies against surface receptors, DEC205, CD11c, and CD40. All targeted NPs stimulated *in vitro* DCs for expression of co-stimulatory molecules and production of IL-12, and induced proliferation of antigen specific IFN-γ producing $CD8^+$ T cells. Subcutaneous vaccination of CD40, DEC205 and CD11c targeted NPs in C57BL/6 mice induced significantly higher frequency of CTLs as compare to non-targeted NPs [24]. In another study, Rosalia et al. have improved the delivery of OVA protein to DCs and induced potent anti-tumor immune response in B16-OVA melanoma model in mice via co-delivery of OVA, Pam3CSK4 (TLR3 agonist) and poly I:C (TLR3 agonist) in anti-CD40 Ab decorated PLGA NPs [25].

DCs can also up-regulate co-inhibitory molecules including PD-L1 and PD-L2. The balance in expression level and activation of co-stimulatory molecules and inhibitory molecules determines the activation state of T cells. Hobo et al. have achieved efficient knockdown of PD-L expression on human monocyte derived DC and superior induction of *ex vivo* antigen-specific T cells via intracellular delivery of PD-L1 and PD-L2 siRNA using cationic lipid nanoparticles (LNP) and delivery of antigen peptide mRNA via electroporation [26]. Moreover, similar groups have also developed DOPE based NPs to delivery PD-L1 and PD-L2 siRNA which increased transfection efficiency and suppression of PD-L1 and PD-L2 [27]. In another study, Cubillos-Ruiz et al. has shown increased uptake of NPs to tumor associated regulatory DCs via delivery of siRNA- PEI nanocomplexes [114]. Delivery of siRNA via PEI complexes converted regulatory DCs to antigen presenting DCs and also enhanced tumoricidal activity of DCs via TLR5 stimulation. Moreover, siRNA delivery via PEI complexes significantly reduced tumor growth and improved survival of ovarian carcinoma bearing mice [28]. Similarly, Teo et al., have increased siRNA uptake and reduced toxicity of NPs, when PD-L1 siRNA was delivered to PD-L1 overexpressed epithelial ovarian cells via PEI-PEG-siRNA complexes. Delivery of PD-L1 siRNA via PEI nanocomplexes resulted into 40% to 50% of PD-L1 knockdown with two fold increased sensitivity of SKOV-3 to T cell killing as compare to scrambled siRNA sequence [29].

2.5. PRINT (Particle Replication in Non-wetting Template) - a platform for delivery of subunit vaccine

PRINT (Particle Replication in Non-Wetting Template) is a unique nanofabrication technique which combines modern soft-lithographic principles from microelectronic industries with the flexible molding properties of PFPE (perfluoropolyether) to produce nano-microparticles with unprecedented control of size and shape. It has been found and developed in the lab of DeSimone at UNC Chapel Hill and its spin out company Liquidia Technologies Inc. which has developed cGMP compliant PRINT plant for its use in phase I clinical trial [30, 31]. Similar to other soft lithographic techniques PRINT involves fabrication of PFPE molds from

master templates, following by filling the mold with a pre-particle solution, solidifying the particles in the mold, then transferring the particles out of the mold and onto a water soluble polymer sheet [31]. PRINT fabrication process is shown in following figure-2.2.

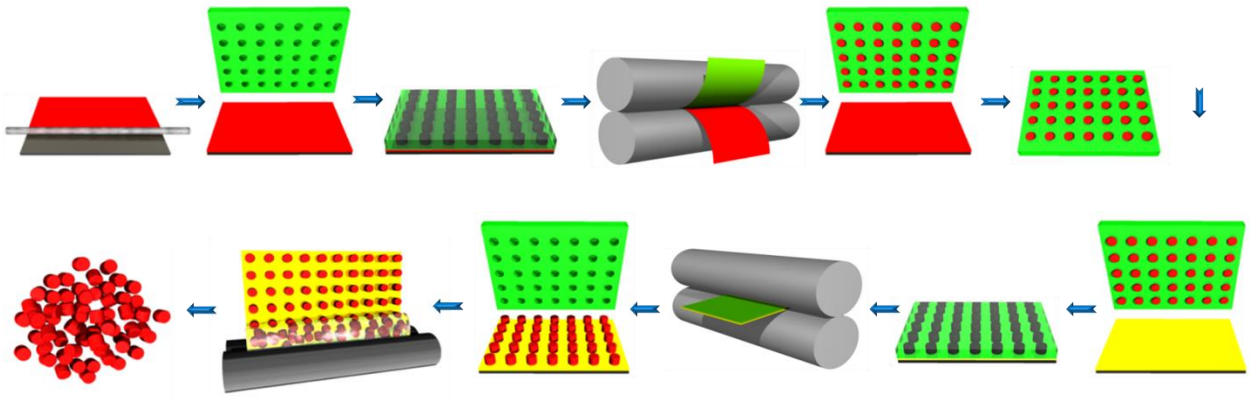

Figure-2.2: PRINT®- fabrication process.
PRINT fabrication process begins with applying pre-particle (precursor) organic solution of polymer or monomer or proteins (red) to a polyethylene terephthalate (PET) delivery sheet (gray) by mayer rod. Then PFPE mold (green) is laminated against the thin layer of pre-particle sheet and passed through a heated nip (gray). The mold cavities are filled with a material of choice. Filled mold is laminated against water soluble polymer sheet (yellow) such as PVA or Plasdone™ and passed through a heated nip. Particles (red dots) are transferred onto harvesting layer sheet. Very monodispersed particles are collected by dissolving sacrificial harvesting layer of water soluble polymer into water.

PRINT begins with the etching the micro-nano cavities of precise size and shape on silicon wafer. Molds are manufactured by applying photocurable elastomeric PFPE to the silicon master template. The low surface energy of PFPE enables complete wetting of the silicone master template which allows patterning of consistently high density features from 10 nm to 1 µm. The pre-particle solutions (combinations of polymers, monomers, proteins, nucleic acids, therapeutic drugs) fill all cavities in the mold by capillary action and/or mechanical forces. Moreover, low surface energy prevents the wetting of the land area between the cavities of mold allowing the production of highly monodisperse nano/micro particles without an interconnected

flash layer [31]. After filling the mold, particles can be removed by transferring them to harvesting sheet composed of water soluble polymers. Common harvesting materials used are poly (vinyl) alcohol (PVA) and Plasdone™. Transferred particles are collected via dissolving the sacrificial harvesting layers in water yielding empty molds and nearly mono-disperse particles. Monodisperse particle can be lyophilized or store for future chemical modification.

The versatility of PRINT technologies allows investigators to fill the mold with different materials such as PLGA, photo curable cross-linked acrylate monomers, proteins, and chemotherapeutics, providing exquisite control over modulus, composition, and surface chemistries [32, 33]. Additionally, fluorescent dyes can be incorporated into appropriate particle compositions to study bio-distribution as well as lymphatic trafficking [12]. Special monomers can also be incorporated into particle matrix to provide different functional handle for addition of surface ligands such as PEG, targeting affibody, or protein antigens [34].

For subunit vaccine delivery, PRINT technology allows for the fabrication of particles that mimic the features of known pathogens (size, shape, and surface composition). Previous work has shown that delivery of trivalent influenza antigenic protein adsorbed onto cationic PLGA PRINT nanoparticles is safe and produced better antigen-specific antibody responses when compared to inactivated virus vaccine [35]. Fromen et al. has shown potent mucosal and humoral immune responses in mice when model antigenic protein conjugated to PEG hydrogel PRINT particles were delivered through intranasal immunization [36]. Moreover, Mueller et al. has shown the importance of particle size in production of antibody response. Model ovalbumin protein conjugated to 80X180 nm PRINT PEG hydrogel particles were more efficiently taken up by key APCs and stimulated helper $CD4^+$ T cell responses to boost humoral immunity as compared to 1 μm sized PRINT PEG hydrogel particles [12]. Although successful delivery of model protein resulted into potent humoral immune response, optimization and development is still needed to induce potent cellular immune response to fight against cancer and intracellular pathogens. The goal of my dissertation project is to design the delivery system for model as well

as tumor antigenic peptides and adjuvants to induce cellular immune response to fight against cancer. The next chapter focuses on the design of a PRINT hydrogel particulate platform for the delivery of model antigenic peptide-SIINFEKL (MHC-I epitope of Ovalbumin) and CpG ODN by utilizing intracellular reduction sensitive environment of APCs.

2.6. REFERENCES

[1] C.H. Kapadia, J.L. Perry, S. Tian, J.C. Luft, J.M. DeSimone, Nanoparticulate immunotherapy for cancer, J Control Release, 219 (2015) 167-180.

[2] C.A. Schutz, L. Juillerat-Jeanneret, H. Mueller, I. Lynch, M. Riediker, C. NanoImpactNet, Therapeutic nanoparticles in clinics and under clinical evaluation, Nanomedicine (Lond), 8 (2013) 449-467.

[3] K. Kataoka, A. Harada, Y. Nagasaki, Block copolymer micelles for drug delivery: design, characterization and biological significance, Adv Drug Deliv Rev, 47 (2001) 113-131.

[4] V.P. Torchilin, Recent advances with liposomes as pharmaceutical carriers, Nat Rev Drug Discov, 4 (2005) 145-160.

[5] M.J. Lawrence, G.D. Rees, Microemulsion-based media as novel drug delivery systems, Adv Drug Deliv Rev, 45 (2000) 89-121.

[6] J.P. Rolland, B.W. Maynor, L.E. Euliss, A.E. Exner, G.M. Denison, J.M. DeSimone, Direct Fabrication and Harvesting of Monodisperse, Shape-Specific Nanobiomaterials, Journal of the American Chemical Society, 127 (2005) 10096-10100.

[7] S. Xu, Z. Nie, M. Seo, P. Lewis, E. Kumacheva, H.A. Stone, P. Garstecki, D.B. Weibel, I. Gitlin, G.M. Whitesides, Generation of monodisperse particles by using microfluidics: control over size, shape, and composition, Angew Chem Int Ed Engl, 44 (2005) 724-728.

[8] D.J. Irvine, M.A. Swartz, G.L. Szeto, Engineering synthetic vaccines using cues from natural immunity, Nat Mater, 12 (2013) 978-990.

[9] V. Manolova, A. Flace, M. Bauer, K. Schwarz, P. Saudan, M.F. Bachmann, Nanoparticles target distinct dendritic cell populations according to their size, Eur J Immunol, 38 (2008) 1404-1413.

[10] J. Kim, D.J. Mooney, In Vivo Modulation of Dendritic Cells by Engineered Materials: Towards New Cancer Vaccines, Nano Today, 6 (2011) 466-477.

[11] S.T. Reddy, A. Rehor, H.G. Schmoekel, J.A. Hubbell, M.A. Swartz, In vivo targeting of dendritic cells in lymph nodes with poly(propylene sulfide) nanoparticles, J Control Release, 112 (2006) 26-34.

[12] S.N. Mueller, S. Tian, J.M. DeSimone, Rapid and Persistent Delivery of Antigen by Lymph Node Targeting PRINT Nanoparticle Vaccine Carrier To Promote Humoral Immunity, Mol Pharm, 12 (2015) 1356-1365.

[13] T. Fifis, A. Gamvrellis, B. Crimeen-Irwin, G.A. Pietersz, J. Li, P.L. Mottram, I.F. McKenzie, M. Plebanski, Size-dependent immunogenicity: therapeutic and protective properties of nano-vaccines against tumors, J Immunol, 173 (2004) 3148-3154.

[14] I.H. Frazer, M. Quinn, J.L. Nicklin, J. Tan, L.C. Perrin, P. Ng, V.M. O'Connor, O. White, N. Wendt, J. Martin, J.M. Crowley, S.J. Edwards, A.W. McKenzie, S.V. Mitchell, D.W. Maher, M.J. Pearse, R.L. Basser, Phase 1 study of HPV16-specific immunotherapy with E6E7 fusion protein

and ISCOMATRIX adjuvant in women with cervical intraepithelial neoplasia, Vaccine, 23 (2004) 172-181.

[15] B.L. Hartwell, L. Antunez, B.P. Sullivan, S. Thati, J.O. Sestak, C. Berkland, Multivalent nanomaterials: learning from vaccines and progressing to antigen-specific immunotherapies, J Pharm Sci, 104 (2015) 346-361.

[16] X. Zhan, K.K. Tran, H. Shen, Effect of the poly(ethylene glycol) (PEG) density on the access and uptake of particles by antigen-presenting cells (APCs) after subcutaneous administration, Mol Pharm, 9 (2012) 3442-3451.

[17] M.F. Bachmann, G.T. Jennings, Vaccine delivery: a matter of size, geometry, kinetics and molecular patterns, Nat Rev Immunol, 10 (2010) 787-796.

[18] S.T. Reddy, A.J. van der Vlies, E. Simeoni, V. Angeli, G.J. Randolph, C.P. O'Neil, L.K. Lee, M.A. Swartz, J.A. Hubbell, Exploiting lymphatic transport and complement activation in nanoparticle vaccines, Nat Biotechnol, 25 (2007) 1159-1164.

[19] S.Y. Seong, P. Matzinger, Hydrophobicity: an ancient damage-associated molecular pattern that initiates innate immune responses, Nat Rev Immunol, 4 (2004) 469-478.

[20] Z. Xu, S. Ramishetti, Y.C. Tseng, S. Guo, Y. Wang, L. Huang, Multifunctional nanoparticles co-delivering Trp2 peptide and CpG adjuvant induce potent cytotoxic T-lymphocyte response against melanoma and its lung metastasis, J Control Release, 172 (2013) 259-265.

[21] E.A. Vasievich, S. Ramishetti, Y. Zhang, L. Huang, Trp2 peptide vaccine adjuvanted with (R)-DOTAP inhibits tumor growth in an advanced melanoma model, Mol Pharm, 9 (2012) 261-268.

[22] S. Tan, T. Sasada, A. Bershteyn, K. Yang, T. Ioji, Z. Zhang, Combinational delivery of lipid-enveloped polymeric nanoparticles carrying different peptides for anti-tumor immunotherapy, Nanomedicine (Lond), 9 (2014) 635-647.

[23] S.L. Demento, W. Cui, J.M. Criscione, E. Stern, J. Tulipan, S.M. Kaech, T.M. Fahmy, Role of sustained antigen release from nanoparticle vaccines in shaping the T cell memory phenotype, Biomaterials, 33 (2012) 4957-4964.

[24] L.J. Cruz, R.A. Rosalia, J.W. Kleinovink, F. Rueda, C.W. Lowik, F. Ossendorp, Targeting nanoparticles to CD40, DEC-205 or CD11c molecules on dendritic cells for efficient CD8(+) T cell response: a comparative study, J Control Release, 192 (2014) 209-218.

[25] R.A. Rosalia, L.J. Cruz, S. van Duikeren, A.T. Tromp, A.L. Silva, W. Jiskoot, T. de Gruijl, C. Lowik, J. Oostendorp, S.H. van der Burg, F. Ossendorp, CD40-targeted dendritic cell delivery of PLGA-nanoparticle vaccines induce potent anti-tumor responses, Biomaterials, 40 (2015) 88-97.

[26] W. Hobo, T.I. Novobrantseva, H. Fredrix, J. Wong, S. Milstein, H. Epstein-Barash, J. Liu, N. Schaap, R. van der Voort, H. Dolstra, Improving dendritic cell vaccine immunogenicity by silencing PD-1 ligands using siRNA-lipid nanoparticles combined with antigen mRNA electroporation, Cancer Immunol Immunother, 62 (2013) 285-297.

[27] M.W. Roeven, W. Hobo, R. van der Voort, H. Fredrix, W.J. Norde, K. Teijgeler, M.H. Ruiters, N. Schaap, H. Dolstra, Efficient Nontoxic Delivery of PD-L1 and PD-L2 siRNA Into Dendritic Cell Vaccines Using the Cationic Lipid SAINT-18, J Immunother, 38 (2015) 145-154.

[28] J.R. Cubillos-Ruiz, X. Engle, U.K. Scarlett, D. Martinez, A. Barber, R. Elgueta, L. Wang, Y. Nesbeth, Y. Durant, A.T. Gewirtz, C.L. Sentman, R. Kedl, J.R. Conejo-Garcia, Polyethylenimine-based siRNA nanocomplexes reprogram tumor-associated dendritic cells via TLR5 to elicit therapeutic antitumor immunity, J Clin Invest, 119 (2009) 2231-2244.

[29] P.Y. Teo, C. Yang, L.M. Whilding, A.C. Parente-Pereira, J. Maher, A.J. George, J.L. Hedrick, Y.Y. Yang, S. Ghaem-Maghami, Ovarian Cancer Immunotherapy Using PD-L1 siRNA Targeted Delivery from Folic Acid-Functionalized Polyethylenimine: Strategies to Enhance T Cell Killing, Adv Healthc Mater, (2015).

[30] J.P. Rolland, B.W. Maynor, L.E. Euliss, A.E. Exner, G.M. Denison, J.M. DeSimone, Direct fabrication and harvesting of monodisperse, shape-specific nanobiomaterials, J Am Chem Soc, 127 (2005) 10096-10100.

[31] W. Jeong, M.E. Napier, J.M. DeSimone, Challenging nature's monopoly on the creation of well-defined nanoparticles, Nanomedicine (Lond), 5 (2010) 633-639.

[32] J.Y. Kelly, J.M. DeSimone, Shape-specific, monodisperse nano-molding of protein particles, J Am Chem Soc, 130 (2008) 5438-5439.

[33] J.L. Perry, K.P. Herlihy, M.E. Napier, J.M. Desimone, PRINT: a novel platform toward shape and size specific nanoparticle theranostics, Acc Chem Res, 44 (2011) 990-998.

[34] J.L. Perry, K.G. Reuter, M.P. Kai, K.P. Herlihy, S.W. Jones, J.C. Luft, M. Napier, J.E. Bear, J.M. DeSimone, PEGylated PRINT nanoparticles: the impact of PEG density on protein binding, macrophage association, biodistribution, and pharmacokinetics, Nano Lett, 12 (2012) 5304-5310.

[35] A.L. Galloway, A. Murphy, J.M. DeSimone, J. Di, J.P. Herrmann, M.E. Hunter, J.P. Kindig, F.J. Malinoski, M.A. Rumley, D.M. Stoltz, T.S. Templeman, B. Hubby, Development of a nanoparticle-based influenza vaccine using the PRINT technology, Nanomedicine, 9 (2013) 523-531.

[36] C.A. Fromen, G.R. Robbins, T.W. Shen, M.P. Kai, J.P. Ting, J.M. DeSimone, Controlled analysis of nanoparticle charge on mucosal and systemic antibody responses following pulmonary immunization, Proc Natl Acad Sci U S A, 112 (2015) 488-493.

Chapter-3: Reduction Sensitive PEG Hydrogels for Co-delivery of Antigen and Adjuvant to Induce Potent CTL*

3.1. Introduction

Vaccines are one of the major discoveries in modern medicine. Contributions include the almost complete elimination of polio, eradication of small pox, and a decrease by more than 95% of the incidence of diseases such as diphtheria, tetanus, pertussis, measles, mumps and rubella [1]. Vaccines have substantially decreased morbidity and mortality related to infectious disease and increased the average life span in the twenty-first century. Despite these successes, there is a clear need to develop vaccines against pathogens like human immunodeficiency virus (HIV), hepatitis C virus (HCV), and diseases such as malaria, tuberculosis, and cancer. Although effective, traditional vaccines utilize live or attenuated pathogens which pose safety concerns due to the administration of unnecessary components of pathogenic micro-organism [2].

New-generation subunit vaccines offer a safer and more specific approach to generate immunity, in which very specific components of pathogenic organisms (e.g. bacterial coat proteins, peptides, carbohydrates or lipids; immunogenic determinants) are administered to protect against disease. Clinical success of subunit vaccines include the use of Fluvirin® (trivalent subunit protein) and Influvac (inactivated purified surface antigens from influenza virus) against influenza, BioThrax® (AVA-anthrax adsorbed vaccine, contains no whole cell or live bacteria) against anthrax, Cervarix® (contains a mixture of human papilloma virus protein antigens with adjuvants alum and monophosphoryl lipid-A) against cervical cancer caused by HPV [3]. Because of our improved understanding of the immune system, more specific and safer

---

*Chintan H. Kapadia, Shaomin Tian, Jillian L. Perry, J. Christopher Luft, Joseph M. DeSimone, *In preparation*

peptide epitopes are being designed based on recombinant technology and epitope focusing [4].

Peptide antigens are easily synthesized, stored and transported. Specific antigenic peptide epitopes can induce an antigen specific cytotoxic T cell (CTL) response, which is of the utmost importance in the elimination of intracellular pathogens, as well as cancer cells. Successful intracellular delivery of peptides to professional APCs (mostly dendritic cells [DCs]) and their cross-presentation to T cells elicit CTLs. For cross-presentation, APCs can process endocytosed antigens by either the classical (also cytosolic pathway) or vacuolar pathway. In the classical pathway, protein antigens are processed into 8 to 12 amino acids fragments by proteasomal degradation machinery in cytosol and loaded onto MHC-I molecules in the endoplasmic reticulum (ER) or phagosome by antigen processing machinery (APM). In the vacuolar pathway, degradation of pathogens/antigens and loading of peptide fragments to MHC-I occurs in the endosome [5]. However, soluble peptides suffer from fast degradation half-life (from a few seconds to minutes depending on their length) [6] and low cellular uptake, resulting in poor cross-presentation by DCs and lower immunogenicity.

Many particulate subunit vaccine delivery systems such as liposomes, nano-beads, solid-lipid nanoparticles, polymeric nanoparticle and micelles, etc. have been investigated as a delivery vehicle to induce protection against HIV, influenza and cancer [7]. Particulate carrier systems can improve immunogenicity of antigens and adjuvants by mimicking the size, shape and/or surface molecule organization of pathogens, in order to facilitate uptake by APCs [8]. Additionally they prevent enzymatic degradation of antigens/adjuvants, and facilitate their intracellular delivery by increasing their local resident time [9]. Depending on their degradation mechanism, the antigen can be released into the late endosome/ lysosome or into cytosol. By optimizing the polymeric material of the nanoparticulate carrier, release of antigen can be triggered by changes in an intracellular pH [10, 11], slower degradation rate of biodegradable polymeric carrier [12-14], or enzyme mediated release of antigen such as endo-lysosomal lipases [15] or α-chymotrypsin [16].

Efficient activation of DCs as well as induction and proliferation of T cells also requires co-stimulatory signals which can be provided by delivering adjuvants [17]. Co-delivery of antigens with adjuvants using particulate carriers can further boost the immune response [18, 19]. Many immune stimulating agents such as alum, oil in water emulsions, various TLR/NLR agonists etc. are being explored in clinical, as well as pre-clinical studies as vaccine adjuvants [20]. TLR agonists such as MPL-A, CpG, resiquimod, poly I:C etc. have been investigated in the development of particulate vaccines [4]. Antigen and adjuvant can be encapsulated, adsorbed, or conjugated to NPs. Sarti el al. demonstrated induction of IgA titers via co-delivery of encapsulated mono-phosphoryl lipid-A (MPL-A) and ovalbumin (ova) through PLGA particles [21]. Particle conjugated CpG and ova have induced $CD8^+$ effector as well as memory T cells in mice [22].

In this study, we have designed a PRINT® NP sub-unit vaccine to deliver a MHC-I epitope (SIINFEKL) of ovalbumin and a TLR-9 agonist, CpG oligonucleotide (ODN). PRINT offers the ability to mold biocompatible nanoparticles with complete control over particle size, shape and chemical composition in a manner heretofore not possible with other particle technologies. High aspect ratio (80 × 80 × 320 nm, aspect ratio = 4) particles were chosen since the rod-shape emulates known pathogens [23] and increased aspect ratio is known to enhance cellular uptake [24]. The antigenic peptide (CSIINFEKL) and adjuvant (CpG ODN) were surface conjugated to NPs through reduction sensitive linkers, taking of the intracellular reducing environment to trigger their release. Two cleavable linkers were investigated, a short SPDP (succinimidyl 3-(2-pyridyldithio) propionate linker, and long NHS-PEG(2k)-OPSS linker. SPDP has been widely used to conjugate amine groups to thiol groups for intracellular delivery of siRNA-polymer conjugates [25, 26], aptamer toxins, aptamer virus capsid conjugates [27, 28], delivery of siRNA or DNA NPs [29-32], or delivery of model antigen ovalbumin via NPs [33-35]. Though, the NHS-PEG-OPSS linker has not been used as extensively in the literature, there is much evidence to the support the hypothesis that linker length is important. For example, Chen

et al showed higher immunostimulatory response gold labeled CpG ODN by increasing the proximity of CpG ODN to gold nanoparticles [36]. Furthermore, Singh et al was able to demonstrate the effect of linker length on gene silencing efficiency of siRNA conjugated to quantum dots [37]. We therefore hypothesized that linker length would play a significant role in the accessibility of bio-molecules to their appropriate receptors. Our work demonstrates the significant role that linker length plays in the development of particulate based sub-unit vaccines. Herein we report the formulation of highly uniform and monodisperse hydrogel PRINT NPs co-conjugated with SIINFEKL and CpG, that are successfully taken up and processed by BMDCs, resulting in their efficient maturation and leading to SIINFEKL cross-presentation and subsequent induction of potent antigen-specific T cell proliferation and cytotoxic activity.

3.2. Materials and Methods

3.2.1. Materials

Poly (ethylene glycol) diacrylate (M_n 700) ($PEG_{700}DA$), 2-aminoethyl methacrylate hydrochloride (AEM), diphenyl (2, 4, 6-trimethylbenzoyl)-phosphine oxide (TPO), thiol modified CpG 1826 (C6-S-S-C6-tccatgacgttcctgacgtt), dithiothreitol (DTT), sucrose and DNAse, RNAse free sterile water were purchased from Sigma-Aldrich. Tetraethylene glycol monoacrylate (HP_4A) was synthesized in house. Cysteine modified OVA257-264 (CSIINFEKL) were purchased from Peptide 2.0. Trifluoroacetic acid, methanol, dimethyl sulfoxide (DMSO), PTFE (polytetrafluoroethylene) syringe filters (13-mm membrane, 0.22-µm pore size), HPLC grade water and acetonitrile were obtained from Fisher Scientific. Conventional filters (2-µm) were purchased from Agilent Technologies, and polyvinyl alcohol (Mw 2000) (PVOH) was purchased from Acros Organics. (N-Succinimidyl 3-(2-pyridyldithio)-propionate (SPDP) was purchased from Thermo Scientific. Ortho-Pyridyldisulfide-PEG-N-Hydroxylsuccinimide ester (NHS-PEG (2k)-OPSS) was purchased from Creative PEGworks. PRINT molds (80 nm × 320 nm) were obtained from Liquidia Technologies. DNA grade NAP-10 columns were purchased

from GE Healthcare. RPMI1640 medium, penicillin and streptomycin, L-glutamine, fetal bovine serum (FBS) were all from Life Technologies.

3.2.2. Methods

3.2.2.1. PRINT nanoparticle fabrication

The PRINT particle fabrication process is described previously [38]. Briefly, the pre-particle solution was prepared by dissolving 3.5 weight percent (wt %) of the various reactive monomers in isopropyl alcohol (IPA). The reactive monomers included: a cure-site monomer (an oligomeric PEG with a nominal molar mass of 700 g/mol terminally functionalized on both end groups with an acryl or acryloxy functionality); a hydrophilic monomer used to make up the majority of the particle composition (tetraethylene glycol monoacrylae, HP4A); an amine containing monomer (aminoethyl methacrylate, AEM) which provides chemical handle to conjugate various linkers and peptides; and a photoinitiator, TPO. Pre-particle solution was composed of 69 wt% HP_4A, 10 wt% $PEG_{700}DA$, 20 wt% AEM, and 1 wt% TPO. Using # 3 mayer rod, a thin film of pre-particle solution was drawn on to corona-treated PET using roll-to-roll lab line (Liquidia Technologies) running at 12 feet per minute. The solvent was evaporated by heat guns. Then 80X80X320 nm, cylinder shaped mold was laminated to delivery sheet and passed through nip (80 psi, 12 feet per minute). After delamination, filled mold were cured by passing through UV LED lamp (λmax =395 nm, 30 psi N_2, 12 feet per minute; Phoseon). Due to UV light initiated radical chain polymerization, monomers cross-linked into polymers to form a hydrogel. After cross-linking the hydrogels inside the mold cavities, filled mold was laminated against PVA harvesting sheet and passed through heated nip (140°C, 80 psi, 12 feet per minute). Particles were removed from mold by splitting the harvesting sheet from the mold. Particles were then harvested by dissolving sacrificial harvesting layer of PVA into water (2 ml of water per 10 feet of harvesting sheet). Particle suspensions were passed through 2 μm filter to remove additional scum layer. To remove excess of PVA, particles were spun down at 14,000 rpm (Eppendorf

Thermomixer R) for 25 minutes, and resuspended into sterile water. This purification procedure was repeated 3 times.

3.2.2.2. Thermogravimetric analysis

Concentrations of particles were determined by thermogravimetric analysis (TGA) using a TA Instrument's Discovery TGA. Aluminum sample pans were tarred before loading the sample. 20 μL of the stock nanoparticle solution were loaded on to the pan. Samples suspended in water were heated at 30 °C/min to 130 °C, followed by a 10 minute isotherm at 130 °C. All samples were then cooled at 30 °C/min to 30 °C, followed by a 2 minute isotherm at 30 °C.

3.2.2.3. Scanning electron microscopy

Particles were visualized by scanning electron microscopy (SEM) using a Hitachi S-4700 SEM. Prior to imaging, SEM samples were coated with 1.5 nm of gold-palladium alloy using a Cressington 108 auto sputter coater.

3.2.2.4. Dynamic light scattering

Particle size and zeta potential (ZP) were measured in sterile water by dynamic light scattering (DLS) on a Zetasizer Nano ZS (Malvern Instruments, Ltd.).

3.2.2.5. Conjugation of linker to NPs

We utilized amine groups from AEM to conjugate cleavable linkers, SPDP and NHS-PEG(2k)OPSS. Theoretical numbers of –NH2 groups contributed from 1 mg of nanoparticles suspension were calculated. Different molar ratios linker to amine groups (such as 0.28, 0.55 and 2.30) were evaluated for the conjugation scheme (Table S1). For the optimized reaction scheme, particles were reacted with a 0.55 times molar excess of linker, resulting in reacting 1 mg of NPs with 0.24 mg of SPDP or 6 mg of NHS-PEG-OPSS in 1 ml of 1X PBS + 0.1% PVA for 2 hours. SPDP (or NHS-PEG(2k)OPSS) was dissolved in DMF. Volume of DMF kept constant at 160 μL regardless of different linker mass used. Total volume of reaction was 1 mL. NPs were continuously agitated for 2 hours at 1400 rpm (Eppendorf Thermomixer R). After 2 hours, unconjugated linker was removed from the, pyridyldithiol decorated NPs via 2 centrifugation

washes (Eppendorf Centrifuge 5417g) with sterile water. Efficiency of linker conjugation was evaluated by incubating 1 mg of NPs in 1 mL of DTT solution. Moles of DTT used was 10 times higher than the moles of linkers added during conjugation procedure. Due to disulfide exchange reaction, pyridine 2 thione is released from pyridyldithiol modified NPs, which can be detected by reading absorbance at 343 nm using Spectra Max M plate reader. Conjugation efficiency was determined by the following formula:

% Conjugation efficiency = (Amount of linker conjugated) X 100 / (Amount of linker charged).....(1)

Conjugation efficiency of linkers were between 50-60%.

3.2.2.6. Conjugation of CSIINFEKL to NPs

Once NPs were modified with SPDP or NHS-PEG(2k)OPSS, they were spun down for 25 mins at 14,000 rpm (Eppendorf Centrifuge 5417g) and resuspended into 800 μL of sterile water. 1 mg/ml of cysteine labeled SIINFEKL (CSIINFEKL) solution was made in sterile water. 200 μL of this solution was mixed with 800 μL of NPs suspension and incubated overnight. NPs were continuously agitated at 1400 rpm (Eppendorf Thermomixer R). The following day, NPs were spun down for 25 mins at 14,000 rpm (Eppendorf Centrifuge 5417g), supernatant was collected and NPs resuspended in 1 mL of sterile water. To remove unbound peptide, NPs were washed in sterile water for 2 times. Due to disulfide exchange with cysteine labelled peptide, pyridine 2 thione is released from pyridyl dithiol modified NPs. By reading the absorption of pyridine 2 thione in the supernatant at 343 nm using Spectra Max M plate reader, the amount of pyridine 2 thione released from NPs can be calculated and thus amount of peptide conjugated was evaluated. Conjugation efficiency of peptide was evaluated as mentioned by equation 1. We found 60-70% conjugation efficiency of peptide to NPs.

3.2.2.7. Reduction and purification of C6 S-S- C6 CpG 1826

CpG 1826 with phosphorothioate backbone was chosen because of slower *in vivo* degradation via nucleases as compared to CpG with phosphodiester [39]. C6 S-S- C6 CpG 1826 was reduced

with 100 mM DTT solution in sodium phosphate buffer of pH 8.0 and purified by gel filtration chromatography using Sephadex NAP-10 column. Unreduced CpG was kept for an hour in presence of 100 mM DTT solution in sodium phosphate buffer of pH 8.0. Sephadex NAP-10 column (DNA grade) was equilibrated by flowing through 15 mL of sterile water (DNAse, RNAse free). After equilibration, 0.75 mL of sample was loaded to column and allowed to pass through completely. Reduced CpG was eluted by passing through 1.2 mL of water. Concentration of CpG was measured by evaluating absorption at 260 nm by using NanoDrop 2000 Spectrophotometer.

3.2.2.8. Conjugation of thiol-CpG 1826 to NPs

Once NPs were modified with SPDP or NHS-PEG(2k)OPSS, NPs were spun down for 25 mins at 14,000 rpm (Eppendorf Centrifuge 5417g) and resuspended into 800 μL of sterile water. 40 μg of thiol CpG 1826 was mixed with 1 mg of linker modified NPs and kept for 8 to 10 hours. Total volume of reaction was 1 mL. NPs were continuously agitated at 1400 rpm (Eppendorf Thermomixer R). Then NPs were spun down for 25 mins at 14,000 rpm (Eppendorf Centrifuge 5417g) and resuspended into 200 μL of 10X PBS. This washing procedure was repeated 3 times to remove adsorbed CpG. To evaluate conjugation of CpG, NPs were incubated in 100 mM DTT for 4 hours. NPs were spun down and supernatant was collected. Conjugation efficiency of CpG was evaluated as mentioned by equation 1. Evaluation of CpG was done by reading absorption at 260nm using NanoDrop 2000 spectrophotometer. We found 70-80% conjugation efficiency of CpG to NPs.

3.2.2.9. Co-conjugation of CSIINFEKL and CpG ODN to NPs

CSIINFEKL peptide and CpG were co-conjugated in 2 step process. For co-conjugation process we used 0.39 mg of SPDP or 12 mg of NHS-PEG(2k)OPSS. After modified with linkers, NPs were conjugated to CSIINFEKL by incubating 1 mg of NPs with 0.2 mg of CSIINFEKL. Unbound peptides were removed by washing NPs in sterile water for 2 times. After the final wash nanoparticles were resuspended in 900 mL of sterile water and 0.04 mg of reduced CpG was

added and left to react for 8-10 hours at 1400 rpm (Eppendorf Thermomix R). After co-conjugation, to evaluate peptide and adjuvant loading, CSIINFEKL and CpG were cleaved from NPs by incubating 1 mg of NPs with 100 mM DTT for 4 hours. After 4 hours, nanoparticles were spun down at 14,000 rpm (Eppendorf Centrifuge 5417g) for 25 mins, and the supernatant was evaluated for released peptide and adjuvant through HPLC Agilent 1200 Series and NanoDrop 2000 spectrophotometer, respectively. Co-conjugation of adjuvant resulted in a reduction of final peptide loading to 50% conjugation efficiency, while CpG loading remained at approximately 50-60% conjugation efficiency.

3.2.2.10. Peptide evaluation via HPLC

Reverse phase high performance liquid chromatography (HPLC) was run on an Agilent1200 series HPLC system using an Agilent C18 column. A Waters 2695 Alliance module equipped with quaternary pump, mobile phase degasser, temperature controlled auto sampler and column thermostat were used for HPLC analysis. The separation was carried out on a zorbax C18(2) column (150mm×4.6mm i.d., 3µm particle size, 100Å pore size) from Phenomenex (Torrance, CA) at column temperature of 50 ^{o}C and sample temperature of 50 ^{o}C. Peptide was eluted using mobile phase gradient, which consist of two solution. Solution A- Water (0.1% TFA-Triflouroacetic acid) and B- Acetonitrile with 0.1% TFA. Gradient method is shown in table-3.1.

Table-3.1: Gradient method for HPLC run

Min	% of Mobile Phase A	% of Mobile Phase B	Flow rate (ml/min)
0	100	0	2
5	100	0	2
25	5	95	2
28	5	95	2
30	100	0	2

Binary linear gradients starting from a mixture of 100% A and 0% B from 0 min to 5 min. From 5 min to 25 min B was increased gradually from 0% to 95%. Then, till 28 mins gradient was kept 5% for A and 95% for B. The mobile phase composition was then changed back to initial solvent

mixture and the column was equilibrated for 2 min before every subsequent run. The flow rate of the mobile phase was set to 2.0 mL/min. The samples for HPLC injections were prepared by cleaving off peptide in 100mM DTT in sterile water. Peptides were detected via UV-VIS detector at 210 nm and concentration was determined by comparing area of peak with standard curve. Know amount of peptides were dissolved with 100mM DTT in sterile water to prepare standard curve.

3.2.2.11. Animals

Female C57BL/6 mice and OT-I TCR transgenic mice were purchased from Jackson Laboratory and used at age 6–12 weeks. All experiments involving mice were carried out in accordance with an animal use protocol approved by the University of North Carolina Animal Care and Use Committee.

3.2.2.12. Preparation of single cell culture from mouse spleens

Spleens were harvested from euthanized mice aseptically. Individual spleens were mechanically dissociated with back of the sterile syringe plunger through 100um cell strainer into RPMI 1640 medium. Red blood cells were lysed by ACK buffer. Cells were then resuspended in R-10 medium (RPMI 1640 medium supplemented with 10% FBS, 10 U/ml penicillin and 10 μg/ml streptomycin, 2mM L-Glutamine) and filtered through 70μm cell strainer to remove any residual tissue fragments.

3.2.2.13. Preparation of BMDCs

Bone marrow was collected from mouse femurs and tibias as reported [40]. Erythrocytes were lysed by ACK lysis buffer (Lonza). Bone marrow cells were then cultured at $2x10^6$/ml in R10 supplemented with 50 μM 2-mercaptoethanol, 10 ng/ml each of IL-4 and granulocyte–macrophage-colony stimulating factor (GM-CSF). The culture was replenished with fresh medium on day 3 without removing old medium. On day 6 or 7, BMDCs were harvested and purified with Opti-Prep density medium (Sigma) to remove dead cells.

3.2.2.14. Antigen presentation assay in BMDCs

To evaluate the effect of linker length on antigen presentation, Day 6 BMDCs (3×10^5 cells) were either untreated or treated with blank hydrogels (with and without linkers), CSIINFEKL (5 μg/ml), CSIINFEKL conjugated to PEG hydrogels via SPDP (short cleavable linker, 5 μg/ml) or CSIINFEKL conjugated to PEG hydrogels via PEG (2k) OPSS (longer cleavable linker 5ug/ml) for 4 hours. After four hour incubation, cells were either washed with PBS of pH~7.4 or citrate-phosphate buffer (pH3.0) for 3 minutes on ice to strip off the MHC-I-peptide complex or NP-peptide/H-2K^b complex from cell surface. Additionally, cells were re-incubated at 37^{o}C for an additional 20 hours post-washes and then stained with CD11c-APC and 25-D1.16-PE (anti-SIINFEKL/H-2K^b complex) antibodies (eBioscience), followed by flow cytometry analysis on Cyan ADP (Dako).

3.2.2.15. *In vitro* T cell proliferation assay

In vitro CD8$^+$ T cell proliferation was done as previously reported [41]. Briefly, day 6 BMDCs were dosed with the samples described ablove for 24 h at 37°C. OT-I CD8$^+$ T cells were isolated from OT-I mouse spleens using CD8α$^+$ T cell Isolation Kit (Miltenyi Biotec) as per manufacturer's instructions and labeled with CFSE (5 μM) in PBS with 0.1% FBS for 10 min at 37°C. BMDCs were then incubate with OT-I-CFSE cells in R-10 medium for 72 h at 37°C. After incubation, cells were stained with CD8 and Vα2 antibodies. Division of OT-I cells as indicated by dilution of CFSE fluorescence in T cells was examined by flow cytometry.

3.2.2.16 BMDC maturation assay

Day 6 BMDCs were treated with samples for 24 h at 370C. Cells were washed and stained with CD40-APC, CD80-FITC and MHC II-eFluor450 (ebioscience), then analyzed by flow cytometry.

3.2.2.17. Immunization Study

All formulations were prepared using low endotoxin grade reagents. To confirm the low endotoxin content of vaccines, formulations were routinely tested for endotoxin content using Pierce LAL Chromogenic Endotoxin Quantitation Kit following instructions. All formulations were prepared 24 hours before injections, resuspended in an isotonic 9.25% sucrose, and

subcutaneously administered in the right flank. SIINFEKL was given at a dose of 100 μg and CpG was injected at a dose of 20 μg. On day 7, mice were sacrificed, spleen and draining lymph nodes were harvested. All studies were repeated twice and each experimental arm contained 4-6 mice.

3.2.2.18. ELISPOT assay

Frequency of antigen specific IFN-γ producing T cells in spleen was evaluated using IFN-γ ELISPOT kit (BD Biosciences). Immobilon-P hydrophobic PVDF plates (Millipore) were briefly treated with 35% ethanol, washed 2 times with PBS and coated overnight with anti-mouse IFN-γ antibody at 4°C. The following day, plates were blocked with 200μl R-10 medium with for 2hrs at room temperature (RT). 100,000 splenocytes in R-10 medium were plated in each well, with or without restimulation with 10 μg/ml of SIINFEKL peptide overnight at 37°C. Spots were then developed following manufacturer's instructions.

3.2.2.19. *In vivo* CTL assay

In vivo CTL assay was performed as previously reported [42]. Briefly, OT-I T cells were isolated from spleen using CD8α$^+$ T cell Isolation Kit (Miltenyi Biotec). C57BL/6 mice were injected intravenously with 10,000 OT-I T cells on day -1. On day 0, mice were either untreated or immunized subcutaneously with a mixture of soluble SIINFEKL and CpG ODN, or NPs-SPDP-CSIINFEKL-CpG, or NPs-PEG(2k)OPSS-CSIINFEKL-CpG. Fifteen days after vaccination, mice were intravenously injected with 5×10^6 splenocytes as target cells. To prepare target cells, splenocytes from wild type C57BL/6 mice were pulsed with SIINFEKL peptide at 1μg/ml in PBS for 1 h at 37C, washed with PBS, and labelled with CSFE at 4 μM in PBS for 10 min at 37°C ($CFSE^{hi}$); or non-peptide pulsed cells were labeled with CSFE at 0.4 μM in PBS for 1 h at 37°C ($CFSE^{lo}$). $CFSE^{hi}$ and $CFSE^{lo}$ cells were mixed at 1:1 ratio to generate target cells for i.v. injections. On day sixteen, mice were euthanized, splenocytes were isolated and cells were stained with anti-CD8 and Vα2 antibodies. Percentage of $CFSE^{hi}$ and $CFSE^{lo}$ were determined with a flow cytometer. The ratio of unpulsed to pulsed target cells in the naïve (unimmunized)

mice defined the 0% lysis level. The percent-specific lysis is determined by loss of the antigen-pulsed $CFSE^{hi}$ population compared with the unpulsed $CFSE^{lo}$ control population using the formula: [1– (ratio in naive mouse/ratio in experimental mouse)] × 100.

3.3. Results

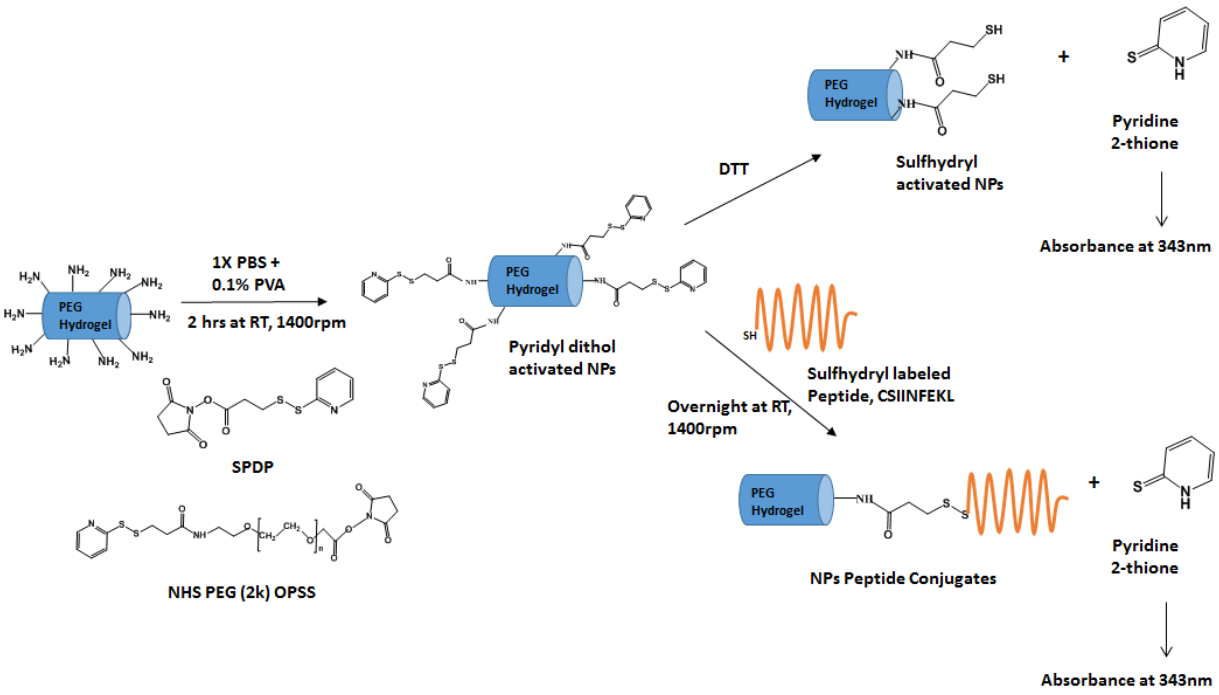

Figure-3.1: Conjugation of cleavable linkers and cysteine labelled SIINFEKL to PEG hydrogels.
PEG hydrogels were first modified with cleavable linkers SPDP or NHS-PEG(2k)-OPSS. NP-linker conjugation was evaluted through the release of pyridine 2-thione after incubation of NPs with DTT. Linker modified particles were incubated with CSIINFEKL, and peptide conjugation was evaluated through the release of pyrigine 2-thione.

3.3.1. Conjugation of CSIINFEKL and CpG to NPs

Pathogen inspired cylinder shaped (80×80×320 nm) cationic PEG hydrogel NPs were fabricated by PRINT® process. It has been established that particles with a net positive charge bind to the negatively charged plasma memberane of the cell surface, thus increasing cellular uptake, as well as enhance endosomal escape of cargos [43]. Our previous work demonstrated that cationic hydrogel particles were able to efficiently deliver siRNA to cytosol, resulting in efficient gene silencing [44, 45]. Furthermore, Fromen et al. demonstrated significanlty higher lung and systemic antibody titers when cationic particles were used to deliver ovalbumin, as compared to anionic particles [46]. Therefore, amine groups on NP surface were used to conjugate cysteine labelled SIINFEKL peptide via reduction sensitive, heterobifunctional linkers- SPDP or NHS-PEG(2k)OPSS in a two step-process (Figure 3.1). First, the succinimidyl

ester of the linker was reacted to the amine groups on the particle, forming an amide bond. The excess linker was then removed via centrifugation washes, followed by reacting the cysteine labeled adjuvant with the pyridine disulfide ring. Linker density was controlled by varying the

Table-3.2: Physical Characterization of nanoparticles conjugated to SPDP.

mg of SPDP loaded	ratio of linker to -NH2 sites	mg of SPDP conjugated	% of NH-2 conjugated	%Conjugation Efficiency	Size (nm)	PDI	ZP (mV)
0.12	0.28	0.10	23.00	83.33	269±8	0.04±0.03	36±5
0.24	0.55	0.19	43.70	79.17	240±5	0.05±0.01	38±1
1	2.30	0.47	108.11	47.16	251±15	0.115±0.023	-21± 2

linker-to-NP ratio (Table 3.2), in an effort to determine maximum linker density while maintaining the positive charge of the nanoparticles. Thus during mono- or dual conjugation of antigenic peptide and CpG, we aimed to keep the overall charge of NPs positive (as indicated by zeta potential) to facilitate better uptake by APCs and to get possible endosomal escape of cargos. As shown in Table S1, as the amount of SPDP charged to the nanoparticle increased from 0.12 mg to 1 mg, the conjugated amount of linker increased; however, conjugation efficiency decreased. At the highest level of SPDP charged, the ZP of NPs became negative (-21± 2 mV) indicating almost complete conversion of amine groups and therefore eliminating this formulation from further development. The amount of SPDP and NHS-PEG(2k)OPSS used for single component conjugation (either peptide or CpG) to modify 1 mg of NPs was 0.24 mg and 6 mg, respectively, which resulted in positively charge particles.

Particles modified with each linker were then incubated overnight with CSIINFEKL in sterile water, resulting in peptide conjugation to the NPs via disulfide exchange. Followed by incubation with thiol-containing CpG (Figure 3.1). For co-conjugation reactions, conjugation efficiency for peptide and CpG was around 50% and 50-60%, respectively.

Following peptide and CpG modification, NPs remained highly uniform in size and shape as visualized by SEM (Figure 3.2). For all formulations the ZP remained greater than +25 mV (Table 3.3) which is desirable for cytosol delivery of antigens into MHC class I presentation pathway. Polydispersity index (PDI) of all sets of nanoparticles was found to be <0.1 which indicates monodisperse nanoparticles with homogenous distribution, and size ranged from 250-280 depending on the surface modification.

Table-3.3: Physical Characterization of PEG hydrogel sub-unit vaccine. (For all formulations, n=4)

Formulations	Size (nm)	PDI	ZP (mV)	mg of linker/mg NP	mg CSIINFEKL/mg NP	mg of CpG ODN / mg of NPs
NPs (Blank)	274 ± 7	0.05 ± 0.01	38 ± 2	N/A	N/A	N/A
NPs-SPDP	259 ± 20	0.05 ± 0.02	36 ± 4	0.1 ± 0.003 to 0.48 ± 0.040	N/A	N/A
NPs-PEG	278 ± 9	0.04 ± 0.03	37 ± 1	0.283 ± 0.016	N/A	N/A
NPs-SPDP-CSIINFEKL	260 ± 15	0.04 ± 0.01	38 ± 2	N/A	0.093 ± 0.01	N/A
NPs-PEG-CSIINFEKL	271 ± 4	0.04 ± 0.01	34 ± 2	N/A	0.08 ± 0.001	N/A
NPs-SPDP-CpG	238 ± 5	0.03 ± 0.01	35 ± 2	N/A	N/A	0.050 ± 0.005
NPs-PEG- CpG	289 ± 7	0.07 ± 0.02	30 ± 4	N/A	N/A	0.048 ± 0.006
NPs-SPDP-CSIINFEKL-CpG	246 ± 3	0.09 ± 0.02	26 ± 11	N/A	0.082 ± 0.032	0.017 ± 0.007
NPs-PEG-CSIINFEKL-CpG	255 ± 7	0.04 ± 0.02	29 ± 11	N/A	0.071 ± 0.013	0.015 ± 0.003

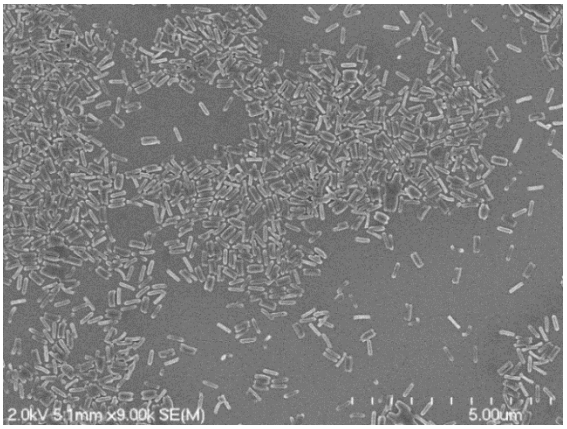

Figure-3.2: Representative SEM image of 80x320 nm PRINT subunit peptide vaccine.

3.3.2. *In vitro* antigen presentation in BMDCs by sub-unit vaccine

In order for vaccines to generate an efficient $CD8^+$ T cell response, DCs must first internalize antigens, process them into 8-12 amino acid peptides and present them to T cell receptors as peptide/MHC-I complexes on cell surface. T cells recognize MHC-I-peptide complex via T cell receptors and in presence of other co-stimulatory signals subsequently proliferate. Since antigen presentation is key to developing an efficient T cell response, the antigen presentation efficiency of our PRINT NP subunit vaccine was evaluated using an *in vitro* assay. 25-D1.16, an antibody that recognizes SIINFEKL/H-$2K^b$ on antigen presenting cells was used to stain BMDCs treated with various samples to quantify antigen cross presentation. As expected, SIINFEKL peptide binds to H-$2K^b$ on the cell surface directly upon 4 hours pulsing, while treatment with blank NP-SPDP or NP-PEG(2k)OPSS and washes with PBS resulted in minimum staining for MHC-I-peptide complex (Figure 3.3A). Interestingly, cells treated with NP-SPDP-CSIINFEKL or NP-PEG(2k)OPSS-CSIINFEKL showed similar surface MHC-I-peptide staining to soluble peptide (Figure 3.3A and Figure 3.3I). The kinetics of NP processing, antigen cleavage, internalization, and MHC-I presentation make it unlikely that the high staining observed with NP-peptides after 4 hours incubation was all due to antigen cross presentation. Instead, the results suggest that SIINFEKL peptide displayed on NPs may bind to MHC class I H-$2K^b$ on the cell surface and form the pMHC complex stainable by 25-D1.16. When unbound peptide or NP-peptide were removed by washes with PBS, followed by another 20 h

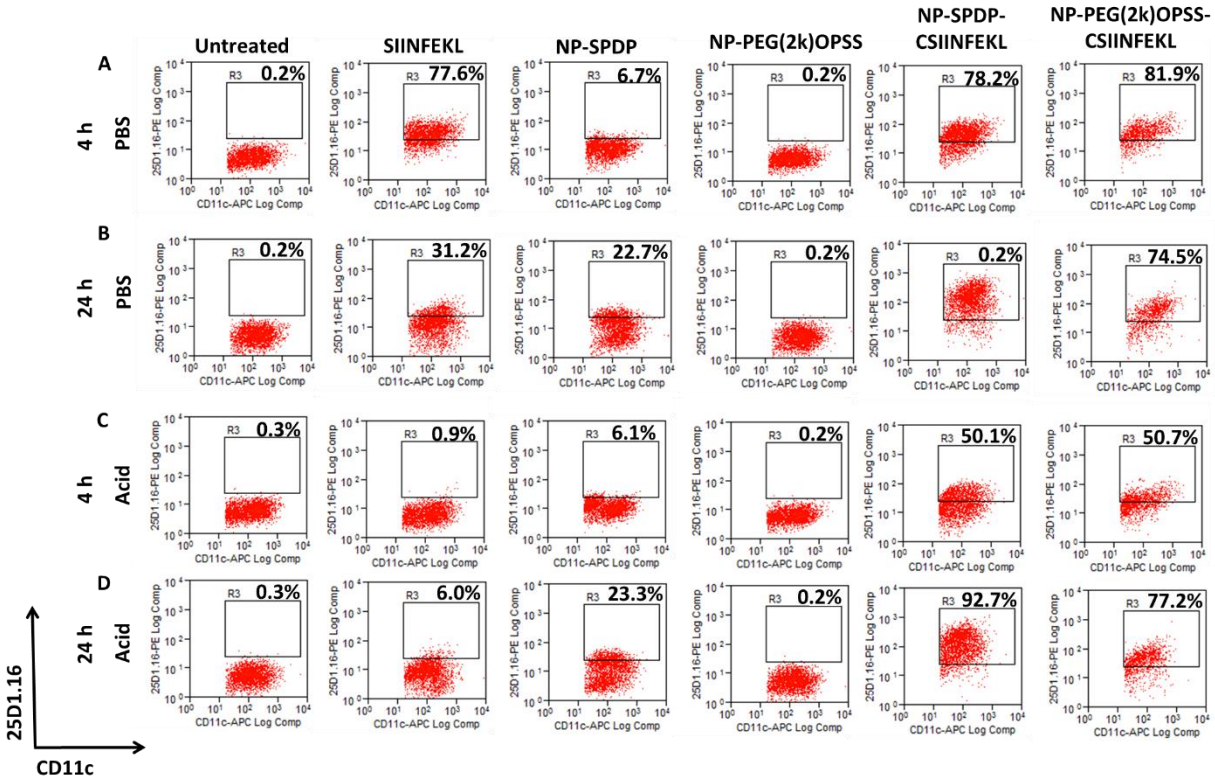
Untreated
SIINFEKL
NP-SPDP
NP-PEG(2k)OPSS
NP-SPDP-CSIINFEKL
NP-PEG(2k)OPSS-CSIINFEKL
A
4 h PBS
B
24 h PBS
C
4 h Acid
D
24 h Acid
R3 0.2%
R3 77.6%
R3 6.7%
R3 0.2%
R3 78.2%
R3 81.9%
R3 0.2%
R3 31.2%
R3 22.7%
R3 0.2%
R3 0.2%
R3 74.5%
R3 0.3%
R3 0.9%
R3 6.1%
R3 0.2%
R3 50.1%
R3 50.7%
R3 0.3%
R3 6.0%
R3 23.3%
R3 0.2%
R3 92.7%
R3 77.2%
25D1.16-PE Log Comp
CD11c-APC Log Comp
25D1.16
CD11c

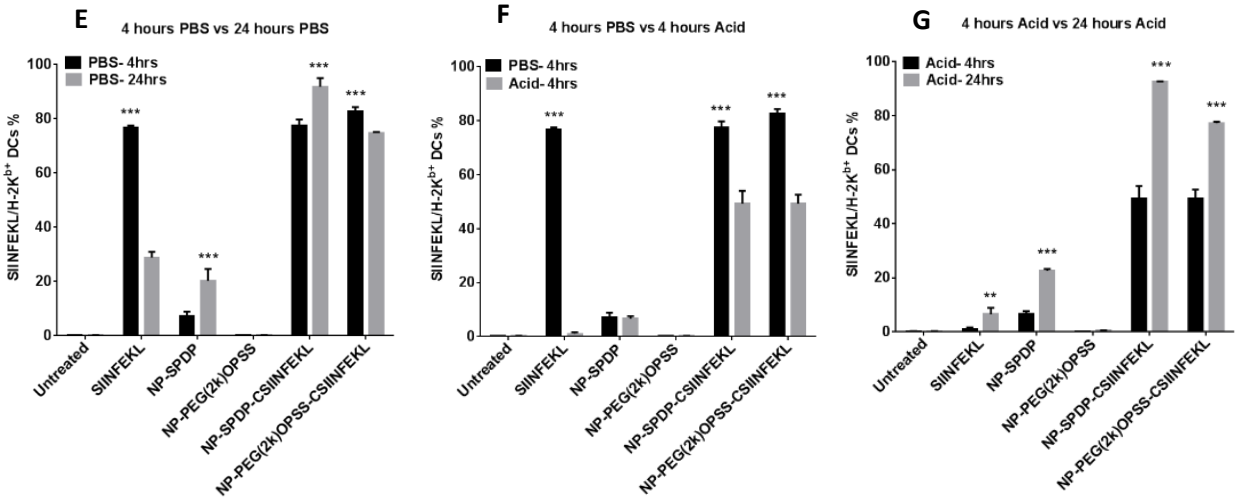
E
4 hours PBS vs 24 hours PBS
PBS- 4hrs
PBS- 24hrs
F
4 hours PBS vs 4 hours Acid
PBS- 4hrs
Acid- 4hrs
G
4 hours Acid vs 24 hours Acid
Acid- 4hrs
Acid- 24hrs
SIINFEKL/H-2K^{b+} DCs %
Untreated
SIINFEKL
NP-SPDP
NP-PEG(2k)OPSS
NP-SPDP-CSIINFEKL
NP-PEG(2k)OPSS-CSIINFEKL

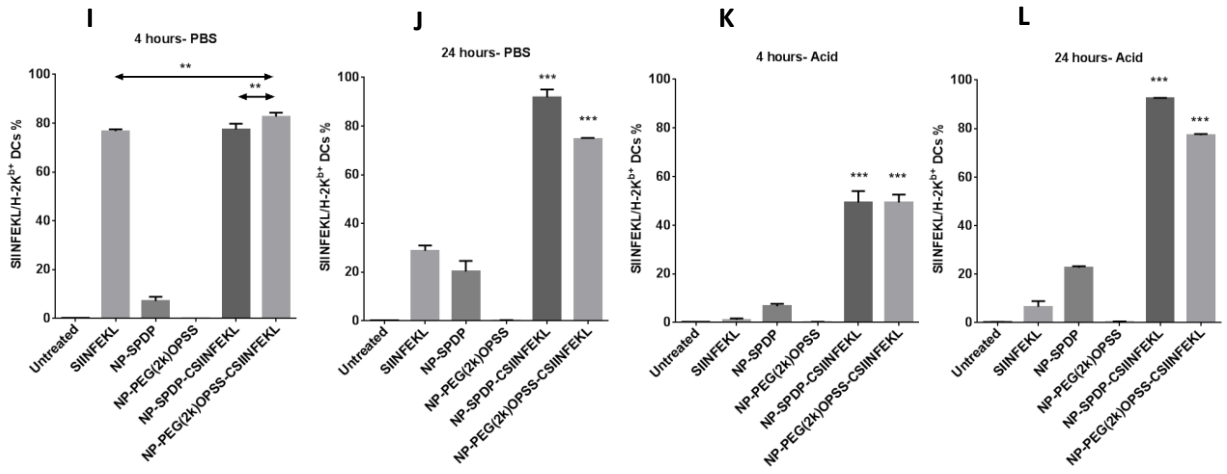

Figure-3.3: Enhanced antigen presentation by NP-peptide in BMDCs.
BMDCs were treated with different formulations for 4 hours and washed with PBS (A), and incubated for another 20 hours (B), or washed with acidic citrate-phosphate buffer (pH3) (C), and incubated for another 20 hours (D). Representative flow cytometry histogram for each group is shown in figure 3.3A to 3.3D. The numbers in the histogram represents the percentage of $CD11c^{+}$ dendritic cells that were positive for p/MHC I. Quantitative analysis of data (E-L). Results are shown as mean ± SD, n=3. E-G, data were analyzed by two-way anova, tukey's post hoc analysis, I-L, data were analyzed by one-way Anova, holm's sidak test, ** $p < 0.01$, *** $p < 0.001$.

culture at 37°C, it was observed that both NP-SPDP-CSIINFEKL and NP-PEG(2k)OPSS-CSIINFEKL led to significantly higher pMHC level than that of soluble peptide pulsed BMDCs (Figure 3.3B, Figure 3.3J). On the other hand, pMHC complexes on soluble peptide pulsed and washed BMDCs decreased over time, suggesting loss of pMHC (Figure 3.3E). These results indicate that NP-conjugation of antigenic peptide not only stabilizes cell surface MHC I through direct binding, but also increase the overall level of cell surface pMHC over time, possibly due to enhanced cell uptake of NP-peptides and more efficient delivery of antigenic peptide into class I presentation pathway.

To further examine the capability of delivering antigenic peptide into cross-presentation pathway by NP-peptide formulations, cells were pulsed with soluble or NP conjugated peptides for 4 hours, and washed with an acidic citrate-phosphate buffer (pH3.0) for 3 minutes to strip off the MHC-I peptide complex from the surface of the BMDCs [47]**.** Cells were then incubated

for another 20 hours at 37°C allowing for internalized antigens to be re-presented onto cell surface. As shown in figure-3.3C, 3.3F citrate-phosphate treatment completely removed SIINFEKL from pMHC complexes for cells treated with soluble SIINFEKL (down to 0.9%), but only partially removed cell bound NP-peptide (down to ~50%) (Figure 3.3K). This result may be due to the increased binding avidity of NP-peptide to cells as a result of multivalent binding of the peptide. As shown in Figure 3.3D, after acidic washes and an additional 20 hour incubation, peptide/MHC I staining for NP-SPDP-CSIINFEKL and NP-PEG(2k)OPSS-CSIINFEKL pulsed cells were 92.7% and 77%, up from around 50% (Figure 3.3G), which was also significantly higher than soluble SIINFEKL (6%) (Figure 3.3L). During the re-incubation period, cells treated with NP conjugated peptide had higher staining of pMHC complex, as compared to cells that did not go through re-incubation period (Figure 3.3G) which indicates higher uptake of NP and cross-presentation of antigenic peptide. In conclusion, the conjugation of peptide to PRINT NPs via cleavable linkers is able to achieve not only higher but also longer lasting cross-presentation of antigenic peptide by BMDCs as compared to soluble peptide.

3.3.3. *In vitro* proliferation of OT-I T cells in BMDCs treated with sub-unit vaccine

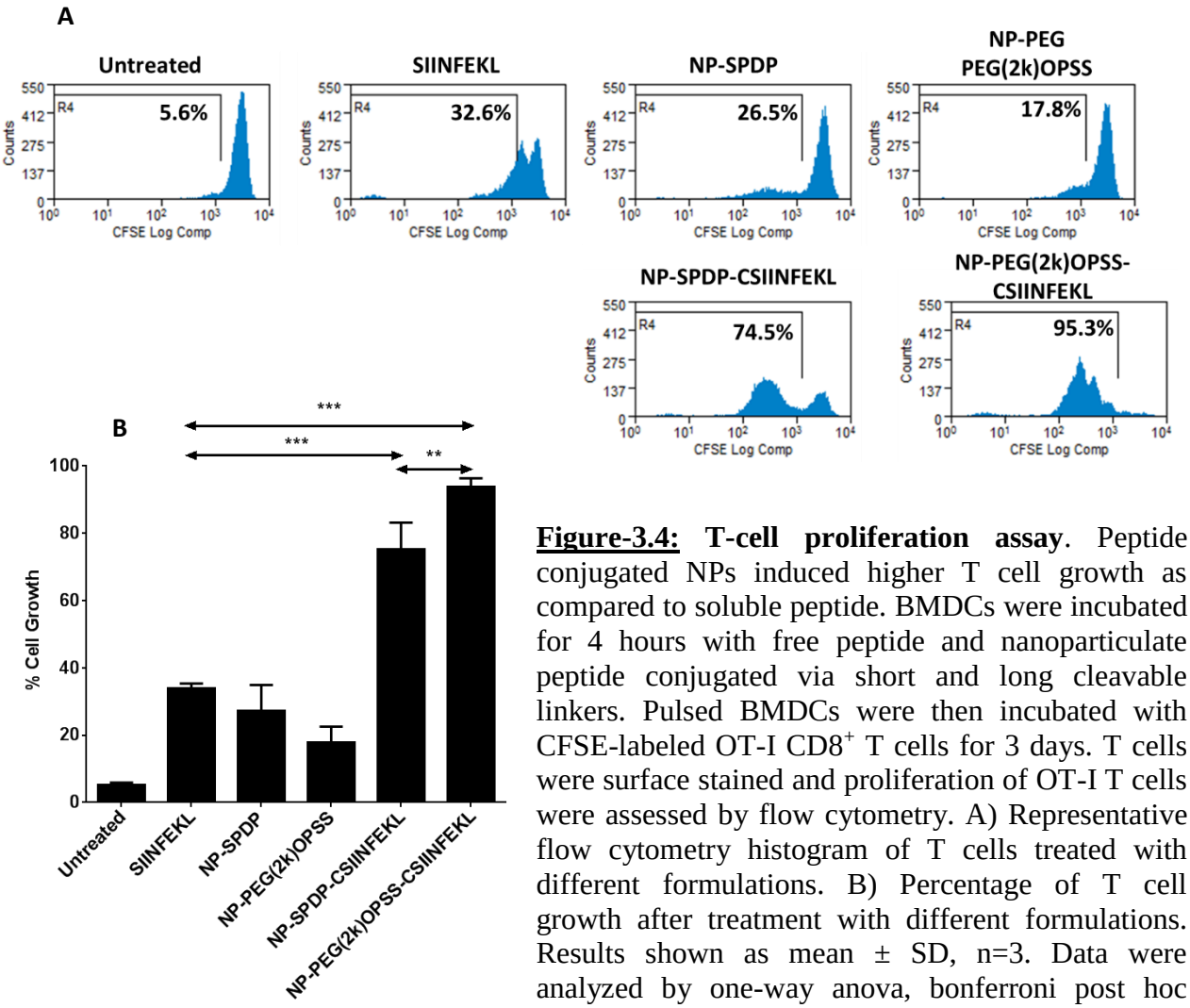

<u>Figure-3.4:</u> T-cell proliferation assay. Peptide conjugated NPs induced higher T cell growth as compared to soluble peptide. BMDCs were incubated for 4 hours with free peptide and nanoparticulate peptide conjugated via short and long cleavable linkers. Pulsed BMDCs were then incubated with CFSE-labeled OT-I $CD8^+$ T cells for 3 days. T cells were surface stained and proliferation of OT-I T cells were assessed by flow cytometry. A) Representative flow cytometry histogram of T cells treated with different formulations. B) Percentage of T cell growth after treatment with different formulations. Results shown as mean ± SD, n=3. Data were analyzed by one-way anova, bonferroni post hoc analysis, ** $p < 0.01$, *** $p < 0.001$.

Next, we evaluated how cross presentation via BMDCs translated into activation and priming of $CD8^+$ T cells. $CD8^+$ T cells derived from OT-I TCR transgenic mice were used to evaluate OVA-specific T cell response for NP and soluble vaccine formulations. In this study, BMDCs, either untreated or treated with soluble SIINFEKL or NP-SIINFEKLNP conjugated peptides were incubated with 5- (and 6-) carboxyfluorescein diacetate succinimidyl ester (CSFE) labelled OT-I T cells for three days. Proliferation of T cells was evaluated by flow cytometry. Representative flow cytometry histogram for each group is shown in figure 3.4A. As shown in

figure 3.4B, BMDCs pulsed with soluble peptide at concentration of 5 μg/ml were able to induce proliferation of cognate $CD8^+$ T cells**.** In comparison, much enhanced T cell proliferation was observed for BMDCs treated with NP conjugated peptide, which indicates higher priming and activation of $CD8^+$ T cells. CSIINFEKL conjugated to PRINT NPs via the longer cleavable linker resulted in approximately 95% of T cell growth, as compared to short cleavable linker (74.5%) and soluble peptide (32.6%). This is consistent with the enhanced antigen presentation by NP-peptide demonstrated above (Figure 3.4B).

3.3.4. Maturation of BMDCs by CpG ODN conjugated PEG hydrogels

It is well known that activation of naïve T cells and development of multiple effector functions depends not only on recognition of MHC-I-peptide complex on APCs by TCRs, but also on a second signal from engagement of co-stimulation receptors. Concurrent delivery of adjuvants have been shown to promote the second signals, further drive clonal expansion of naïve T cells and aid in their differentiation into armed effector T cells.[17] The CD40 ligand and CD28 expressed on T cell surface bind to co-stimulatory molecules CD40 and CD80 on the surface of DCs, respectively. CD40 provides signals for activation, while CD80 provides signals for proliferation. The ability of PRINT NPs to deliver CpG ODN to provide co-stimulatory signals were tested in BMDCs. BMDCs were incubated with soluble CpG ODN or NP-CpG for 18 hours. After incubation, cells were analyzed for expression of CD80 and CD40 via flow

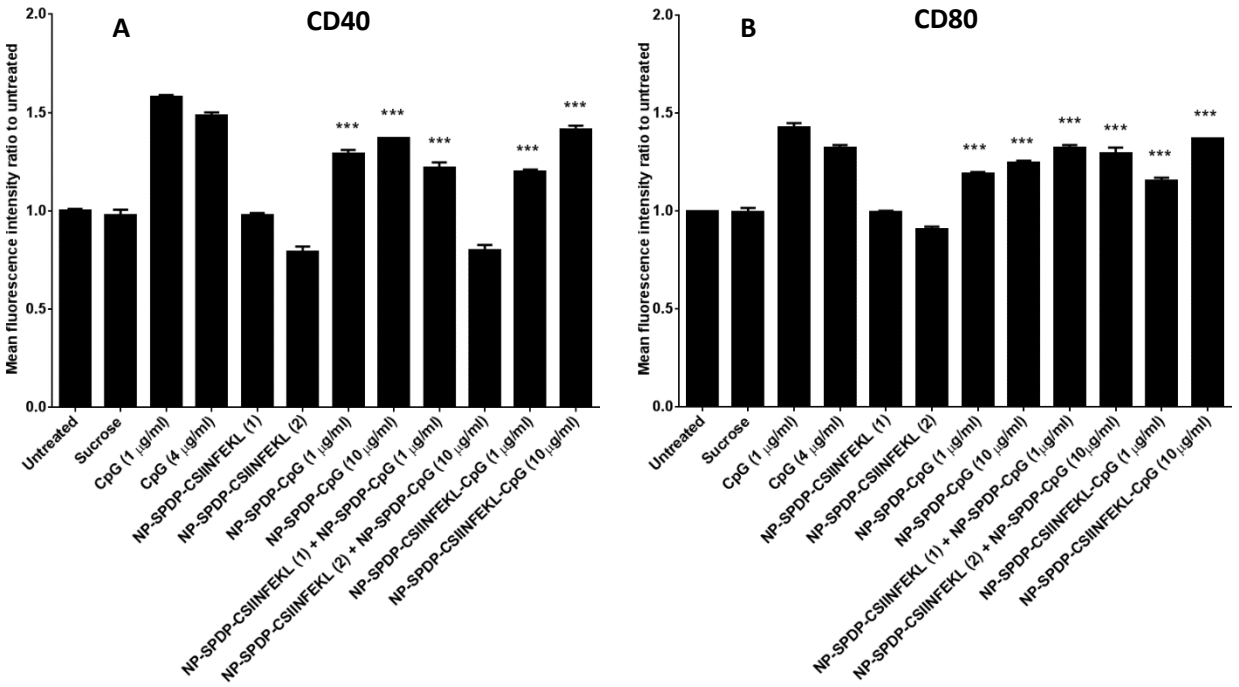

Figure-3.5: Up-regulation of maturation markers by NP-CpG on BMDCs.
BMDCs were treated with various samples for 24 hours with 1, 4 or 10 µg/ml of CpG. Equivalent amount of NPs were dosed in case of NP-peptide. NP-SPDP-CSIINFEKL (1) has equivalent dose of NPs to 1 µg/ml particulate CpG and NP-SPDP-CSIINFEKL (2) has equivalent dose of NPs to 10 µg/ml particulate CpG. The expression of co-stimulatory molecules were detected by flow cytometry analysis of fluorescence labelled CD40 and CD80 antibodies. Ratio of MFI from sample to MFI of untreated is plotted in A) for CD40 and B) for CD80. Results are shown here as mean ± SD, n=3. Data were analyzed by one-way anova, bonferroni post hoc analysis, *** $p < 0.001$.

cytometry. Expressions of co-stimulatory molecules were presented as a ratio of mean fluorescent intensity (MFI) to untreated cells. Treatment with CpG conjugated PRINT NPs at 1 µg/mL or 10 µg/mL concentrations, induced upregulation of CD40 and CD80 on BMDCs as compared to untreated cells, as potently as soluble CpG. Therefore the functionality of CpG is well retained during conjugation to nanoparticles. No upregulation of either marker was found when BMDCs were treated with CSIINFEKL conjugated NPs. Lack of response indicates the limitation of delivering antigen alone for maturation of BMDCs. CD40 and CD80 were both upregulated when CpG ODN were combined with antigenic CSIINFEKL peptide either via co-conjugation of CpG ODN and SIINFEKL on a single NP, or when delivered on separate NPs

(NP-CpG + NP-Peptide), indicating the helper effect of adjuvant in presence of antigen (Figure 3.5A and B).

3.3.5. Induction of IFN-γ producing SIINFEKL specific CD8⁺ T cells in mice

After evaluating the efficiency of antigen presentation and maturation of BMDCs as well as OT-I T cell proliferation, PRINT NP subunit vaccines were analyzed for their efficacy to induce IFN-γ producing antigen specific T cells in mice. Frequency of antigen-specific IFN-γ producing T cells in spleens of mice 7 days post immunization was evaluated *ex vivo* by ELISPOT. First we evaluated whether co-conjugation of antigen and adjuvant are necessary by vaccinating mice with NP-SPDP-CSIINFEKL + NP-SPDP-CpG and NP-SPDP-CSIINFEKL-CpG.

We found that mice treated with NPs co-conjugated to antigenic peptide and CpG induced significantly higher $CD8^+$ T cell response as compared to mice treated with separately conjugated NPs (Figure 3.6). Similar results were also reported by Schlosser et al. when they co-encapsulate TLR ligands- CpG or poly I: C and antigen in the same delivery system [48]. Next we tested both the vaccine formulations for their ability to induce IFN-ϒ producing $CD8^+$ T cells. As shown in figure 3.7A, there is a significant difference in induction of IFN-γ producing $CD8^+$ T cells when mice were immunized with NPs-SPDP-CSIINFEKL-CpG and NPs-PEG(2k)OPSS-CSIINFEKL-CpG as compared to mice receiving a mixture of soluble antigen and adjuvant. Co-conjugation of adjuvant and antigen resulted in 10 times higher induction of IFN-γ producing T cells as compared to NPs conjugated to antigen alone. IFN-γ producing T cells response was minimum in case of negative control-blank PRINT NPs.

Secretion of IFN-γ by antigen-specific $CD8^+$ T cells into culture medium upon restimulation over 3 days was also examined by ELISA. Similar to T cell frequency analysis, the bulk production of IFN-γ was also significantly higher for mice treated with NP formulations with co-conjugated peptide and adjuvant as compared to NP conjugated with just antigen, or

soluble antigen and adjuvant (Figure 3.7B), again confirming the importance of co-delivery of CpG adjuvant for IFN-γ production.

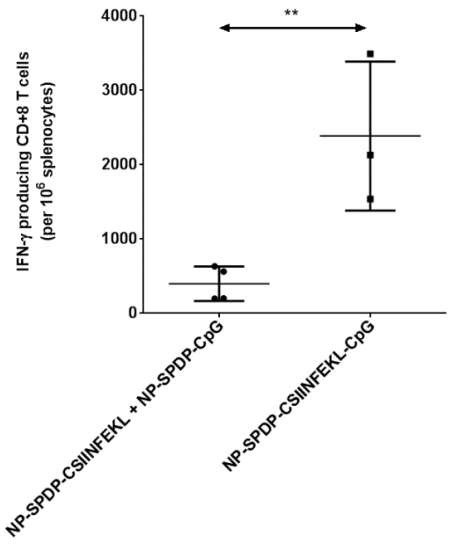

<u>Figure-3.6:</u> Evaluation of IFN-γ producing CD8⁺ T cells: Separate vs co-conjugation of antigen and adjuvant.

Co-conjugation of peptide and CpG ODN has induced higher numbers of IFN-γ producing SIINFEKL specific $CD8^+$ T cells in spleen as compared to separate conjugation**.** Mice were immunized with various samples containing 100 µg peptide and/or 20 µg CpG via s.c injection in left flank. One week later, splenocytes were isolated and re-stimulated with SIINFEKL for 20 h for IFN-γ ELISPOT assay. Results are shown as mean ± SD, n=3-4. Data were analyzed by Student's t-Test** $p < 0.01$.

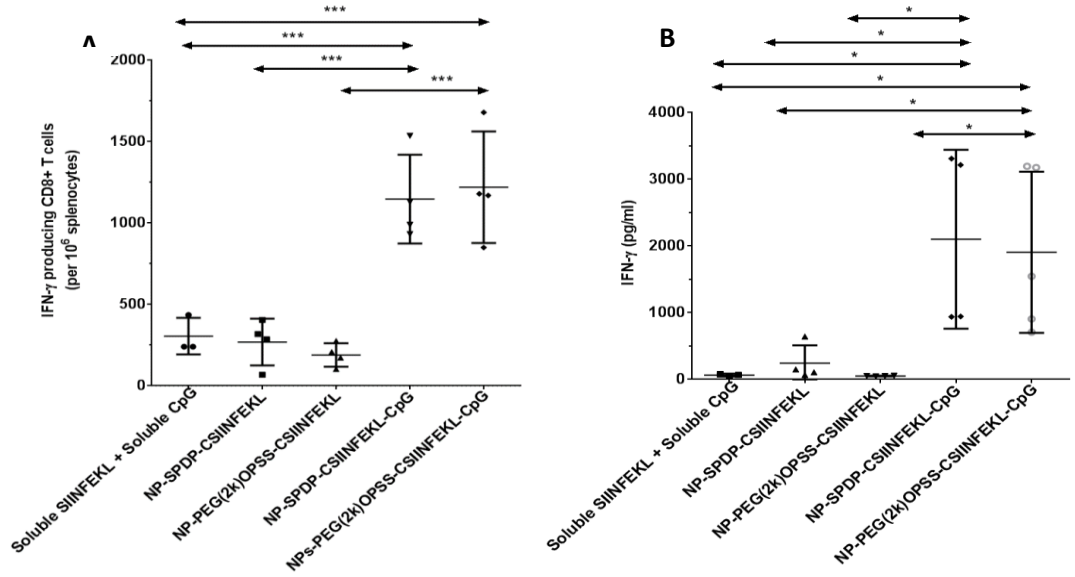

<u>Figure-3.7:</u> Induction of IFN-γ producing SIINFEKL specific $CD8^+$ T cells in spleen.

Mice were immunized with various samples containing 100 µg peptide and/or 20 µg CpG via s.c injection in left flank. One week later, splenocytes were isolated and re-stimulated with SIINFEKL for 20 h for IFN-γ ELISPOT assay (A), or for 72 h for ELISA analysis of secreted IFN-γ in medium (B). Results are shown as mean ± SD, n=4. Data were analyzed by one-way anova, Holm-Sidak's multiple comparison test, *$p < 0.05$, *** $p < 0.001$.

3.3.6. *In vivo* CTL response in mice after immunization with SIINFEKL and CpG co-conjugated NPs

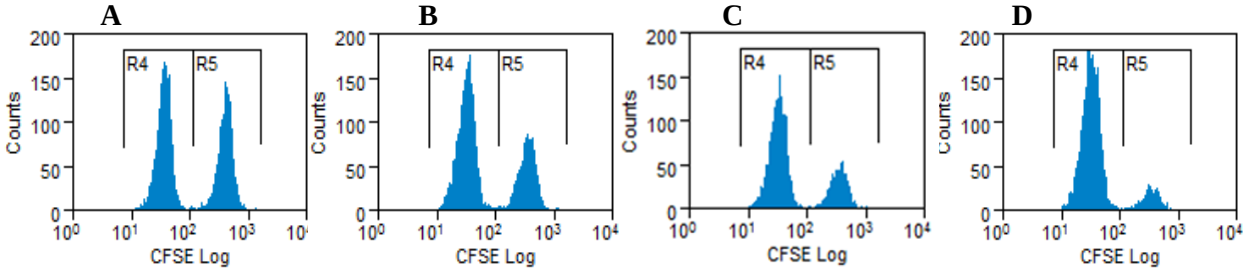

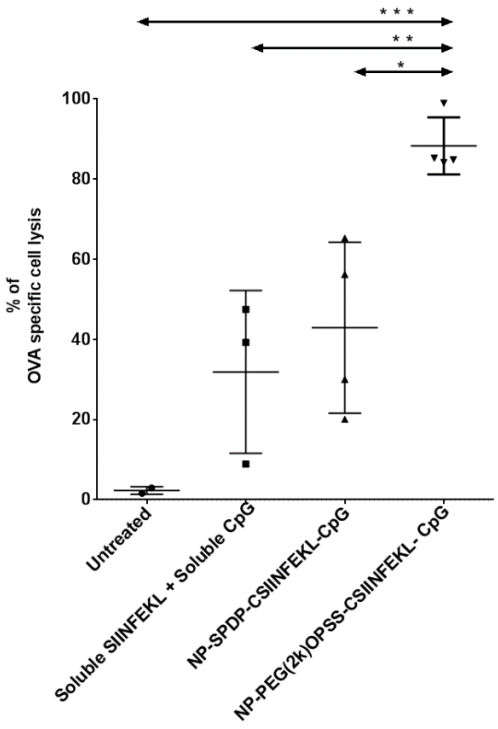

<u>Figure-3.8:</u> *In vivo* CTL response after vaccination with model peptide hydrogel cancer vaccine.
NPs-PEG(2k)OPSS-CSIINFEKL-CpG is more effective at killing target cells compared to NPs-SPDP-CSIINFEKL-CpG. Purified OT-I $CD8^+$ T cells were adoptively transferred into C57BL/6 mice. Two days later, mice were kept a) untreated or immunized with either b) soluble SIINFEKL + soluble CpG or c) NPs-SPDP- CSIINFEKL-CpG or d) NPs-PEG OPSS-CSIINFEKL-CpG. Fifteen days later, CFSE labeled wild type splenocytes (non-peptide pulsed $CFSE^{hi}$ and peptide pulsed $CFSE^{lo}$, 1:1) were i.v. transferred into immunized mice. After twenty hours, splenocytes were isolated and population of target cells was determined by flow cytometry. Representative histogram analysis of untreated (A), soluble SIINFEKL + soluble CpG (B), NPs-SPDP-CSIINFEKL-CpG (C) and NPs-PEG(2k)OPSS-CSIINFEKL-CpG (D). Quantitation of specific lysis from flow cytometry data in A-D (E). Results are shown here as mean ± SD, n=4. Data were analyzed by one-way anova, Holm-Sidak's multiple comparison test, *$p < 0.05$, ** $p < 0.01$, *** $p < 0.001$.

Induction of CTLs is critical in generating an antitumor immune response. We evaluated PRINT NP subunit vaccines for their ability to induce CTLs. through an *in vivo* CTL assay [42].

Fifteen days after immunizations with mixture of soluble SIINFEKL and soluble CpG or NP-SPDP-CSIINFEKL-CpG or NP-PEG(2k)OPSS-CSIINFEKL-CpG, mice were adoptively transferred with SIINFEKL pulsed, $CSFE^{hi}$ and control non-pulsed, $CSFE^{lo}$ target cells. On day sixteen, peptide pulsed and non-pulsed target cells in mouse spleens were differentiated by flow cytometry by two distinct population with high and low CFSE fluorescence (R5 and R4, respectively in Figure 3.8A-D). $CSFE^{hi}$ population was decreased for peptide pulsed cells in mice immunized with a mixture of soluble peptide and soluble CpG (Figure 3.8B), NPs-SPDP-CSIINFEKL-CpG (Figure 3.8C) and NPs-PEG(2k)OPSS-CSIINFEKL-CpG (Figure 3.8D). Moreover, the percentage of OVA specific cell killing was 90% for mice treated with NPs-PEG (2k) OPSS-CSIINFEKL-CpG, which is significantly higher than mice treated with soluble antigen with soluble adjuvant (35%) and NPs-SPDP-CSIINFEKL-CpG ODN (50%) (Figure 3.8E). Results from these assays reveal that the longer linker is more efficient at *in vivo* target cell killing as compared to short linker.

3.4. Discussion

Here we have shown: i) successful co-conjugation via reduction sensitive linkers of model antigenic peptide-SIINFEKL and CpG ODN to hydrogel NPs; ii) delivery of CSIINFEKL via NPs to DCs that induced cross-presentation of SIINFEKL via MHC-I protein molecules and subsequently stimulated *in vitro* proliferation of OT-I T cells; iii) delivery of CpG ODN via NPs provided "adjuvanted" effect by inducing maturation of DCs as demonstrated by upregulation of CD80 and CD40; iv) co-delivery of CSIINFEKL and CpG ODN induced IFN-γ producing robust $CD8^+$ T cells and v) co-delivery of CSIINFEKL and CpG ODN by reduction sensitive hydrogel system elicited potent CTLs that kill antigen specific target cells.

Within last decade PRINT NPs have evolved into a unique delivery platform for various agents such as chemotherapeutics, fluorescent dyes, quantum dots, siRNA and proteins [44, 49-51]. Due to the versatility of the PRINT platform, it has been employed to study the impact of various particle parameters in a biological system such as bio-distribution of intravenously

administered NPs as well as lymphatic trafficking of particles after intramuscular administration [52, 53]. Utilizing immunologically inert materials to mimic size, shape, and surface functionality of pathogens, PRINT provides an excellent platform to engineer subunit vaccines investigating various combinations of antigens and adjuvants to tune the immune response [54]. Galloway et al. showed enhanced humoral response when mice were treated with trivalent influenza protein adsorbed cationic PLGA PRINT particles [55]. In an effort to induce mucosal immune response, Fromen et al. showed higher antibody titers of ovalbumin protein when delivered via intranasal immunization by PRINT hydrogels [46]. Building this platform, the work presented herein is the first PRINT system to induce potent CTL response by co-delivering antigenic peptides and CpG ODN through reduction sensitive linkers.

Disulfide linkers have been widely used in antibody drug-conjugates (ADCs) to allow for release of chemotherapeutic drugs in intracellular reductive environment and delivering antigenic proteins [56]. Eby et al. conjugated ovalbumin to polymeric micelles via pyridyl disulfide. One advantage of this technique is that triggered release of the cargo only happens upon cellular internalization, due to the presence of various reductive enzymes in the endosome, lysosome, and cytosol. Therefore, employing reduction sensitive linkers to conjugate CpG ODN and SIINFEKL to NPs, we were able to deliver CpG, resulting in stimulation of TLR-9 and the triggered release of co-stimulatory molecules to enhance T cell activation, while also delivering SIINFEKL, to be cross-presented to the surface of APCs (vacuolar pathway) [5]. More experimental studies are required to understand the mechanism of NP uptake, trafficking, and antigen release.

Employing peptide antigens has many advantages including enhanced safety, specificity, and stability. Furthermore, synthesizing eight to nine amino acid peptides for MHC-I/ HLA binding domains is uncomplicated and can be readily synthesized in large quantities. Using defined peptide epitopes allows for the generation of very specific arms of effector T cells without the health risk of inducing autoimmune or adverse reactions which may occur in

response to whole protein antigens [57]. Moreover, peptides can be chemically modified to improve their solubility, stability, and antigenicity. In our studies, the cysteine modification added to the peptide for conjugation purposes did not interfere with MHC I binding to SIINFEKL. However, ensuring peptide modification does not alter MHC binding will need to be investigated for each unique application to confirm the appropriate antigen/peptide is being presented [58].

Another important parameter of PRINT hydrogel vaccine design is the positive surface charge provided by AEM in the composition. Cationic formulations enhance NP cellular internalization and endosomal escape thereby delivering cargo in the reductive environment of cytosol [44, 45] . Being able to take advantage of these cellular events should favor antigen cross presentation through the classical pathway. Neumann et al. has also reported inflammasome activation by cationic charged particles alone, which may potentially provide adjuvanticity and contribute to the high potency of our particle vaccines [59, 60]. Additionally, positively charged particles remain trapped at the injection site because of collagen fibers and negatively charged proteins (glycosaminoglycans) of extracellular matrix (ECM) [61]. Our previous study suggested 80×80×320nm cationic particles have minimal lymphatic drainage [53]. Thus our NP vaccines most likely rely on the uptake by tissue resident DCs at the injection site for antigen presentation, such as migratory $CD103^+$ DCs in peripheral tissues, a subset of DCs very potent in antigen cross presentation [5]. These results, uniquely and for the first time, demonstrate the ability to perform well-controlled mechanistic studies to investigate the effect of optimizing particulate vaccine parameters in terms of immune cell targeting, APC uptake/activation, and nanoparticle vaccine efficacy.

3.5. Conclusion

In summary, we have investigated the use of an engineered PEG hydrogel subunit vaccine to harness the power of our own immune system to generate CTLs to validate this approach in the fight against cancer. We have designed and developed a model platform NP sub-

unit vaccine to co-deliver antigenic peptide and CpG ODN. These NPs were successfully internalized and processed by BMDCs, resulting in BMDC maturation, subsequent cross-presentation of antigenic peptide, and induction of potent antigen-specific T cells. Taken together, results from this study provided a highly specific and effective platform to develop vaccines against infectious disease and cancer.

3.6. REFERENCES

[1] R. Rappuoli, C.W. Mandl, S. Black, E. De Gregorio, Vaccines for the twenty-first century society, Nat Rev Immunol, 11 (2011) 865-872.

[2] P.M. Moyle, I. Toth, Modern subunit vaccines: development, components, and research opportunities, ChemMedChem, 8 (2013) 360-376.

[3] M.A. Curran, W. Montalvo, H. Yagita, J.P. Allison, PD-1 and CTLA-4 combination blockade expands infiltrating T cells and reduces regulatory T and myeloid cells within B16 melanoma tumors, Proc Natl Acad Sci U S A, 107 (2010) 4275-4280.

[4] L.A. Brito, D.T. O'Hagan, Designing and building the next generation of improved vaccine adjuvants, J Control Release, 190 (2014) 563-579.

[5] O.P. Joffre, E. Segura, A. Savina, S. Amigorena, Cross-presentation by dendritic cells, Nat Rev Immunol, 12 (2012) 557-569.

[6] J. Neefjes, H. Ovaa, A peptide's perspective on antigen presentation to the immune system, Nat Chem Biol, 9 (2013) 769-775.

[7] M. Black, A. Trent, M. Tirrell, C. Olive, Advances in the design and delivery of peptide subunit vaccines with a focus on toll-like receptor agonists, Expert Rev Vaccines, 9 (2010) 157-173.

[8] M.F. Bachmann, G.T. Jennings, Vaccine delivery: a matter of size, geometry, kinetics and molecular patterns, Nat Rev Immunol, 10 (2010) 787-796.

[9] C.H. Kapadia, J.L. Perry, S. Tian, J.C. Luft, J.M. DeSimone, Nanoparticulate immunotherapy for cancer, J Control Release, 219 (2015) 167-180.

[10] E. Yuba, C. Kojima, A. Harada, Tana, S. Watarai, K. Kono, pH-Sensitive fusogenic polymer-modified liposomes as a carrier of antigenic proteins for activation of cellular immunity, Biomaterials, 31 (2010) 943-951.

[11] S. Flanary, A.S. Hoffman, P.S. Stayton, Antigen delivery with poly(propylacrylic acid) conjugation enhances MHC-1 presentation and T-cell activation, Bioconjug Chem, 20 (2009) 241-248.

[12] S.L. Demento, W. Cui, J.M. Criscione, E. Stern, J. Tulipan, S.M. Kaech, T.M. Fahmy, Role of sustained antigen release from nanoparticle vaccines in shaping the T cell memory phenotype, Biomaterials, 33 (2012) 4957-4964.

[13] M. Diwan, M. Tafaghodi, J. Samuel, Enhancement of immune responses by co-delivery of a CpG oligodeoxynucleotide and tetanus toxoid in biodegradable nanospheres, J Control Release, 85 (2002) 247-262.

[14] A.L. Silva, R.A. Rosalia, A. Sazak, M.G. Carstens, F. Ossendorp, J. Oostendorp, W. Jiskoot, Optimization of encapsulation of a synthetic long peptide in PLGA nanoparticles: low-burst release is crucial for efficient CD8(+) T cell activation, Eur J Pharm Biopharm, 83 (2013) 338-345.

[15] J.J. Moon, H. Suh, A. Bershteyn, M.T. Stephan, H. Liu, B. Huang, M. Sohail, S. Luo, S.H. Um, H. Khant, J.T. Goodwin, J. Ramos, W. Chiu, D.J. Irvine, Interbilayer-crosslinked multilamellar vesicles as synthetic vaccines for potent humoral and cellular immune responses, Nat Mater, 10 (2011) 243-251.

[16] Y. Zhu, W. Meng, H. Gao, N. Hanagata, Hollow Mesoporous Silica/Poly(l-lysine) Particles for Codelivery of Drug and Gene with Enzyme-Triggered Release Property, The Journal of Physical Chemistry C, 115 (2011) 13630-13636.

[17] T.P. Janeway CA Jr, Walport M, et al. , Immunobiology: The Immune System in Health and Disease., Garland Science, New York, 2001.

[18] S.P. Kasturi, I. Skountzou, R.A. Albrecht, D. Koutsonanos, T. Hua, H.I. Nakaya, R. Ravindran, S. Stewart, M. Alam, M. Kwissa, F. Villinger, N. Murthy, J. Steel, J. Jacob, R.J. Hogan, A. Garcia-Sastre, R. Compans, B. Pulendran, Programming the magnitude and persistence of antibody responses with innate immunity, Nature, 470 (2011) 543-547.

[19] A. Beletskii, A. Galloway, S. Rele, M. Stone, F. Malinoski, Engineered PRINT((R)) nanoparticles for controlled delivery of antigens and immunostimulants, Hum Vaccin Immunother, 10 (2014) 1908-1913.

[20] M. Singh, D. O'Hagan, Advances in vaccine adjuvants, Nat Biotech, 17 (1999) 1075-1081.
[21] F. Sarti, G. Perera, F. Hintzen, K. Kotti, V. Karageorgiou, O. Kammona, C. Kiparissides, A. Bernkop-Schnurch, In vivo evidence of oral vaccination with PLGA nanoparticles containing the immunostimulant monophosphoryl lipid A, Biomaterials, 32 (2011) 4052-4057.

[22] A. de Titta, M. Ballester, Z. Julier, C. Nembrini, L. Jeanbart, A.J. van der Vlies, M.A. Swartz, J.A. Hubbell, Nanoparticle conjugation of CpG enhances adjuvancy for cellular immunity and memory recall at low dose, Proc Natl Acad Sci U S A, 110 (2013) 19902-19907.

[23] M.E. Lebel, K. Chartrand, D. Leclerc, A. Lamarre, Plant Viruses as Nanoparticle-Based Vaccines and Adjuvants, Vaccines (Basel), 3 (2015) 620-637.

[24] S.E. Gratton, P.A. Ropp, P.D. Pohlhaus, J.C. Luft, V.J. Madden, M.E. Napier, J.M. DeSimone, The effect of particle design on cellular internalization pathways, Proc Natl Acad Sci U S A, 105 (2008) 11613-11618.

[25] C.L. Waite, C.M. Roth, PAMAM-RGD conjugates enhance siRNA delivery through a multicellular spheroid model of malignant glioma, Bioconjug Chem, 20 (2009) 1908-1916.

[26] A.W. York, F. Huang, C.L. McCormick, Rational design of targeted cancer therapeutics through the multiconjugation of folate and cleavable siRNA to RAFT-synthesized (HPMA-s-APMA) copolymers, Biomacromolecules, 11 (2010) 505-514.

[27] B.A. Cohen, M. Bergkvist, Targeted in vitro photodynamic therapy via aptamer-labeled, porphyrin-loaded virus capsids, J Photochem Photobiol B, 121 (2013) 67-74.

[28] T.C. Chu, J.W. Marks, 3rd, L.A. Lavery, S. Faulkner, M.G. Rosenblum, A.D. Ellington, M. Levy, Aptamer:toxin conjugates that specifically target prostate tumor cells, Cancer Res, 66 (2006) 5989-5992.

[29] J.S. Lee, J.J. Green, K.T. Love, J. Sunshine, R. Langer, D.G. Anderson, Gold, poly(beta-amino ester) nanoparticles for small interfering RNA delivery, Nano Lett, 9 (2009) 2402-2406.

[30] H.R. Kim, I.K. Kim, K.H. Bae, S.H. Lee, Y. Lee, T.G. Park, Cationic solid lipid nanoparticles reconstituted from low density lipoprotein components for delivery of siRNA, Mol Pharm, 5 (2008) 622-631.

[31] V. Bagalkot, X. Gao, siRNA-aptamer chimeras on nanoparticles: preserving targeting functionality for effective gene silencing, ACS Nano, 5 (2011) 8131-8139.

[32] H.Q. Mao, K. Roy, V.L. Troung-Le, K.A. Janes, K.Y. Lin, Y. Wang, J.T. August, K.W. Leong, Chitosan-DNA nanoparticles as gene carriers: synthesis, characterization and transfection efficiency, J Control Release, 70 (2001) 399-421.

[33] B. Slutter, P.C. Soema, Z. Ding, R. Verheul, W. Hennink, W. Jiskoot, Conjugation of ovalbumin to trimethyl chitosan improves immunogenicity of the antigen, J Control Release, 143 (2010) 207-214.

[34] B. Slutter, S.M. Bal, I. Que, E. Kaijzel, C. Lowik, J. Bouwstra, W. Jiskoot, Antigen-adjuvant nanoconjugates for nasal vaccination: an improvement over the use of nanoparticles?, Mol Pharm, 7 (2010) 2207-2215.

[35] K.C. Sheng, M. Kalkanidis, D.S. Pouniotis, S. Esparon, C.K. Tang, V. Apostolopoulos, G.A. Pietersz, Delivery of antigen using a novel mannosylated dendrimer potentiates immunogenicity in vitro and in vivo, Eur J Immunol, 38 (2008) 424-436.

[36] N. Chen, M. Wei, Y. Sun, F. Li, H. Pei, X. Li, S. Su, Y. He, L. Wang, J. Shi, C. Fan, Q. Huang, Self-assembly of poly-adenine-tailed CpG oligonucleotide-gold nanoparticle nanoconjugates with immunostimulatory activity, Small, 10 (2014) 368-375.

[37] N. Singh, A. Agrawal, A.K. Leung, P.A. Sharp, S.N. Bhatia, Effect of nanoparticle conjugation on gene silencing by RNA interference, J Am Chem Soc, 132 (2010) 8241-8243.

[38] S.W. Jones, R.A. Roberts, G.R. Robbins, J.L. Perry, M.P. Kai, K. Chen, T. Bo, M.E. Napier, J.P. Ting, J.M. Desimone, J.E. Bear, Nanoparticle clearance is governed by Th1/Th2 immunity and strain background, J Clin Invest, 123 (2013) 3061-3073.

[39] G.K. Mutwiri, A.K. Nichani, S. Babiuk, L.A. Babiuk, Strategies for enhancing the immunostimulatory effects of CpG oligodeoxynucleotides, J Control Release, 97 (2004) 1-17.

[40] A. Madaan, R. Verma, A.T. Singh, S.K. Jain, M. Jaggi, A stepwise procedure for isolation of murine bone marrow and generation of dendritic cells, 2014, (2014).

[41] B.J. Quah, H.S. Warren, C.R. Parish, Monitoring lymphocyte proliferation in vitro and in vivo with the intracellular fluorescent dye carboxyfluorescein diacetate succinimidyl ester, Nat Protoc, 2 (2007) 2049-2056.

[42] E. Ingulli, Tracing tolerance and immunity in vivo by CFSE-labeling of administered cells, Methods Mol Biol, 380 (2007) 365-376.

[43] E. Frohlich, The role of surface charge in cellular uptake and cytotoxicity of medical nanoparticles, Int J Nanomedicine, 7 (2012) 5577-5591.

[44] D. Ma, S. Tian, J. Baryza, J.C. Luft, J.M. DeSimone, Reductively Responsive Hydrogel Nanoparticles with Uniform Size, Shape, and Tunable Composition for Systemic siRNA Delivery in Vivo, Mol Pharm, 12 (2015) 3518-3526.

[45] S.S. Dunn, S. Tian, S. Blake, J. Wang, A.L. Galloway, A. Murphy, P.D. Pohlhaus, J.P. Rolland, M.E. Napier, J.M. DeSimone, Reductively responsive siRNA-conjugated hydrogel nanoparticles for gene silencing, J Am Chem Soc, 134 (2012) 7423-7430.

[46] C.A. Fromen, G.R. Robbins, T.W. Shen, M.P. Kai, J.P. Ting, J.M. DeSimone, Controlled analysis of nanoparticle charge on mucosal and systemic antibody responses following pulmonary immunization, Proc Natl Acad Sci U S A, 112 (2015) 488-493.

[47] W.J. Storkus, H.J. Zeh, 3rd, R.D. Salter, M.T. Lotze, Identification of T-cell epitopes: rapid isolation of class I-presented peptides from viable cells by mild acid elution, J Immunother Emphasis Tumor Immunol, 14 (1993) 94-103.

[48] E. Schlosser, M. Mueller, S. Fischer, S. Basta, D.H. Busch, B. Gander, M. Groettrup, TLR ligands and antigen need to be coencapsulated into the same biodegradable microsphere for the generation of potent cytotoxic T lymphocyte responses, Vaccine, 26 (2008) 1626-1637.

[49] M.J. Hampton, J.L. Templeton, J.M. DeSimone, Direct patterning of CdSe quantum dots into sub-100 nm structures, Langmuir, 26 (2010) 3012-3015.

[50] R.A. Roberts, T.K. Eitas, J.D. Byrne, B.M. Johnson, P.J. Short, K.P. McKinnon, S. Reisdorf, J.C. Luft, J.M. DeSimone, J.P. Ting, Towards programming immune tolerance through geometric manipulation of phosphatidylserine, Biomaterials, 72 (2015) 1-10.

[51] J.Y. Kelly, J.M. DeSimone, Shape-specific, monodisperse nano-molding of protein particles, J Am Chem Soc, 130 (2008) 5438-5439.

[52] K.G. Reuter, J.L. Perry, D. Kim, J.C. Luft, R. Liu, J.M. DeSimone, Targeted PRINT Hydrogels: The Role of Nanoparticle Size and Ligand Density on Cell Association, Biodistribution, and Tumor Accumulation, Nano Lett, 15 (2015) 6371-6378.

[53] S.N. Mueller, S. Tian, J.M. DeSimone, Rapid and Persistent Delivery of Antigen by Lymph Node Targeting PRINT Nanoparticle Vaccine Carrier To Promote Humoral Immunity, Mol Pharm, 12 (2015) 1356-1365.

[54] R.A. Roberts, T. Shen, I.C. Allen, W. Hasan, J.M. DeSimone, J.P. Ting, Analysis of the murine immune response to pulmonary delivery of precisely fabricated nano- and microscale particles, PLoS One, 8 (2013) e62115.

[55] A.L. Galloway, A. Murphy, J.M. DeSimone, J. Di, J.P. Herrmann, M.E. Hunter, J.P. Kindig, F.J. Malinoski, M.A. Rumley, D.M. Stoltz, T.S. Templeman, B. Hubby, Development of a nanoparticle-based influenza vaccine using the PRINT technology, Nanomedicine, 9 (2013) 523-531.

[56] G. Saito, J.A. Swanson, K.D. Lee, Drug delivery strategy utilizing conjugation via reversible disulfide linkages: role and site of cellular reducing activities, Adv Drug Deliv Rev, 55 (2003) 199-215.

[57] C.L. Slingluff, The Present and Future of Peptide Vaccines for Cancer: Single or Multiple, Long or Short, Alone or in Combination?, Cancer journal (Sudbury, Mass.), 17 (2011) 343-350.
[58] A. Yamada, T. Sasada, M. Noguchi, K. Itoh, Next-generation peptide vaccines for advanced cancer, Cancer Science, 104 (2013) 15-21.

[59] S. Neumann, K. Burkert, R. Kemp, T. Rades, P. Rod Dunbar, S. Hook, Activation of the NLRP3 inflammasome is not a feature of all particulate vaccine adjuvants, Immunol Cell Biol, 92 (2014) 535-542.

[60] F.A. Sharp, D. Ruane, B. Claass, E. Creagh, J. Harris, P. Malyala, M. Singh, D.T. O'Hagan, V. Petrilli, J. Tschopp, L.A. O'Neill, E.C. Lavelle, Uptake of particulate vaccine adjuvants by dendritic cells activates the NALP3 inflammasome, Proc Natl Acad Sci U S A, 106 (2009) 870-875.

[61] X. Zhan, K.K. Tran, H. Shen, Effect of the poly(ethylene glycol) (PEG) density on the access and uptake of particles by antigen-presenting cells (APCs) after subcutaneous administration, Mol Pharm, 9 (2012) 3442-3451.

Chapter 4: Induction of Antitumor Protective Immune Response by Sustain Release Delivery of Antigen and Adjuvant*

4.1. Introduction

Harnessing the power of a patient's own immune system to target, fight and eradicate cancer cells without destroying healthy cells is a highly attractive and innovative approach for cancer management. Despite many efforts made to develop successful cancer vaccines, translation of cancer vaccines to clinic is challenging. FDA approval of sipuleucel‑T (Provenge®, Dendreon Corporation, Seattle, USA) in April 2010 for the treatment of metastatic castration-resistant prostate cancer (mCRPC) has created lot of encouragement and promises in the field of active immunotherapy. Various types of cancer vaccines including cell (T cells, dendritic cell (DC) and tumor cell) based vaccines, subunit vaccines, and genetic vaccines, are being evaluated in pre-clinical and clinical studies [1, 2]. Among them, sub-unit vaccines provide very safe and effective way to induce protective immunity against cancer. T-cell epitope peptides identified from tumor associated antigens (TAA) and various immunostimulatory adjuvants such as TLR/NLR agonists can be delivered to induce potent CTLs (cytotoxic T-lymphocytes) as well as memory response against tumors [3, 4]. Due to advancements in the field of nanotechnology, particulate delivery of DNA, siRNA, chemotherapeutics, proteins, and peptides to the specific target tissue is now possible [5]. Nanoparticle carriers can improve solubility, bioavailability, and therapeutic index of protected cargo. They are able to protect proteins and peptide antigens from degradation, and deliver them to specific antigen presenting cells, resulting in higher cellular uptake, antigen cross-presentation, and induction of cellular response. Many particulate delivery systems have been

*Chintan H. Kapadia, Shaomin Tian, Jillian L. Perry, David Sailer, J. Christopher Luft, Joseph M. DeSimone, *In preparation*

explored in pre-clinical studies for the delivery of antigenic peptides and adjuvants for cancer vaccine [6, 7]. For particulate based vaccines, antigens and adjuvants can be either adsorbed, encapsulated, or conjugated to nanoparticles. Various labile and non-labile linkers have been utilized to conjugate antigens on the surface of NPs for intracellular delivery, resulting in improved antibody titers and induction of potent cellular immune response [8-13].

Various cross-inkers are also used extensively in the antibody-drug conjugate (ADC) field, in which it was discovered that linker chemistry plays an important role in the overall safety, stability, and potency of the ADCs. Cleavable linkers such as disulfide, hydrazine, and dipeptides, are widely used in the ADC field to conjugate cytotoxic small molecules to antibodies for targeted drug delivery [14]. Although reduction sensitive (disulfide) and acid labile (hydrazine) linkers were designed to release the drug in the intracellular environment, they underwent rapid cleavage at off target sites. The half-life of various peptides conjugated to hemoglobin via disulfide bonds in 0.5 mM GSH is <1 hour (8-45 mins) [15]. It has become apparent that the reduced potency and higher adverse effects of disulfide linked ADCs is associated to its non-specific cleavage and drug release in circulation. Thus efforts have been made to design new linkers, to provide higher stability in circulation, decrease off-target adverse effects, and improve the antitumor activity. Sterically hindered disulfide linkers improved biological stability and antitumor activity of cargo as compared to un-hindered disulfide linkers [16, 17]. Furthermore, maleimide based linkers utilize a Michael addition reaction to link a reduced thiol, resulting in the formation of a stable thioether linkage [18]. In a seminal paper by Baldwin and Kiick, it was shown that thioether bonds undergo retro and exchange reactions in the presence of other thiol compounds at physiological pH and temperature [19]. Furthermore, they found that based upon the Michael donor's reactivity, the kinetics of the retro reactions and extent of exchange could be tuned from 20 hours to 80 hours in highly reductive environment (10 mM GSH) [19]. Moreover, in a comparative study done by Genentech and Immunogen, they found that thioether linked ADC's had improved efficacy and pharmacokinetics, and reduced toxicity in mouse breast cancer models as compared

to disulfide linked ADC's [20]. These findings resulted in FDA approval of the thioether linked ADC Kadcyla® in 2013 for the treatment of patients with HER2+ metastatic breast cancer. Thioether linkage is also used in another FDA approved ADC, Adcetris® (brentuximab vedotin) which is prescried for the treatment of relapsed Hodgkin Lymphoma[21]. These results provided the novel controlled release strategy to deliver drugs or biomolecules via thioether linkages. Antigens and/or adjuvants delivered via thioether linkage could provide more stable and controlled release of subunit vaccine components for prolong activation of immune cells. To this end, we have evaluated the effect of linker chemistry (disulfide versus thioether) on subunit vaccine efficacy.

Controlled or sustained release of antigen is possibly advantageous in the generation, maturation, and extension of immune responses [22-25]. To this point, Yumeki et al. has shown that cationized OVA adsorbed to DNA hydrogel NPs had sustained release of OVA for 24 hours and induced a better antitumor immune response as compared to the soluble OVA protein [26]. Zhang et al. has also shown persistent antibody titer up to 10 weeks by providing sustain release of CpG ODN and OVA up to 60 days when encapsulated within PLGA micro-emulsions [27]. In chapter 3, we have shown the design of PRINT based NPs to co-deliver of CSIINFEKL and CpG ODN by conjugating them to NPs via disulfide linkers. These NPs were successfully internalized and processed by BMDCs resulting in antigen cross-presentation, maturation of BMDCs, and induction of antigen specific IFN-γ producing potent $CD8^+$ T cells. In the studies presented herein, we have generated a better antitumor protective response through sustained release of model antigenic peptide CSIIFENKL and CpG ODN linked to NPs through thioether linkage, as compared to the same subunit vaccines utilizing disulfide linkage. We compared the *in vitro* and *in vivo* efficacy of PRINT subunit vaccines as a function of cargo release. For these studies, both antigen and adjuvant were conjugated to NPs either through disulfide linkage or thioether linkage. CSIINFEKL peptide release in highly reductive environment (10 mM GSH) were evaluated for each formulation. We further compared the formulations for their efficiency in

antigen cross-presentation in BMDCs, activation and maturation of BMDCs, as well as induction of antigen specific TNF-Ɣ producing $CD8^+$ T cells. Lastly, both formulations were evaluated for their potency to provide protection against tumor challenge in EG7 mouse tumor model. Our work demonstrates better antigen cross-presentation in BMDCs, as well as better activation and maturation of BMDCs treated with thioether formulation as compared to disulfide formulation. These enhancements translated to a 2-fold improvement in tumor growth inhibition for mice treated with the thioether formulation over the disulfide formulation.

4.2. Materials and Methods

4.2.1. Materials

Poly (ethylene glycol) diacrylate (M_n 700) ($PEG_{700}DA$), 2-aminoethyl methacrylate hydrochloride (AEM), diphenyl (2, 4, 6-trimethylbenzoyl)-phosphine oxide (TPO), thiol modified CpG 1826 (C6-S-S-C6-tccatgacgttcctgacgtt), dithiothreitol (DTT), sucrose and DNase, RNase free sterile water were purchased from Sigma-Aldrich. Tetraethylene glycol monoacrylate (HP_4A) was synthesized in house. Cysteine modified OVA257-264 (CSIINFEKL) were purchased from Peptide 2.0. Trifluoroacetic acid, methanol, dimethyl sulfoxide (DMSO), PTFE (polytetrafluoroethylene) syringe filters (13-mm membrane, 0.22-µm pore size), HPLC grade water and acetonitrile were obtained from Fisher Scientific. Conventional filters (2-µm) were purchased from Agilent Technologies, and polyvinyl alcohol (Mw 2000) (PVOH) was purchased from Acros Organics. (N-Succinimidyl 3-(2-pyridyldithio)-propionate (SPDP) and SMCC (succinimidyl 4-(N-maleimidomethyl) cyclohexane-1-carboxylate) were purchased from Thermo Scientific. PRINT molds (80 nm × 320 nm) were obtained from Liquidia Technologies. DNA grade NAP-10 columns were purchased from GE Healthcare. RPMI1640 medium, penicillin and streptomycin, L-glutamine, fetal bovine serum (FBS) were all from Life Technologies.

4.2.2. Methods

4.2.2.1. PRINT nanoparticle fabrication

PRINT nanoparticles were fabricated as mentioned in 3.2.2.1.

4.2.2.2. Thermogravimetric analysis

Thermogravimetric analysis was performed as mentioned in 3.2.2.2.

4.2.2.3. Scanning electron microscopy (SEM)

SEM was performed as mentioned in 3.2.2.3.

4.2.2.4. Dynamic light scattering

Particle size and zeta potential were measured in sterile water by dynamic light scattering (DLS) on a Zetasizer Nano ZS (Malvern Instruments, Ltd.).

4.2.2.5. Conjugation of linker to NPs

We utilized amine groups from AEM to conjugate SPDP and SMCC. Conjugation of SPDP to NPs was performed as mentioned in 3.2.2.5. For reaction of NPs with SMCC, equal moles of SMCC as to SPDP (0.26 mg of SMCC) was reacted to NPs in 1 ml of 1X PBS + 0.1% PVA for 2 hours. SMCC or SPDP were dissolved in DMF. Similar protocol was followed as mentioned in 3.2.2.5.

4.2.2.6. Conjugation of CSIINFEKL to linker modified NPs

Conjugation reaction of CSIINFEKL via SPDP was performed as mentioned in 3.2.2.6. Similar protocol was followed to conjugate CSIINFEKL to NPs via SMCC except conjugation reaction was done in 1X PBS. At the end of the conjugation process, loading of SMCC conjugated peptide was evaluated by performing standard BCA assay (Thermo Scientific) on particle conjugated peptides. Loading of SPDP conjugated CSIINFEKL was evaluated by utilizing HPLC technique. Conjugation efficiency of peptide was evaluated using the following equation.

% Conjugation efficiency = (Amount of linker conjugated) X 100 / (Amount of linker charged)..... (1)

Conjugation efficiency of peptide is around 60-70% for both the linkers.

4.2.2.7. Reduction and purification of C6 S-S- C6 CpG 1826

Reduction and purification of C6 S-S- C6 CpG 1826 was done as mentioned in 3.2.2.7.

4.2.2.8. Conjugation of Thiol-CpG 1826 to NPs

Conjugation of CpG ODN to NPs via SPDP was done by following procedure mentioned in 3.2.2.8. Similar protocol was followed to conjugated CpG ODN to NPs via SMCC except conjugation of CpG was performed in 1X PBS instead in sterile water. For both the formulations, evaluation of CpG was done via UV/VIS spectroscopy at 260 nm by using NanoDrop 2000 Spectrophotometer as mentioned above.

4.2.2.9. Co-conjugation of CSIINFEKL and CpG ODN to NPs

Co-conjugation of CSIINFEKL and CpG ODN to NPs via SPDP was done by following procedure mentioned in 3.2.2.9. Similar protocol was followed to co-conjugate CSIINFEKL and CpG ODN to NPs via SMCC except that conjugation was performed in 1X PBS instead of sterile water. Disulfide liked CSIINFEKL was evaluated via HPLC as mentioned in 3.2.2.10. SMCC linked CSIINFEKL was evaluated via standard BCA assay (Thermo Scientific). Blank reading for BCA assay was taken in SMCC modified NPs. For both the formulations, evaluation of CpG was done via UV/VIS spectroscopy at 260 nm by using NanoDrop 2000 Spectrophotometer as mentioned above.

4.2.2.10. Peptide release study

CSIINFEKL was conjugated to nanoparticles via SPDP and SMCC as mentioned earlier. After conjugation of peptide, 5 mg of NPs were incubated in 10mM GSH (sterile water of pH 7.0) at 37^{o} C. pH of the solution was adjusted to 7.0 by using 4 µM sodium hydroxide. (One of the reason to use sterile water is because peptide is insoluble in buffer because of higher salt concentration). 80uL of aliquot were collected at 0.5, 1, 2, 8, 24, 48 and 72 hours. Collected samples were spun down at 14000 RPM and supernatant were collected. Quantity of released peptide in the supernatant was evaluated by HPLC-MS.

4.2.2.11. Peptide evaluation via HPLC

Quantification of CSIINFEKL was done by HPLC as mentioned in 3.2.2.10.

4.2.2.12. Liquid chromatography- Mass spectrometry (LC-MS)

Reverse phase high performance liquid chromatography (HPLC) was run on an Agilent1200 series HPLC system equipped with quaternary pump, mobile phase degasser, temperature controlled auto sampler and column thermostat. The separation was carried out on a Zorbax Eclipse XDB-C18 (100 mm×2.1 mm i.d., 3.5 µm particle size) from Agilent Technologies (Santa Clara, CA) at column temperature of 40 ^{o}C. Peptide was eluted using mobile phase gradient at a flowrate of 300 µL/ min. Mobile phase consist of two solutions. Solution A- Water with 0.1% formic acid and B- Acetonitrile with 0.1% formic acid. Gradient method is shown in table-4.1.

Table-4.1: Gradient method for LC-MS run

Min	% of Mobile Phase A	% of Mobile Phase B
0	98	2
1	98	2
17	50	50
18	5	95
23	5	95
24	98	2
30	98	2

An Agilent 6520 Accurate Mass Quadrupole Time-of-Flight Mass Spectrometer (Q-TOF LC/MS) system was used for the detection of peptide species. Separated peptide species from the C18 column were analyzed with electrospray ionization (ESI) in positive ion mode by scanning the instrument over the mass range of 100-3000 amu.

4.2.2.13. Animals

Female C57BL/6 mice were purchased from Jackson Laboratory and used at age 6–12 weeks. All experiments involving mice were carried out in accordance with an animal use protocol approved by the University of North Carolina Animal Care and Use Committee.

4.2.2.14. Preparation of splenocytes and WBCs

Splenocytes were isolated as mentioned in 3.2.2.12. To isolate leukocytes from blood, mice were bled submandibularly into 500 µl PBS with 7 mM EDTA. Diluted blood was then laid onto 500 µl

Lympholyte-mammal (Cedarlane) and spun at 600 g for 20 min. White blood cells were collected from the layer at the interface, washed with DPBS.

4.2.2.15. Preparation of BMDCs

BMDCs were prepared and cultured as mentioned in 3.2.2.13.

4.2.2.16. Antigen presentation assay in BMDCs

To evaluate the effect of linker chemistry on antigen presentation, Day 6 BMDCs (3×10^5 cells) were either untreated or treated with blank hydrogels (with and without linkers), CSIINFEKL (5 µg/ml), CSIINFEKL conjugated to PEG hydrogels via SPDP (short cleavable linker, 5 µg/ml) or CSIINFEKL conjugated to PEG hydrogels via PEG (2k) OPSS (longer cleavable linker 5ug/ml) for 4 hours. After four hour incubation, cells were either washed with PBS of pH~7.4 or citrate-phosphate buffer (pH3.0) for 3 minutes on ice to strip off the MHC-I-peptide complex or NP-peptide/H-2K^b complex from cell surface. Additionally, cells were re-incubated at 37^{o}C for an additional 24 hours, 48 hours and 72 hours post-washes and then stained with CD11c-APC and 25-D1.16-PE (anti-SIINFEKL/H-2K^b complex) antibodies (eBioscience), followed by flow cytometry analysis on Cyan ADP (Dako).

4.2.2.17 BMDC maturation assay

BMDC maturation assay was performed as mentioned in 3.2.2.16.

4.2.2.18. Immunization Study

7 days immunization studies were performed as mentioned in 3.2.2.17.

4.2.2.19. ELISPOT assay

Enzyme-linked immunospot assay was performed as mentioned in 3.2.2.18.

4.2.2.20. Tumor challenge study

C57BL/6 mice were vaccinated subcutaneously with different formulations on day -28 and day -7, respectively. Seven days after booster dose, on day zero, 9.3 x 10^5 EG7 cells were subcutaneously injected in the left flank region. Tumors were measured using digital calipers (Thermo Fisher Scientific, Pittsburgh, PA) every 2–3 days, recording the longest diameter as length and the

perpendicular dimension as width. Tumor volume was calculated as (0.5 × length × width × height). All the mice were euthanized humanely once untreated mice were reached tumor burden i.e. 20mm in measurement in either dimensions. At the end of study splenocytes were harvested and SIINFEKL specific IFN-γ producing T cells (from spleen) were evaluated via ELISPOT assay.

4.3. Results

4.3.1 Conjugation of CSIINFEKL and CpG to NPs

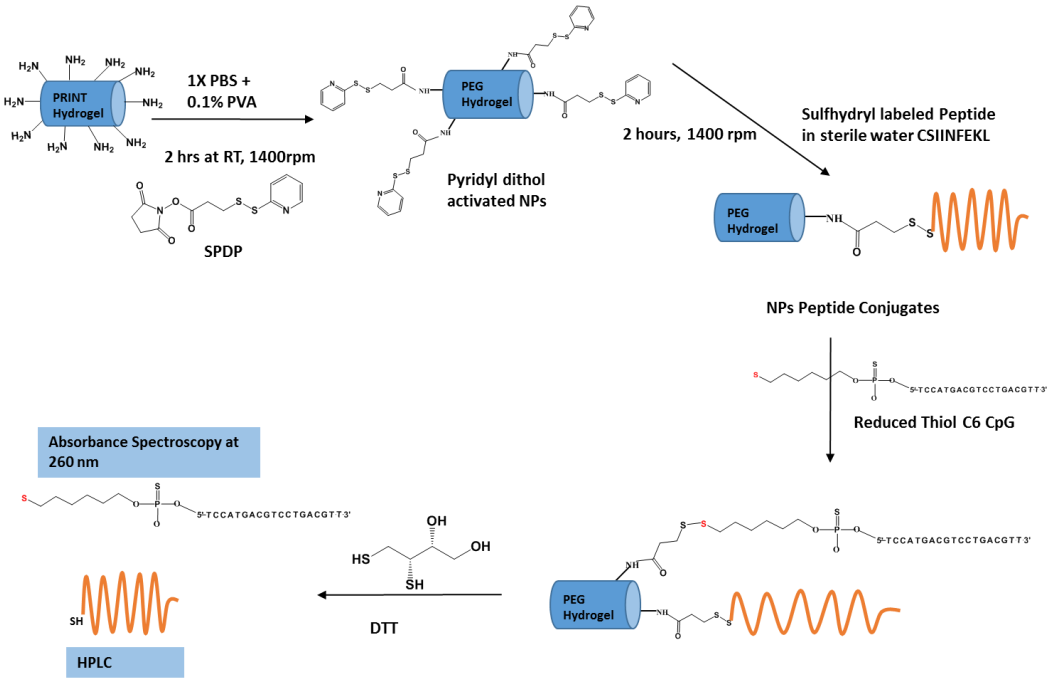

Figure-4.1: Co-conjugation of CSIINFEKL and CpG ODN to NPs via SPDP.
NPs were first modified with SPDP. Pyridyl disulfide modified particles were incubated with CSIINFEKL and then with CpG ODN. Evaluation of CSIINFEKL and CpG ODN conjugated to NPs were performed by HPLC and absorption spectroscopy, respectively.

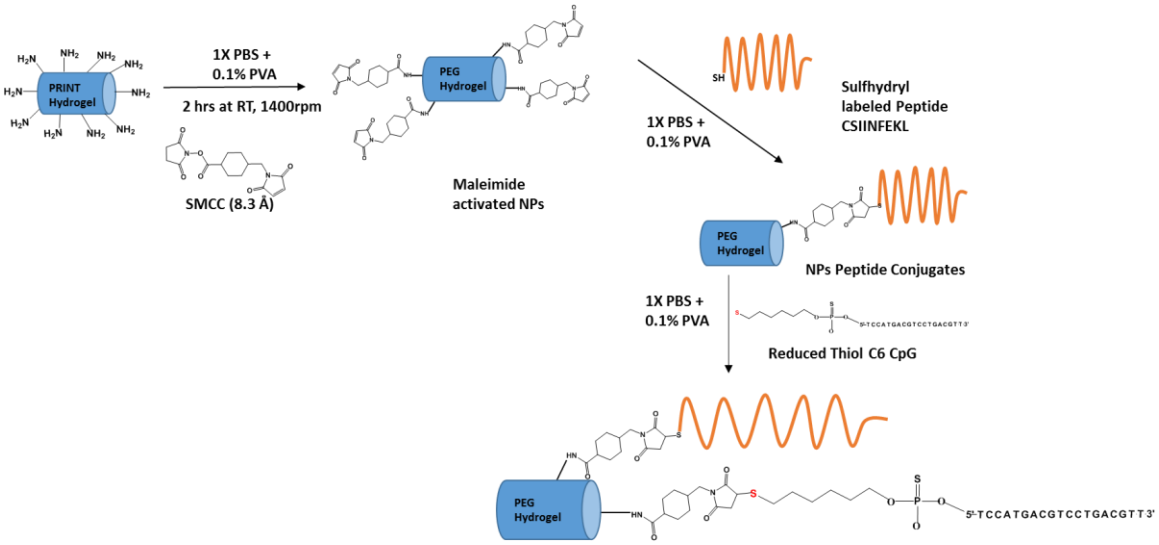

Figure-4.2: Co-conjugation of CSIINFEKL and CpG ODN to NPs via SMCC.
NPs were first modified with SMCC. Maleimide modified particles were incubated with CSIINFEKL and then with CpG ODN. Evaluation of CSIINFEKL and CpG ODN conjugated to NPs were performed by BCA protein assay and absorption spectroscopy, respectively.

Amine groups on NP surface were used to conjugate cysteine labelled SIINFEKL peptide via reduction sensitive, heterobifunctional linkers- SPDP (Figure 4.1) or SMCC (Figure 4.2) in a two step-process. First, the succinimidyl ester of the linker was reacted to the amine groups on the particle, forming an amide bond. After removal of the excess linker (via centrifugation washes), the cysteine labeled adjuvant was reacted with either the pyridine disulfide of the SPDP linker or maleimide ring of the SMCC linker. Particles were modified with equal moles of SMCC and SPDP to ensure similar linker densities and particle surface charge. After modification with either of linkers, NPs were then incubated overnight with CSIINFEKL resulting in peptide conjugation to the NPs via disulfide exchange (for SPDP) or Michael addition (for SMCC)followed by incubation with thiol-containing CpG.

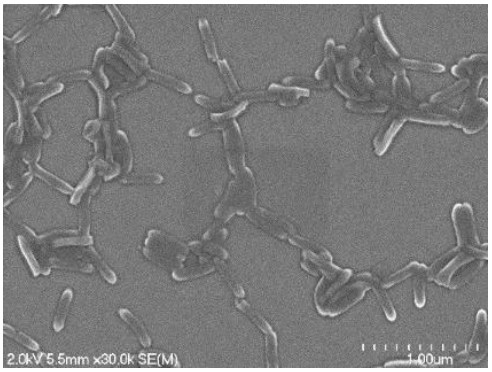

Figure-4.3: SEM image of 80×320 nm PEG hydrogel.

Table-4.2: Physical Characterization of NPs

Formulations	Size (nm)	PDI	ZP (mV)
NP-SPDP-CSIINFEKL-CpG	246 ± 3	0.09 ± 0.02	26 ± 11
NP-SMCC-CSIINFEL-CpG	270 ± 9	0.12 ± 0.09	24 ± 10

After peptide and CpG modifications, NPs remained highly uniform in size and shape as visualized by SEM (Figure 4.3). For all formulations the ZP remained around +25 mV (Table 4.2) which is desirable for cytosol delivery of antigens into MHC class I presentation pathway. Polydispersity index (PDI) of all sets of nanoparticles was around 0.1 which indicates

monodisperse nanoparticles with homogenous distribution, and size ranged from 240-270 depending on the surface modification.

4.3.2. Release of antigenic peptide from NPs in highly reductive environment (10 mM GSH)

Release profiles of CSIINFEKL in highly reductive environment was evaluated by incubating the peptide modified particles (5 mgs) in 10 mM GSH (sterile water, pH 7.0) at 37° C. At various time points, aliquots of equal volume were collected and the quantity of released peptide was evaluated by HPLC-MS. Data from HPLC-MS analysis revealed three major species of peptide in the mixture, (a) free peptide, CSIINFEKL, b) glutathione bound peptide, GSH-CSIINFEKL and c) peptide dimer, LKEFNIISC-CSIINFEKL. CSIINFEKL conjugated through the disulfide linker had rapid release profile in first 2 hours, with an initial burst release of 80% in 1 hour (Figure 4.4).

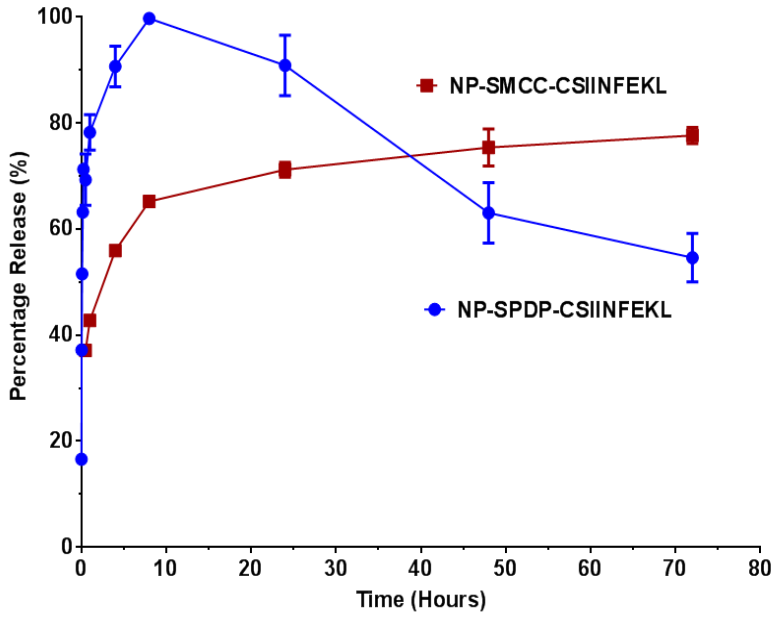

Figure-4.4: Release of antigenic peptide CSIINFEKL from NPs CSIINFEKL conjugated NPs were incubated in 10mM GSH (sterile water of pH 7.0) at 37° C. Samples were collected at different time points and quantity of released peptide was measured by HPLC. Percentage release of A) total peptide and B) 3 major species of CSIINFEKL. Thioether bonded peptide has relatively slower release profile as compared to disulfide bonded peptide. Results are shown as mean ± SD, n=2.

Similarly, Trimble et al. reported rapid release of angiotensin II analog N-acetly-CGDKVYIHPF in 0.5 mM GSH with an half-life of 8-45 mins, when conjugated to hemoglobin via disulfide linker [15]. In comparison, thioether linked CSIINFEKL had a very stable and sustained release profile

till 72 hours (Figure 4.4), with a maximum of ~60% released in 8 hours. As seen in figure 4.4, release of total peptide (i.e. CSIINFEKL + GSH-CSIINFEKL + LKEFNIISC-CSIINFEKL) remained relatively constant and stable for thioether linked CSIINFEKL. Surprisingly, we found decrease in total peptide (i.e. CSIINFEKL + GSH-CSIINFEKL + LKEFNIISC-CSIINFEKL) release after 8 hours when CSIINFEKL was conjugated to NPs via disulfide linker (figure 4.4). This is due to the present of other peptide species with glutathione in the supernatant overtime. This was further confirmed by identifying different possible species (such as CSIINFEK, FNIISCCSIIN, GSH-CSIINFEK and FNIISCCSIINFEKL) present in the mixture by performing time of flight (TOF) mass-spec analysis on 0.5 hrs and 48 hrs samples from both the formulations as shown in Appendix Figure 1-6. We found similar species (peptide fragments) from both samples which could be due to interactions of released peptide fragments with other peptide fragments or with GSH. Presence of different peptide fragments in higher amount in the samples of NP-SPDP-CSIINFEKL as compared to NP-SMCC-CSIINFEKL could be due to rapid release of CSIINFEKL from disulfide linked NPs which possibly resulted into decrease in total peptide.

4.3.3 Cross-presentation of CSIINFEKL in BMDCs

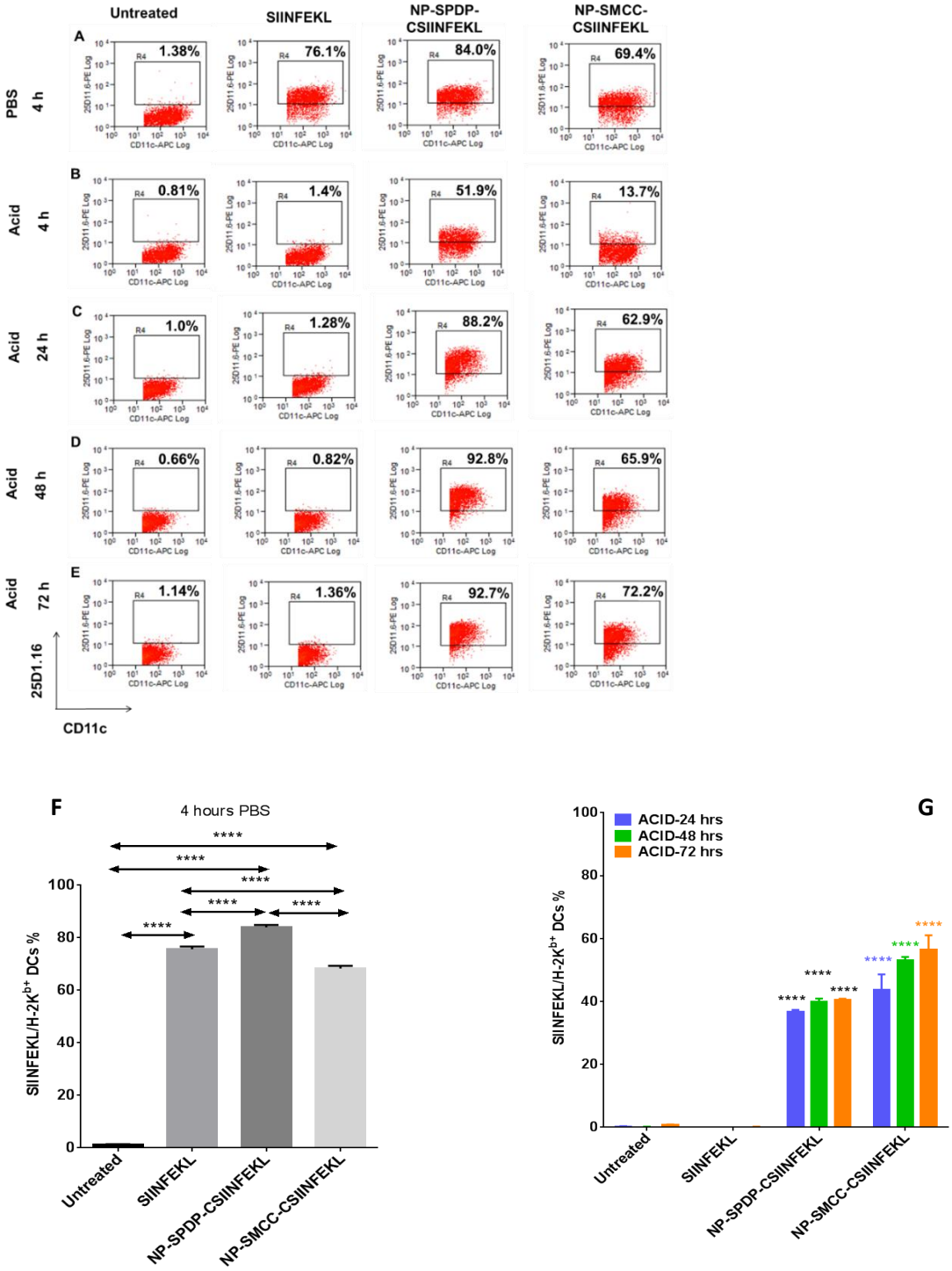

<u>Figure-4.5:</u> Modified antigen presentation assay in BMDCs.
BMDCs were treated with different formulations for 4 hours and washed with PBS (A), or washed with acidic citrate-phosphate buffer (pH3) (B, C, D, E), and certain acidic buffer washed samples

were further incubated for another 24 h (C), 48 h (D) and 72 h (E). Representative flow cytometry histogram for each group is shown in figure 4.5A to 4.5E. The numbers in the histogram represents the percentage of CD11c+ dendritic cells that were positive for pMHC I. Results are shown as mean ± SD, n=3. Data of pMHC I staining after 4 hours post PBS treatment were analyzed in (F) via one-way Anova, Tukey's post comparison test. Readings of 4 h acid treated cells were subtracted from 24 h, 48 h and 72 h acid treated cells. Data was analyzed by two-way anova, tukey's post hoc analysis, **** $p < 0.0001$

In the event of infection, DCs collect pathogens from peripheral sites and process them into small peptide fragments, which then bind to MHC-I/II molecules in endosome or ER (endoplasmic reticulum) and are transported back to the surface of DCs. $CD4^+$ or $CD8^+$ T cells can recognize these MHC I/II-peptide complexes via TCR (T cell receptors) and receive signals for proliferation. As shown in figure-2, when exposed to intracellular concentrations of GSH, CSIINFEKL bound to NPs via SMCC had a slower and more stable release profile as compared to CSIINFEKL bound by SPDP. It was hypothesized that this difference in release profile would result in linker specific pattern of cross-presentation of antigenic peptide overtime for BMDCs treated with the particulate vaccines. Prolongation of antigen presentation was evaluated via antigen presentation assay as mentioned in method section. BMDCs were either untreated or treated with soluble CSIINFEKL, NP-SPDP-CSIINFEKL, or NP-SMCC-CSIINFEKL for 4 hrs and washed with PBS. To quantify the antigen cross-presentation, BMDCs were stained with the 25-D1.16 antibody which recognizes SIINFEKL/H-$2K^b$ on APCs. As seen in Figure 4.5A and F, staining of p-MHC-I complexes was significantly higher in BMDCs treated with soluble CSIINFEKL and NP-SPDP-CSIINFEKL as compared to BMDCs treated with NP-SMCC-CSIINFEKL. Most likely, the higher antigen presentation in BMDCs at early (4h) time points is due to the rapid release of CSIINFEKL from the disulfide linked NP.

To further examine the mechanism of the NP-peptide formulations to deliver antigenic peptide, BMDCs were treated with soluble CSIINFEKL, NP-SPDP-CSIINFEKL, or NP-SMCC-CSIINFEKL, and washed with acidic citrate-phosphate buffer (pH3.0) for 3 minutes to strip off the MHC-I peptide complex from the surface of the BMDCs [28]. Cells were then incubated at 37°C for another 24 hrs, 48 hrs and 72 hrs to allow for internalized antigens to be processed and

re-presented onto the cell surface. As shown in Figure 4B, citrate-phosphate treatment completely removed SIINFEKL from p-MHC complexes for cells treated with soluble SIINFEKL (down to 1.4 %), but was unable to completely remove cell bound NP-peptide (Figure 4.5B). For cells treated with NP-SMCC-CSIINFEKL, the staining of p-MHC-I complexes was reduced to 13%, but was only decreased to 51% for cells treated with NP-SPDP-CSIINFEKL. This could be due in part to differences in avidity of the particulate bound peptide. Therefore, in an effort to find the absolute change in the antigen presentation, the percentage of p-MHC-I complex staining at 4 hrs after acid treatment was subtracted from the percentage of p-MHC-I complex staining at the later time points. At each time point, particle conjugated CSIINFEKL induce significantly higher antigen presentation in BMDCs as compare to soluble SIINFEKL. A gradual increase in antigen cross-presentation was observed for both NP formulations over time after acid treatment, (Figure 4.5C, D, E) with 10-15% higher cross-presentation over time for cells treated with NP-SMCC-CSIINFEKL than cells treated with NP-SPDP-CSIINFEKL (Figure 4.5G). This is in direct agreement with the release rates observed in Figure 2, the slower release from the thioether bond results in prolonged antigen release and higher bioavailability of full peptides, and therefore improved antigen presentation over time.

4.3.4 Maturation of BMDCs by particulate conjugated CpG ODN

Activation of naïve T cells through recognition of MHC-I-peptide complex on APCs can be enhanced through the simultaneous delivery of adjuvants, which can further drive clonal expansion of naïve T cells and aid in their differentiation into armed effector T cells. The CD40 ligand and CD28 on T cell surfaces can bind to co-stimulatory molecules such as CD40 and CD80 on the surface of DCs. Maturation of DCs with upregulation of these co-stimulatory molecules is necessary for T cell activation and proliferation. The ability of particulate vaccines to deliver CpG ODN and provide co-stimulatory signals as a function of linker chemistry was tested in BMDCs. BMDCs were incubated with soluble CpG ODN or NP-CpG for 18 hours. After incubation, cells were analyzed for

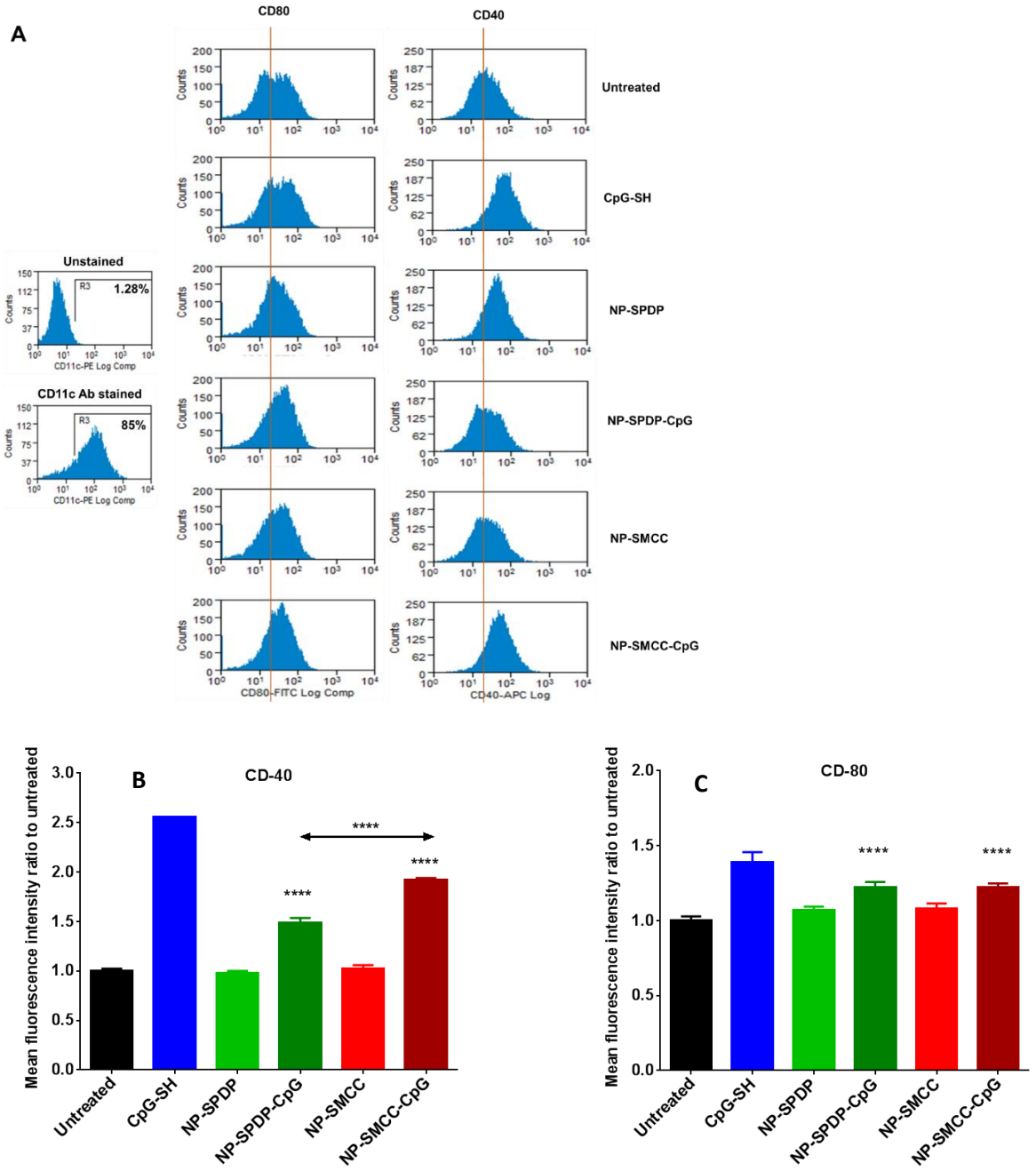

<u>Figure-4.6:</u> Up-regulation of maturation markers by NP-CpG on BMDCs.
BMDCs were treated with various samples for 24 hours with 1 µg/ml of CpG. Equivalent amount of NPs were dosed in case of NP-SPDP and NP-SMCC. The expression of co-stimulatory molecules were detected by flow cytometry analysis of fluorescence labelled CD80 and CD40 antibodies. Flow cytometry histograms for all the samples including both markers are shown in A. Ratio of MFI from sample to MFI of untreated is plotted in B) for CD40 and C) for CD80. Results are shown here as mean ± SD, n=3. Untreated cells were compared with cells treated with NP-CpG. Data were analyzed by one-way anova, Holm-Sidak's multiple comparison test, **** $p < 0.0001$.

expression of CD80 and CD40 via flow cytometry. Flow cytometry histogram for both markers are shown in Figure-4.6A. Expressions of co-stimulatory molecules were presented as a ratio of mean fluorescent intensity (MFI) to untreated cells. Treatment with CpG conjugated PRINT NPs at 1 µg/mL concentration, induced upregulation of CD80 (Figure 4.6B) and CD40 (Figure 4.6C) on BMDCs as compared to untreated cells. Upregulation of CD80 induced by NP-SPDP-CpG and NP-SMCC-CpG was as potent as soluble CpG. Moreover, expression of CD40 was higher in cells when they were treated with NP-SMCC-CpG as compared to NP-SPDP-CpG which could be due to the extended release of CpG in intracellular reductive environment.

4.3.5 *In vitro* release of IL-6 by BMDCs treated with NP conjugated CpG

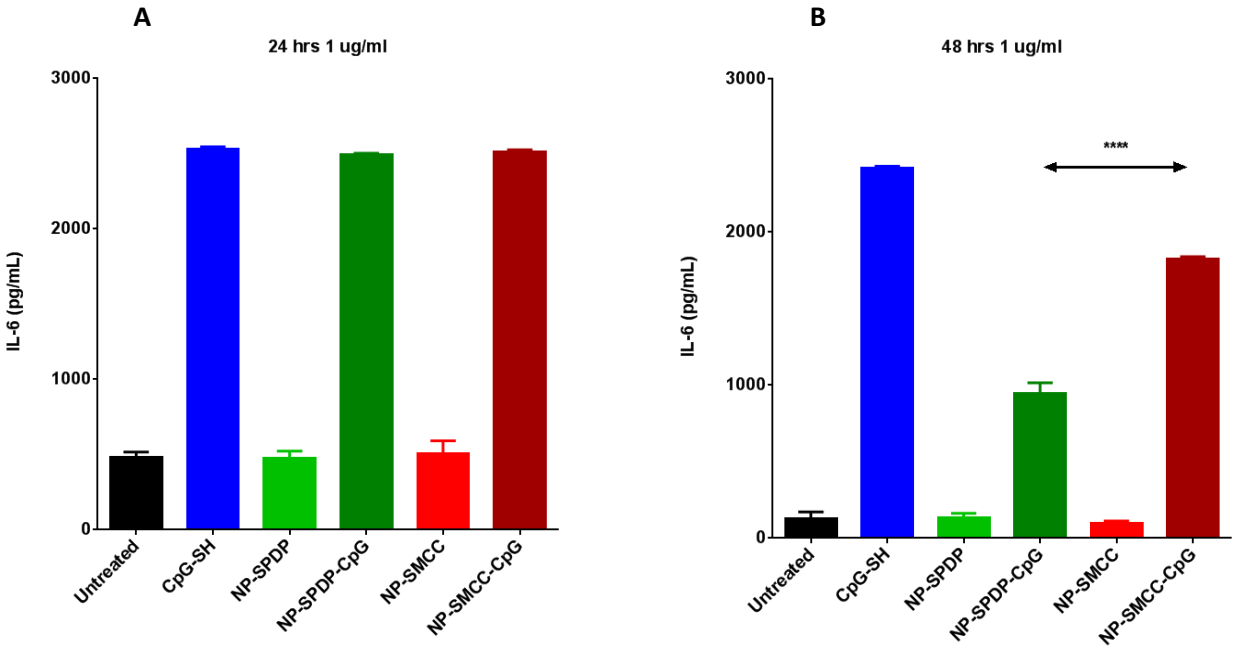

Figure-4.7: Secretion of IL-6 from BMDCs treated with particulate conjugated CpG. BMDCs were treated with various samples for 24 hours with 1 µg/ml of CpG. Equivalent amount of NPs were dosed in case of NP-SPDP and NP-SMCC. At the end of 24 hours, cells were spun down, media were collected and replaced with fresh media. Cells were kept growing for another 24 hours and then media were collected. The release of IL-6 in media was detected by ELISA assay on collected media. IL-6 concentrations in pg/ml for 24 hours and 48 hours are shown in A) and B), respectively. Results are shown here as mean ± SD, n=3. Cells treated with NP-SPDP-CpG were compared with cells treated with NP-SMCC-CpG by two-tailed, unpaired, Student's t-test, **** $p < 0.0001$.

Cytokines play a central role in maintaining the homeostasis of CD8 T lymphocytes. IL-6 is a pro-inflammatory cytokine which plays a very critical role in T cell activation, proliferation and survival [29]. IL-6 can stimulate TCR-independent proliferation and functional differentiation of $CD8^+$ T cells, and synergize with TCR signals to augment $CD8^+$ T cell proliferation [30]. CpG ODN has been shown to stimulate DCs by inducing secretion of IL-6 [31]. NP bound CpG was evaluated for its ability to stimulate the secretion of IL-6. The release of IL-6 by BMDCs were performed by treating BMDCs with various CpG formulations at a concentration of 1μg/ml for 24 hours. After 24 hours, cells were spun down and supernatant collected. To evaluate whether different formulations would have prolonged effect on IL-6 release, cells were replenished with fresh media after 24 hours and incubated at 37°C for another 24 hours. ELISA was performed to determine the concentration of released IL-6 at each time point. Concentrations of IL-6 are shown in figure 4.7 A) for 24 hours, and in figure 4.7 B) for 48 hours. After 24 hours, cells treated with soluble CpG or particulate CpG secreted similar amounts (~2500 pg/ml) of IL-6 proving that CpG retained its activity after conjugation to NPs. Although at the 48 h time point the concentrations of secreted IL-6 were lower for NP-CpG as compared to soluble CpG, the level of released IL-6 from BMDCs treated with NP-SMCC-CpG remained higher than the cells treated with NP-SPDP-CpG. This further supports the evidence that slower and prolong release of adjuvant can produce higher effects.

4.3.6 *In vivo* induction of antigen specific IFN-γ producing $CD8^+$ T cells

Both formulations were analyzed for their efficacy to induced SIINFEKL specific IFN-γ producing $CD8^+$ T cells in mice. Frequency of IFN-γ producing $CD8^+$ T cells were analyzed by performing *ex vivo* ELISPOT assay on isolated splenocytes and WBCs. As shown in Figure-4.8A and 4.8B, there is a significant difference in induction of IFN-γ producing $CD8^+$ T cells (16 times higher) when mice were immunized with NP-SPDP-CSIINFEKL-CpG and NP-SMCC-CSIINFEKL-CpG as compared to mice receiving a mixture of soluble antigen and adjuvant. In case of both the linkers, co- conjugation of adjuvant and antigen resulted in 4-5 times higher

induction of IFN-γ producing T cells in spenocytes as well as 10 times higher induction in WBCs, as compared to NPs conjugated

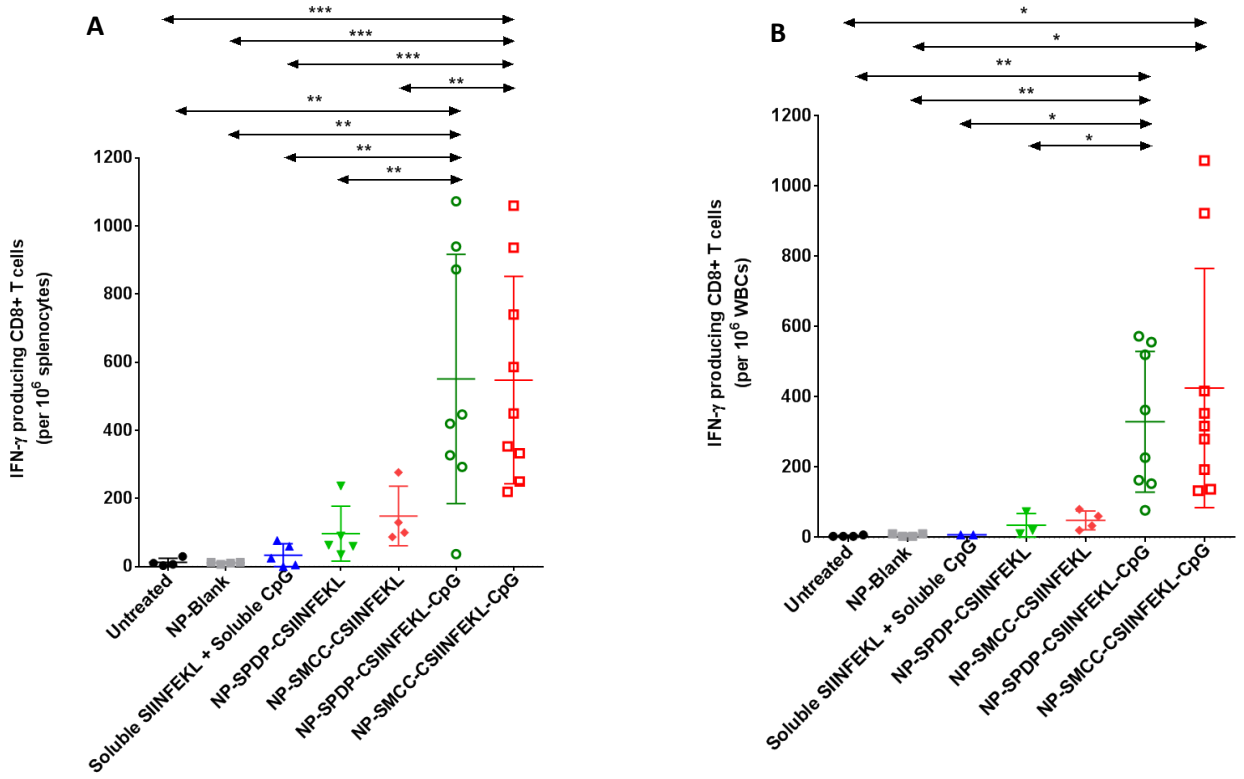

<u>Figure-4.8:</u> Induction of IFN-γ producing SIINFEKL specific CD8⁺ T cells in a) spleen and b) circulating blood.
Mice were immunized with various samples containing 100 µg peptide and/or 20 µg CpG via s.c injection in left flank. One week later, splenocytes and WBCs were isolated and re-stimulated with SIINFEKL for 20 h for IFN-γ ELISPOT assay, a) splenocytes and b) WBCs. Results are shown as mean ± SD, n=4-9. Data were analyzed by one-way anova, Holm-Sidak's multiple comparison test, *p < 0.05, *** p < 0.001.

to antigen alone. IFN-γ producing T cells response was minimum in case of negative control-blank PRINT NPs as well as in untreated mice. Despite the different design and antigen release profile, in this 7 day study, there was no observed difference in induction of CD8⁺ T cells between the NP formulations.

4.3.7 Protection against tumor growth- EG7 mouse tumor model

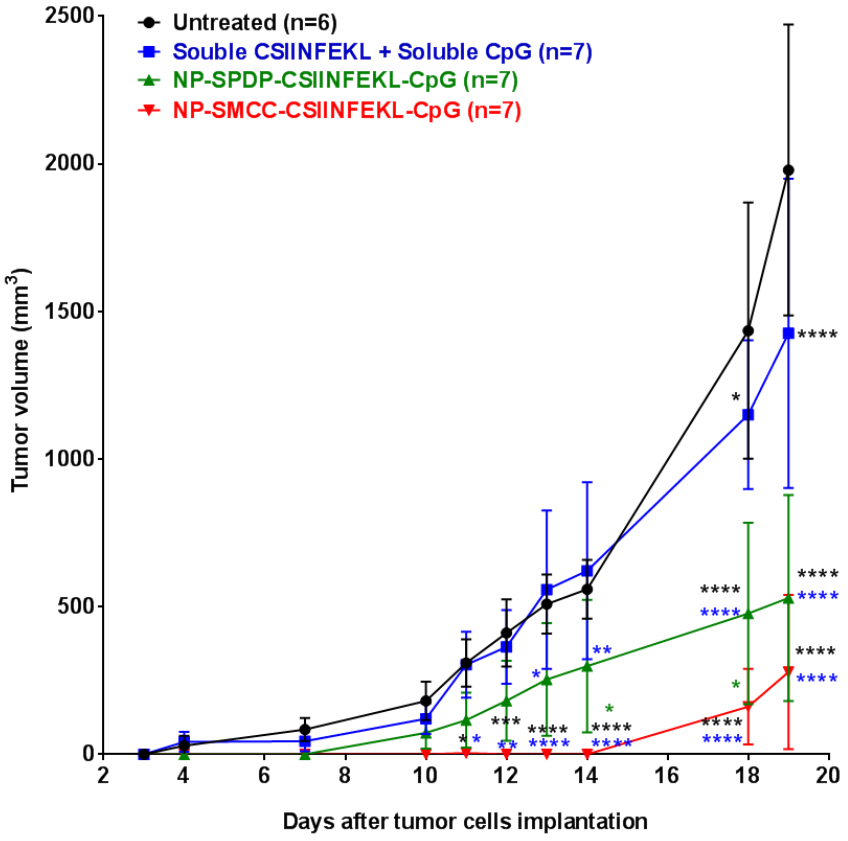

<u>Figure-4.9:</u> Tumor growth challenge study. C57BL/6 mice were vaccinated with prime dose and booster dose on day -28 and day -7, respectively. On day 0, seven days after booster dose, 9.3 x 10^5EG7 cells were subcutaneously injected in the left flank (opposite side of vaccination). Tumor growth was measured by the Animal Core Facility. All the mice were euthanized humanely once untreated mice were reached tumor burden i.e. 20 mm in measurement in either dimensions. Mice vaccinated with the PEG hydrogel subunit vaccine has significantly inhibited EG7-OVA tumor growth as compared to the untreated mice, and mice treated with soluble peptide + soluble CpG. Moreover, 14 days after tumor cells implantation, all 7 mice treated with the non-cleavable linker vaccine have total inhibition of tumor growth. Data were analyzed by two-way ANOVA followed by Bonferroni's post-test. *, $p<0.05$; **, $p<0.01$; ***, $p<0.001$; ****, $p<0.0001$.

To determine how the induction of IFN-γ producing $CD8^+$ T cells in mice would translate to protection against tumor growth the subunit vaccines were evaluated in a tumor challenge study. C57BL6/J mice were either kept untreated, or vaccinated with either a mixture of soluble CSIINFEKL and soluble CpG dissolved in sterile water, or with NP-SPDP-CSIINFEKL-CpG, or with NP-SMCC-CSIINFEKL-CpG on day -28. A booster dose was given on day -7. Seven days after the booster dose, on day 0, mice were inoculated with ~10^6 EG7.OVA thymoma cells in the right flank (opposite side of vaccine administration). Tumor growth was measured as mentioned in

method section throughout the study. As shown in Figure-4.9, untreated mice and mice treated with the mixture of soluble peptide and CpG started developing tumors on day 3,

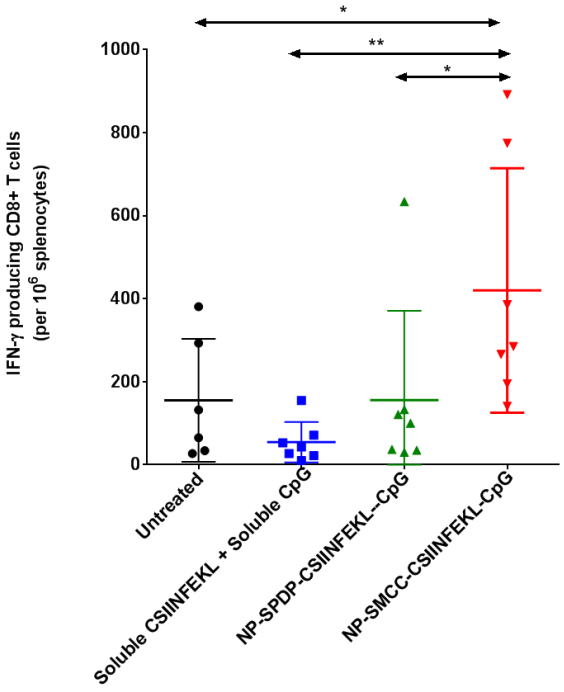

Figure-4.10: Evaluation of antigen specific IFN-γ producing CD8⁺ T Cells
On day 20 mice were euthanized and SIINFEKL specific IFN-γ producing T cells (from spleen) were evaluated via ELISPOT assay. Induction of IFN-γ producing CD8⁺ T cells is significantly higher in mouse treated with non-cleavable sub-unit vaccine as compare to untreated mice and mice treated with other formulations. Data were analyzed by Student's T test. *, $p<0.05$.

while mice vaccinated with NP-SPDP-CSIINFEKL-CpG exhibited inhibition of tumor growth until day 7. Interestingly, all mice vaccinated with NP-SMCC-CSIINFEKL-CpG experienced tumor inhibition until day 14. Furthermore, to evaluate whether delayed tumor growth was due to higher induction of CD8⁺ T cells, we isolated splenocytes at the end of the study and analyzed IFN-γ producing CD8⁺ T cells via ELISPOT. We found that frequency of IFN-γ producing CD8⁺ T cells was higher in mice vaccinated with NP-SMCC-CSIINFEKL-CpG as compared to the other formulations (Figure 4.10). Results from these studies further conclude that CSIINFEKL and CpG co-conjugated to NP via SMCC provide better protection against tumor challenge as compared to conventional disulfide linked subunit vaccine.

4.4 Discussion

Previously we have shown induction of potent CTLs by co-delivery of SIINFEKL and CpG through hydrogel NPs. Here we further demonstrated induction of CSIINFEKL specific IFN-γ producing $CD8^+$ T cells as well as protective antitumor immune response in EG7 tumor mouse model by delivering formulations of CSIINFEKL and CpG ODN via PRINT hydrogel NPs that enable sustained release of cargos. We observed different peptide release rates for peptides bound to NPs via either a disulfide or thioether linkages. The disulfide linkage was rapidly cleaved, and peptide release reached a maximum at 1 hour in 10 mM GSH, whereas peptide bound through the thioether linkage was released more slowly, with the maximum peptide release at 8 hours. These release rates were able to effect *in vitro* BMDC antigen presentation over time when antigenic peptide is conjugated, as well as production of IL-6 when CpG is conjugated. We observed that BMDCs treated with CSIINFEKL conjugated NPs linked via thioether linker had a higher and prolonged antigen presentation as compared to BMDCs treated with disulfide linked CSIINFEKL. While both formulations induced maturation of BMDCs and prolonged the release of IL-6, the effect was higher in cells treated with CSIINFEKL conjugated NPs via thioether linker. Furthermore, the peptide release kinetics resulted in differences in tumor protection *in vivo*. Mice treated with either formulation had significantly lower tumor growth as compared to mice treated with soluble CSIINFEKL and CpG, however, due to the more stable and controlled release of CSIINFEKL from thioether linked NP formulation, tumor growth was controlled for up to 14 days, versus only 7 days for the disulfide linked NP formulation.

These results are in agreement with recent literature showing how vaccine formulations with prolonged release of antigen have higher chance of inducing stronger and persistent immune response [32, 33]**.** The initial and following availability of antigen and/or adjuvant could be important for generation of desired immune response. Compared to soluble vaccine components, nanoparticle-mediated delivery can provide much better control over release kinetics and bio-distribution of their cargos in lymphoid tissues upon immunizations. Controlled release of antigen

has been achieved by encapsulating antigen into different polymeric nano-microparticles, [34] which resulted in higher and more persistent antibody titers. These carrier systems have been reviewed elsewhere [35-37]. Though these results were promising, it has not been evaluated throughout the literature how extended release translates to induction of CTL response for the treatment of cancer.

In our nanoparticle-based vaccine formulations, sustained release of CSIINFEKL peptide was achieved up to 3 days by conjugating to NPs via thioether linkers, in a reducing environment. Release profile of CSIINFEKL from NPs could be different in intracellular environment due to presence of many other variables such as peptidases, thioredoxin etc. Disulfide linked CSIINFEKL had initial burst release from NPs but thioether linked CSIINFEKL provided more stable and prolonged release of peptide. Baldwin and Kiirck had shown that N-ethylmaleimide can undergo exchange reaction with presence of other thiols such as glutathione when conjugated to 4-mercaptophenylacetic acid (MPA), N-acetylcysteine, or 3-mercaptopropionic acid (MP). The half-life of glutathione-maleimide adduct formation were dependent of reactivity of Michael donor [19]. Moreover, thiol exchange can be attenuated by designing self-hydrolyzing maleimide [21]. Therefore, by changing the Michael donor's reactivity or by designing self-hydrolyzing maleimide linkers, we could further tune the release of antigenic peptide and thus *in vivo* immune response.

$CD4^+$ T cells assist in generation of functional and protective $CD8^+$ T cells as well as antibodies through B cells [38]. They directly interact with $CD8^+$ T cells via CD40 ligand to boost the $CD8^+$ T cells response. Also help from $CD4^+$ T cells is required for generation of memory $CD8^+$ T cells [39]. Immunization of mice with whole ovalbumin protein conjugated pluronic stabilized polypropylene disulfide (PPS) NPs induced stronger $CD4^+$ T cells, CTLs and effector memory response in mice with EG7 and B16F10 tumor [9, 10]. Although whole protein delivery induces $CD4^+$ T cells to boost CTLs, synthesis and large scale manufacturing of tumor antigen proteins is a big challenge. In this study we have focused on $CD8^+$ T cell epitope peptides for generating CTLs

and have demonstrated the efficacy for the system. We anticipate that using similar conjugation strategies, MHC-II epitope peptides can be easily associated to NPs and co-delivered with CTLs epitope peptides to induce $CD4^+$ T cell help to boost $CD8^+$ T cellresponse and memory. The nanoparticle platform provides an ideal setting for delivery of multiple peptides concurrently on same particle, or different epitopes on different nanoparticles. These are currently being explored with tumor associated antigenic peptides.

4.5. Conclusion

Here we have designed controlled release delivery system to deliver CSIINFEKL and CpG ODN by conjugating them to hydrogel NPs either via disulfide (SPDP) or thioether (SMCC) linkers. CSIINFEKL linked to NPs via thioether linker provided stable and sustained release as compared to rapid release when conjugated via disulfide linker. Both formulations were successfully internalized and processed by BMDCs, resulting in BMDC maturation, subsequent cross-presentation of antigenic peptide, and induction of IL-6 secretion. Thioether linked CSIINFEKL and CpG ODN resulted in stronger and prolonged effect on BMDCs maturation, secretion of IL-6, and antigen cross-presentation. Both formulations significantly inhibited EG7 tumor growth in mice, however, co-delivery of CSIINFEKL and CpG ODN via thioether conjugated NPs resulted in 2 times stronger antitumor efficacy as compared to disulfide linked CSIINFEKL and CpG. Taken together, this study provides a highly effective approach to induce antitumor immunity by tuning the release of antigenic peptide via changing the conjugation chemistry.

4.6. REFERENCES

[1] I. Melero, G. Gaudernack, W. Gerritsen, C. Huber, G. Parmiani, S. Scholl, N. Thatcher, J. Wagstaff, C. Zielinski, I. Faulkner, H. Mellstedt, Therapeutic vaccines for cancer: an overview of clinical trials, Nat Rev Clin Oncol, 11 (2014) 509-524.

[2] C. Guo, M.H. Manjili, J.R. Subjeck, D. Sarkar, P.B. Fisher, X.Y. Wang, Therapeutic cancer vaccines: past, present, and future, Adv Cancer Res, 119 (2013) 421-475.

[3] Z. Xu, S. Ramishetti, Y.C. Tseng, S. Guo, Y. Wang, L. Huang, Multifunctional nanoparticles co-delivering Trp2 peptide and CpG adjuvant induce potent cytotoxic T-lymphocyte response against melanoma and its lung metastasis, J Control Release, 172 (2013) 259-265.

[4] E.A. Vasievich, S. Ramishetti, Y. Zhang, L. Huang, Trp2 peptide vaccine adjuvanted with (R)-DOTAP inhibits tumor growth in an advanced melanoma model, Mol Pharm, 9 (2012) 261-268.

[5] C.A. Schutz, L. Juillerat-Jeanneret, H. Mueller, I. Lynch, M. Riediker, C. NanoImpactNet, Therapeutic nanoparticles in clinics and under clinical evaluation, Nanomedicine (Lond), 8 (2013) 449-467.

[6] L. Zhao, A. Seth, N. Wibowo, C.-X. Zhao, N. Mitter, C. Yu, A.P.J. Middelberg, Nanoparticle vaccines, Vaccine, 32 (2014) 327-337.

[7] C.H. Kapadia, J.L. Perry, S. Tian, J.C. Luft, J.M. DeSimone, Nanoparticulate immunotherapy for cancer, J Control Release, 219 (2015) 167-180.

[8] J.J. Moon, H. Suh, A.V. Li, C.F. Ockenhouse, A. Yadava, D.J. Irvine, Enhancing humoral responses to a malaria antigen with nanoparticle vaccines that expand Tfh cells and promote germinal center induction, Proc Natl Acad Sci U S A, 109 (2012) 1080-1085.

[9] C. Nembrini, A. Stano, K.Y. Dane, M. Ballester, A.J. van der Vlies, B.J. Marsland, M.A. Swartz, J.A. Hubbell, Nanoparticle conjugation of antigen enhances cytotoxic T-cell responses in pulmonary vaccination, Proc Natl Acad Sci U S A, 108 (2011) E989-997.

[10] A. de Titta, M. Ballester, Z. Julier, C. Nembrini, L. Jeanbart, A.J. van der Vlies, M.A. Swartz, J.A. Hubbell, Nanoparticle conjugation of CpG enhances adjuvancy for cellular immunity and memory recall at low dose, Proc Natl Acad Sci U S A, 110 (2013) 19902-19907.

[11] S. Hirosue, I.C. Kourtis, A.J. van der Vlies, J.A. Hubbell, M.A. Swartz, Antigen delivery to dendritic cells by poly(propylene sulfide) nanoparticles with disulfide conjugated peptides: Cross-presentation and T cell activation, Vaccine, 28 (2010) 7897-7906.

[12] T. Fifis, A. Gamvrellis, B. Crimeen-Irwin, G.A. Pietersz, J. Li, P.L. Mottram, I.F. McKenzie, M. Plebanski, Size-dependent immunogenicity: therapeutic and protective properties of nano-vaccines against tumors, J Immunol, 173 (2004) 3148-3154.

[13] K. Perica, A. Tu, A. Richter, J.G. Bieler, M. Edidin, J.P. Schneck, Magnetic field-induced T cell receptor clustering by nanoparticles enhances T cell activation and stimulates antitumor activity, ACS Nano, 8 (2014) 2252-2260.

[14] C. Peters, S. Brown, Antibody-drug conjugates as novel anti-cancer chemotherapeutics, Biosci Rep, 35 (2015).

[15] S.P. Trimble, D. Marquardt, D.C. Anderson, Use of designed peptide linkers and recombinant hemoglobin mutants for drug delivery: in vitro release of an angiotensin II analog and kinetic modeling of delivery, Bioconjug Chem, 8 (1997) 416-423.

[16] B.A. Kellogg, L. Garrett, Y. Kovtun, K.C. Lai, B. Leece, M. Miller, G. Payne, R. Steeves, K.R. Whiteman, W. Widdison, H. Xie, R. Singh, R.V. Chari, J.M. Lambert, R.J. Lutz, Disulfide-linked antibody-maytansinoid conjugates: optimization of in vivo activity by varying the steric hindrance at carbon atoms adjacent to the disulfide linkage, Bioconjug Chem, 22 (2011) 717-727.

[17] P.E. Thorpe, P.M. Wallace, P.P. Knowles, M.G. Relf, A.N. Brown, G.J. Watson, R.E. Knyba, E.J. Wawrzynczak, D.C. Blakey, New coupling agents for the synthesis of immunotoxins containing a hindered disulfide bond with improved stability in vivo, Cancer Res, 47 (1987) 5924-5931.

[18] G.T. Hermanson, Chapter 6 - Heterobifunctional Crosslinkers, in: Bioconjugate Techniques (Third edition), Academic Press, Boston, 2013, pp. 299-339.

[19] A.D. Baldwin, K.L. Kiick, Tunable degradation of maleimide-thiol adducts in reducing environments, Bioconjug Chem, 22 (2011) 1946-1953.

[20] G.D. Lewis Phillips, G. Li, D.L. Dugger, L.M. Crocker, K.L. Parsons, E. Mai, W.A. Blattler, J.M. Lambert, R.V. Chari, R.J. Lutz, W.L. Wong, F.S. Jacobson, H. Koeppen, R.H. Schwall, S.R. Kenkare-Mitra, S.D. Spencer, M.X. Sliwkowski, Targeting HER2-positive breast cancer with trastuzumab-DM1, an antibody-cytotoxic drug conjugate, Cancer Res, 68 (2008) 9280-9290.

[21] R.P. Lyon, J.R. Setter, T.D. Bovee, S.O. Doronina, J.H. Hunter, M.E. Anderson, C.L. Balasubramanian, S.M. Duniho, C.I. Leiske, F. Li, P.D. Senter, Self-hydrolyzing maleimides improve the stability and pharmacological properties of antibody-drug conjugates, Nat Biotechnol, 32 (2014) 1059-1062.

[22] L. Feng, X.R. Qi, X.J. Zhou, Y. Maitani, S.C. Wang, Y. Jiang, T. Nagai, Pharmaceutical and immunological evaluation of a single-dose hepatitis B vaccine using PLGA microspheres, J Control Release, 112 (2006) 35-42.

[23] S.M. Sivakumar, N. Sukumaran, L. Nirmala, R. Swarnalakshmi, B. Anilbabu, L. Siva, J. Anbu, T.S. Shanmugarajan, V. Ravichandran, Immunopotentiation of hepatitis B vaccine using biodegradable polymers as an adjuvant, J Microbiol Immunol Infect, 43 (2010) 265-270.

[24] I. Preis, R.S. Langer, A single-step immunization by sustained antigen release, J Immunol Methods, 28 (1979) 193-197.

[25] S. Lofthouse, Immunological aspects of controlled antigen delivery, Adv Drug Deliv Rev, 54 (2002) 863-870.

[26] Y. Umeki, K. Mohri, Y. Kawasaki, H. Watanabe, R. Takahashi, Y. Takahashi, Y. Takakura, M. Nishikawa, Induction of Potent Antitumor Immunity by Sustained Release of Cationic Antigen from a DNA-Based Hydrogel with Adjuvant Activity, Advanced Functional Materials, 25 (2015) 5758-5767.

[27] X.Q. Zhang, C.E. Dahle, N.K. Baman, N. Rich, G.J. Weiner, A.K. Salem, Potent antigen-specific immune responses stimulated by codelivery of CpG ODN and antigens in degradable microparticles, J Immunother, 30 (2007) 469-478.

[28] W.J. Storkus, H.J. Zeh, 3rd, R.D. Salter, M.T. Lotze, Identification of T-cell epitopes: rapid isolation of class I-presented peptides from viable cells by mild acid elution, J Immunother Emphasis Tumor Immunol, 14 (1993) 94-103.

[29] I. Rochman, W.E. Paul, S.Z. Ben-Sasson, IL-6 increases primed cell expansion and survival, J Immunol, 174 (2005) 4761-4767.

[30] J. Gagnon, S. Ramanathan, C. Leblanc, A. Cloutier, P.P. McDonald, S. Ilangumaran, IL-6, in synergy with IL-7 or IL-15, stimulates TCR-independent proliferation and functional differentiation of CD8+ T lymphocytes, J Immunol, 180 (2008) 7958-7968.

[31] T. Sparwasser, E.S. Koch, R.M. Vabulas, K. Heeg, G.B. Lipford, J.W. Ellwart, H. Wagner, Bacterial DNA and immunostimulatory CpG oligonucleotides trigger maturation and activation of murine dendritic cells, Eur J Immunol, 28 (1998) 2045-2054.

[32] A.A. Walters, C. Krastev, A.V.S. Hill, A. Milicic, Next generation vaccines: single-dose encapsulated vaccines for improved global immunisation coverage and efficacy, Journal of Pharmacy and Pharmacology, 67 (2015) 400-408.

[33] R.M. Kuntz, W. Mark Saltzman, Polymeric controlled delivery for immunization, Trends in Biotechnology, 15 (1997) 364-369.

[34] C.-Y. Lin, S.-J. Lin, Y.-C. Yang, D.-Y. Wang, H.-F. Cheng, M.-K. Yeh, Biodegradable polymeric microsphere-based vaccines and their applications in infectious diseases, Human Vaccines & Immunotherapeutics, 11 (2015) 650-656.

[35] R. Nakaoka, Y. Tabata, Y. Ikada, Enhanced antibody production through sustained antigen release from biodegradable granules, Journal of Controlled Release, 37 (1995) 215-224.

[36] C. Thomasin, G. Corradin, Y. Men, H.P. Merkle, B. Gander, Tetanus toxoid and synthetic malaria antigen containing poly(lactide)/poly(lactide-co-glycolide) microspheres: importance of polymer degradation and antigen release for immune response, Journal of Controlled Release, 41 (1996) 131-145.

[37] M. Zhu, R. Wang, G. Nie, Applications of nanomaterials as vaccine adjuvants, Human Vaccines & Immunotherapeutics, 10 (2014) 2761-2774.

[38] S. Zhang, H. Zhang, J. Zhao, The role of CD4 T cell help for CD8 CTL activation, Biochem Biophys Res Commun, 384 (2009) 405-408.

[39] M.K. MacLeod, J.W. Kappler, P. Marrack, Memory CD4 T cells: generation, reactivation and re-assignment, Immunology, 130 (2010) 10-15.

Chapter-5: Future Directions and Summary

5.1. Future directions

Here we have shown that intracellular delivery of antigenic peptides and adjuvants by particulate subunit vaccine induced potent CTLs as well as provide a protective response against tumor growth. By varying the nature of linker used in the conjugation process we can provide sustained release of conjugated antigen resulting in higher antigen cross-presentation, maturation of DCs, induction of IL-6, and better protective immune response. In this section, I am discussing different strategies to optimize subunit vaccines to develop a better immune response to combat cancer.

One of the parameters that we could study is the density of antigens or adjuvants on the surface of nanoparticles. Better subunit vaccines can be designed by understanding the optimum density of antigen required to produce a maximum immune response. Reuter et al. has shown the significance of ligand (antibody / affibody) density on the surface of particles for their internalization, biodistribution, and tumor uptake [1]. Little S. has pointed out the importance of multivalent ligand display in particulate vaccine design. Plasmodium Vivax, a malarial parasite, displays antigenic protein circumsporozoite protein (CSP) and structure similar to TLR-4 agonist. As shown in figure 5.1, when B cells come in contact with this parasite, multivalent binding of CSP and TLR-4 agonist to B-cell receptor (BCR) induce clustering of B-cells via cross-linking of BCRs. This natural multivalent binding is capable of inducing potent and persistent humoral response [2]. Moon et al. was able to generate a better suited antibody response against malaria by delivering CSP protein antigen and TLR-4 agonist MPL-A (monophosphoryl lipid-A) via novel multilamellar lipid vesicle delivery system (ICMV), than when antigen and MPL-A was delivered in a soluble form [3]. Homhuan et al. showed that decreasing the protein density from virosome

surface (envelope proteins of Newcastle disease virus (NDV)) failed to induce serum haemaglutinin-inhibition (HAI) antibody titers, possibly due to loss of highly organized viral surface structure [4]. PRINT provides us an ideal platform to precisely control surface density of antigens and adjuvants via various conjugation strategies. As mentioned in chapter-3 and 4, different linker chemistries can be used to tune the release of conjugated antigens. By controlling the antigen and adjuvant density on the surface of the NP we could further control the uptake of subunit vaccine to DCs and thus potentially maximize the cross-presentation and cellular immune response.

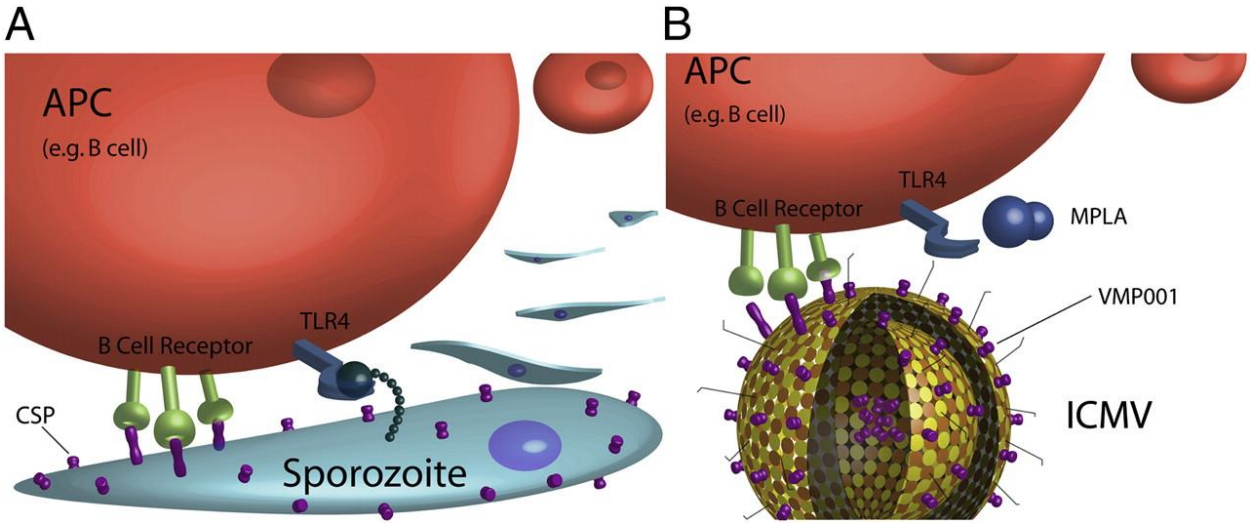

<u>Figure-5.1:</u> Multivalent display of antigen and TLR4 agonist to an antigen presenting cell (APC) such as a B cell by a malarial sporozoite and a nanoparticle/adjuvant formulation.
P. vivax displays circumsporozoite proteins (CSP) prominently on its surface, as well as structures that likely serve as TLR4 agonists (12, 13). Clustering of B-cell receptors is achieved as a result of the natural, repetitive display of the CSP. This combination of persistent, multivalent antigen presentation in context with particular, parasite-associated "danger signals" would be recognized by the immune system in a way that would produce immune responses that are well-suited to combat the parasite. (B) Synthetic ICMVs [as described in [3]] can be designed to display a subunit CSP antigen (VMP001) through both sustained release and multivalent presentation on their surface. When administered along with the TLR4 agonist MPLA, these nanoparticles produce an immune response that is better suited to combat malaria than when antigen and conventional adjuvant are delivered alone. Figure and caption are reprinted from [2] PNAS, Vol 109, Issue 4, Steven R. Little; Reorienting our view of particle-based adjuvants for subunit vaccines, 999-1000, Copyright (2012), with permission from PNAS.

As discussed in the chapter-2 size of the naoparticulate carriers plays a very important role in controlling the immune response. Size of the NP carrier is known to influence their uptake, lymphatic drainage and extracellular trafficking. Smaller size particles of <100 nm drain directly to the lymph nodes and penetrate deeper into lymph node to interact with immature DCs, B-cells and T cells [5, 6]. Many have shown better lymphatic trafficking [7], better humoral response as well as stronger antitumor immunity by smaller sized particle (40 nm) as compared to bigger sized (100 nm) [8]. PRINT platform provides us an unprecedented control over particle size to fabricate various size of particles ranges from 50 nm to 3 μm. For future studies, subunit vaccine can be redesigned by utilizing smaller size particle such as 50X60 nm. Different sizes of PRINT hydrogel subunit vaccines can then be compared for their lymphatic trafficking, uptake by APCs, antigen cross-presentation and *in vivo* induction of $CD8^+$ T cells. Smaller size particles could possibly increase their lymphatic uptake and could increase induction of CTLs.

For future vaccine design, MHC-II epitope peptide can be co-delivered with MHC-I epitope peptide to induce $CD4^+$ T cells to boost $CD8^+$ T cells response and to create memory response. CD4+ T cells assist in the generation of functional and protective $CD8^+$ T cells as well as antibodies through B-cells [9]. They directly interact with $CD8^+$ T cells via CD40 ligand to boost the $CD8^+$ T cells response. If $CD8^+$ T cells are primed in presence of $CD4^+$ T cells, $CD8^+$ T cells go through a second round of clonal expansion once re-stimulated again in absence of $CD4^+$ T cells [10]. To this point, Titta et al. found that delivering MHC-II epitope with MHC-I epitope in form of whole protein induced potent CTLs and memory response. Immunization of mice with whole ovalbumin protein conjugated pluronic stabilized polypropylene disulfide (PPS) NPs induced stronger $CD4^+$ T cells, CTLs and effector memory response in mice with EG7 and B16F10 tumors [11, 12]. Although whole protein delivery induce $CD4^+$ T cells to boost CTLs, synthesis and large scale manufacturing of tumor antigenic peptide is the biggest challenge. Immunogenicity from unknown components of whole proteins and safety is also concern. Not many studies have been performed to evaluate the help provided from MHC-II epitope peptides

in the generation and persistence of $CD8^+$ T cells via particulate vaccines. Mansour et al. has significantly inhibited the growth of tumor in B16F10 melanoma mice model byo-delivery of helper peptide PADRE (pan DR epitope-AKXVAAWTLKAAA-OH) with Trp-2: 181-188 (VYDFFVWL) and p-53: 232-240 (KYICNSSCM) [13]. Due to advancement in the field of cDNA-expression cloning techniques and the use of autologous antibodies to identify peptides of TAA, large numbers of peptide epitopes for many tumor antigens can be synthesized. Multivalent long peptide vaccines (with extra flanking amino acids) or hybrid peptide vaccines (consisting of CTL and helper peptide epitopes) or peptide cocktail vaccines (mixture of MHC-I epitopes of multiple antigens) have been evaluated in clinical trials resulted into moderate to robust immune response [14-16]. Delivering such peptides via particulate subunit vaccine should be considered to design better vaccines. Future PRINT subunit vaccine could contain multiple antigenic peptide epitopes on the same particle or a mixture of different NPs conjugated to separate MHC-I and MHC-II helper epitopes.

Moreover, different intracellular receptors such as TLRs, NLRs (nod like receptors), RIG- I like receptor (retinoic acid inducible gene I like receptor), STINGs (DNA sensors, Stimulators of interferon genes) etc. which recognize different 'danger signals' from pathogen associated molecular patterns (such as unemthylated DNA from bacteria or viruses, bacterial coat proteins and lipids etc) can be simultaneously stimulated by delivering multiple immune stimulating agents and/or agonists such as CpG ODN (TLR-9 agonis), resiquimod and imiquimod (agonist of TLR-7/8), muramyl dipeptide (agonist of NOD2), cyclic dinucleotides (agonist of STING) etc. Single or multiple aduvants can be co-formulated with antigens to enhance immune response. Co-delivery of TLR7 agonist R837 and TLR4 agonist, MPL-A in PLGA NP with HA protein, synergistically increased antigen specific neutralizing antibodies in mice as compared to NP containing antigen plus single TLR ligand [17]. Furthermore, it was reported that immunization of mice with NPs containing antigen and two adjuvants, protected mice completely against lethal avian and swine influenza virus strains, and induced robust

immunity against pandemic H1N1 influenza in rhesus macaques [17]. Additionally, Napolitani et al. found that agonist of TLR3 and TLR4 potently synergize with agonist of TLR8 and induced 50-100 times higher secretion of IL-12 and IL-23 as compared to single TLR agonist [18]. Furthermore, co-delivery of TLR4 agonist glucopyranosyl lipid adjuvant-stable emulsion (GLA-SE) and TLR-9 agonist CpG ODN with mycobacterium tuberculosis antigenic protein ID93 synergistically induced Th1 type protective immune response in mice [19]. PRINT NPs can be used to study the synergistic effect of multiple adjuvants with antigens. As shown in chapter-3 and 4, adjuvant effect of CpG significantly increased the numbers of IFN- γ producing $CD8^+$ T cells. Future PRINT subunit vaccine design could include multiple adjuvants to further induce production of multiple cytokines via activating many intracellular PRRs, which could decrease the dosage and frequency of vaccine administration and increase the speed and duration of immune response.

5.2. Summary

As discuss earlier (chapter-1) induction of high frequency of potent CTLs response and inhibition of immunosuppressive tumor environment are necessary to achieve successful immune response in fight against cancer. Although, different types of cancer vaccines have achieved lot of success in pre-clinical and clinical trials [20-22] due to generation of durable, no-toxic antitumor immune response, immunosuppressive tumor microenvironment is the biggest hurdle making clinical translation of cancer vaccines difficult. The ability to block key pathways by which tumor cells seek to evade or suppress the immune response is critical to realize the full potential of cancer vaccines. In 2010, FDA approval of ipilimumab (an antibody against CTLA-4) has changed the landscape of immunotherapy research and provided new promise for cancer treatment. Since then many other immunotherapies have been approved by FDA such as blinatumomab (Blincyto®, a novel class of bispecific T cell engagers, which consists of two monoclonal antibodies, one binds to T cells and another binds on cancer cell and induce killing of cancer cell) for use in the treatment of B cell acute lymphoblastic leukemia, PD-1 inhibitors

pembrolizumab (Keytruda® made by Merck) and nivolumab (Opdivo® made by Bristol-Myers Squibb) for the treatment of lung cancer and talimogene laherparepvec (Imlygic™ made by Amgen) for the treatment of advanced melanoma [23]. Successful elimination of tumors can be achieved by combining cancer immunotherapy to revert the immunosuppression to boost the effect of T cells and NK cells with cancer vaccine to induce potent immune cells against multiple tumor antigens. Optimizing the effectiveness of cancer vaccine will require targeting the antitumor immune response at multiple levels, and this may be achieved through synergistic combinations. Examples include combining immune checkpoint inhibitors or epigenetic immune modulators with cancer vaccines, or by combining chemotherapy and cancer vaccines with targeted drug delivery vehicles carrying inhibitors/modulators of immunosuppressive TME. Recently, pre-clinical and clinical studies have been done incorporating combination of cancer vaccine with immunotherapies which includes combination of OX40 ligand, anti-CTLA4 and Her2 vaccination; PD1 blockade with CTLA4 blockade; nivolumab in combination with GM.CD40L vaccine; combination immunotherapy of GM.CD40L vaccine with CCL21; etc. resulted into synergistic antitumor response which was better as compared to cancer vaccine or immunotherapy alone [24-29].

Combination strategies with immunotherapy have provided cancer patients with novel treatments that have the potential to elicit durable control of disease and improvement in quality of life. The ability of an activated immune response to generate: 1) a diverse T cell repertoire that adapts to heterogeneous and genetically unstable tumors, 2) persistent memory T cells with specificity for tumor antigens, which provide efficient recall responses against recurrent disease, and 3) re-establish the “normal cellular environment” make it absolutely essential to expand our efforts to find rational combinations to unleash antitumor immune responses for the benefit of cancer patients. We are revealing the complex regulatory mechanisms that enable cancer to escape immune surveillance and develop into our worst nightmare. Therefore, as the scientific community continues to investigate and learn about

highly complex and dynamic system that is cancer, we must also continue to assess the effectiveness of an evolving immune response, define the immune response that contributes to clinical benefit, and then, hopefully, drive every patient's immune response to combat their cancer most effectively. Properly done, it seems likely that more effective treatments and/or cures for many types of cancer will become reality.

5.3 REFERENCES

[1] K.G. Reuter, J.L. Perry, D. Kim, J.C. Luft, R. Liu, J.M. DeSimone, Targeted PRINT Hydrogels: The Role of Nanoparticle Size and Ligand Density on Cell Association, Biodistribution, and Tumor Accumulation, Nano Lett, 15 (2015) 6371-6378.

[2] S.R. Little, Reorienting our view of particle-based adjuvants for subunit vaccines, Proc Natl Acad Sci U S A, 109 (2012) 999-1000.

[3] J.J. Moon, H. Suh, A.V. Li, C.F. Ockenhouse, A. Yadava, D.J. Irvine, Enhancing humoral responses to a malaria antigen with nanoparticle vaccines that expand Tfh cells and promote germinal center induction, Proc Natl Acad Sci U S A, 109 (2012) 1080-1085.

[4] A. Homhuan, S. Prakongpan, P. Poomvises, R.A. Maas, D.J. Crommelin, G.F. Kersten, W. Jiskoot, Virosome and ISCOM vaccines against Newcastle disease: preparation, characterization and immunogenicity, Eur J Pharm Sci, 22 (2004) 459-468.

[5] V. Manolova, A. Flace, M. Bauer, K. Schwarz, P. Saudan, M.F. Bachmann, Nanoparticles target distinct dendritic cell populations according to their size, Eur J Immunol, 38 (2008) 1404-1413.

[6] D.J. Irvine, M.A. Swartz, G.L. Szeto, Engineering synthetic vaccines using cues from natural immunity, Nat Mater, 12 (2013) 978-990.

[7] S.T. Reddy, A.J. van der Vlies, E. Simeoni, V. Angeli, G.J. Randolph, C.P. O'Neil, L.K. Lee, M.A. Swartz, J.A. Hubbell, Exploiting lymphatic transport and complement activation in nanoparticle vaccines, Nat Biotechnol, 25 (2007) 1159-1164.

[8] T. Fifis, A. Gamvrellis, B. Crimeen-Irwin, G.A. Pietersz, J. Li, P.L. Mottram, I.F. McKenzie, M. Plebanski, Size-dependent immunogenicity: therapeutic and protective properties of nano-vaccines against tumors, J Immunol, 173 (2004) 3148-3154.

[9] S. Zhang, H. Zhang, J. Zhao, The role of CD4 T cell help for CD8 CTL activation, Biochem Biophys Res Commun, 384 (2009) 405-408.

[10] M.K. MacLeod, J.W. Kappler, P. Marrack, Memory CD4 T cells: generation, reactivation and re-assignment, Immunology, 130 (2010) 10-15.

[11] A. de Titta, M. Ballester, Z. Julier, C. Nembrini, L. Jeanbart, A.J. van der Vlies, M.A. Swartz, J.A. Hubbell, Nanoparticle conjugation of CpG enhances adjuvancy for cellular immunity and memory recall at low dose, Proc Natl Acad Sci U S A, 110 (2013) 19902-19907.

[12] C. Nembrini, A. Stano, K.Y. Dane, M. Ballester, A.J. van der Vlies, B.J. Marsland, M.A. Swartz, J.A. Hubbell, Nanoparticle conjugation of antigen enhances cytotoxic T-cell responses in pulmonary vaccination, Proc Natl Acad Sci U S A, 108 (2011) E989-997.

[13] M. Mansour, B. Pohajdak, W.M. Kast, A. Fuentes-Ortega, E. Korets-Smith, G.M. Weir, R.G. Brown, P. Daftarian, Therapy of established B16-F10 melanoma tumors by a single vaccination of CTL/T helper peptides in VacciMax, J Transl Med, 5 (2007) 20.

[14] G.G. Kenter, M.J. Welters, A.R. Valentijn, M.J. Lowik, D.M. Berends-van der Meer, A.P. Vloon, J.W. Drijfhout, A.R. Wafelman, J. Oostendorp, G.J. Fleuren, R. Offringa, S.H. van der Burg, C.J. Melief, Phase I immunotherapeutic trial with long peptides spanning the E6 and E7 sequences of high-risk human papillomavirus 16 in end-stage cervical cancer patients shows low toxicity and robust immunogenicity, Clin Cancer Res, 14 (2008) 169-177.

[15] K.A. Chianese-Bullock, W.P. Irvin, Jr., G.R. Petroni, C. Murphy, M. Smolkin, W.C. Olson, E. Coleman, S.A. Boerner, C.J. Nail, P.Y. Neese, A. Yuan, K.T. Hogan, C.L. Slingluff, Jr., A multipeptide vaccine is safe and elicits T-cell responses in participants with advanced stage ovarian cancer, J Immunother, 31 (2008) 420-430.

[16] A. Yamada, T. Sasada, M. Noguchi, K. Itoh, Next-generation peptide vaccines for advanced cancer, Cancer Sci, 104 (2013) 15-21.

[17] S.P. Kasturi, I. Skountzou, R.A. Albrecht, D. Koutsonanos, T. Hua, H.I. Nakaya, R. Ravindran, S. Stewart, M. Alam, M. Kwissa, F. Villinger, N. Murthy, J. Steel, J. Jacob, R.J. Hogan, A. Garcia-Sastre, R. Compans, B. Pulendran, Programming the magnitude and persistence of antibody responses with innate immunity, Nature, 470 (2011) 543-547.

[18] G. Napolitani, A. Rinaldi, F. Bertoni, F. Sallusto, A. Lanzavecchia, Selected Toll-like receptor agonist combinations synergistically trigger a T helper type 1-polarizing program in dendritic cells, Nat Immunol, 6 (2005) 769-776.

[19] M.T. Orr, E.A. Beebe, T.E. Hudson, J.J. Moon, C.B. Fox, S.G. Reed, R.N. Coler, A Dual TLR Agonist Adjuvant Enhances the Immunogenicity and Protective Efficacy of the Tuberculosis Vaccine Antigen ID93, PLoS ONE, 9 (2014) e83884.

[20] M. Noguchi, T. Sasada, K. Itoh, Personalized peptide vaccination: a new approach for advanced cancer as therapeutic cancer vaccine, Cancer Immunol Immunother, 62 (2013) 919-929.

[21] J. Schlom, Therapeutic cancer vaccines: current status and moving forward, J Natl Cancer Inst, 104 (2012) 599-613.

[22] C.H. Kapadia, J.L. Perry, S. Tian, J.C. Luft, J.M. DeSimone, Nanoparticulate immunotherapy for cancer, J Control Release, 219 (2015) 167-180.

[23] http://www.cancerresearch.org/our-strategy-impact/timeline-of-progress/timeline-detail, in.

[24] T. Keler, E. Halk, L. Vitale, T. O'Neill, D. Blanset, S. Lee, M. Srinivasan, R.F. Graziano, T. Davis, N. Lonberg, A. Korman, Activity and safety of CTLA-4 blockade combined with vaccines in cynomolgus macaques, J Immunol, 171 (2003) 6251-6259.

[25] C.G. Drake, Combination immunotherapy approaches, Ann Oncol, 23 Suppl 8 (2012) viii41-46.

[26] S.N. Linch, M.J. Kasiewicz, M.J. McNamara, I.F. Hilgart-Martiszus, M. Farhad, W.L. Redmond, Combination OX40 agonism/CTLA-4 blockade with HER2 vaccination reverses T-cell anergy and promotes survival in tumor-bearing mice, Proc Natl Acad Sci U S A, 113 (2016) E319-327.

[27] J. Duraiswamy, K.M. Kaluza, G.J. Freeman, G. Coukos, Dual blockade of PD-1 and CTLA-4 combined with tumor vaccine effectively restores T-cell rejection function in tumors, Cancer Res, 73 (2013) 3591-3603.

[28] NIVOLUMAB, https://clinicaltrials.gov/ct2/show/NCT02466568?term=combination+of+cancer+vaccine+with+immunotherapy&rank=11

[29] CCL21, https://clinicaltrials.gov/ct2/show/NCT01433172?term=combination+of+cancer+vaccine+with+immunotherapy&rank=6

APPENDIX

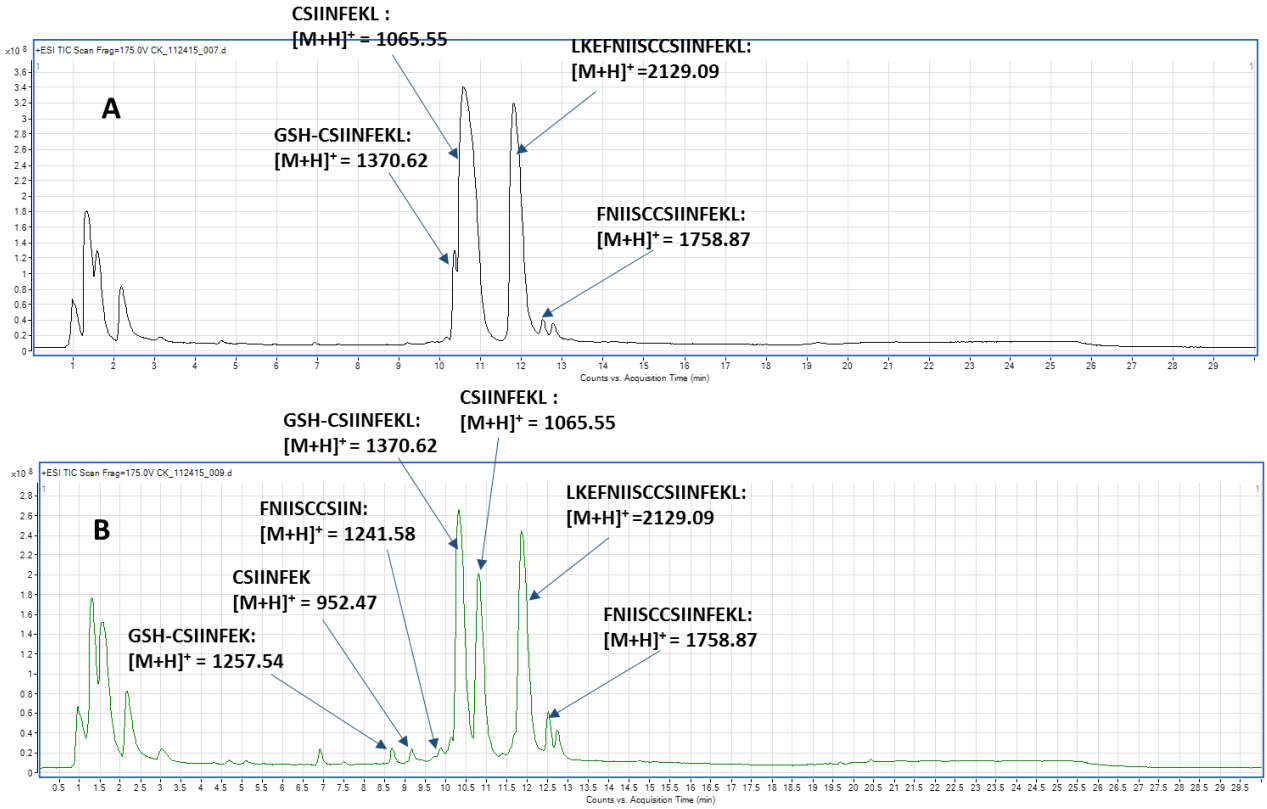

Figure-1: Total ion chromatogram (TIC) of supernatant from A) NP-SPDP-CSIINFEKL (0.5 hours) and B) NP-SPDP-CSIINFEKL (48 hours). Individual mass-spectrum of each species is shown in figure-2 and 3.

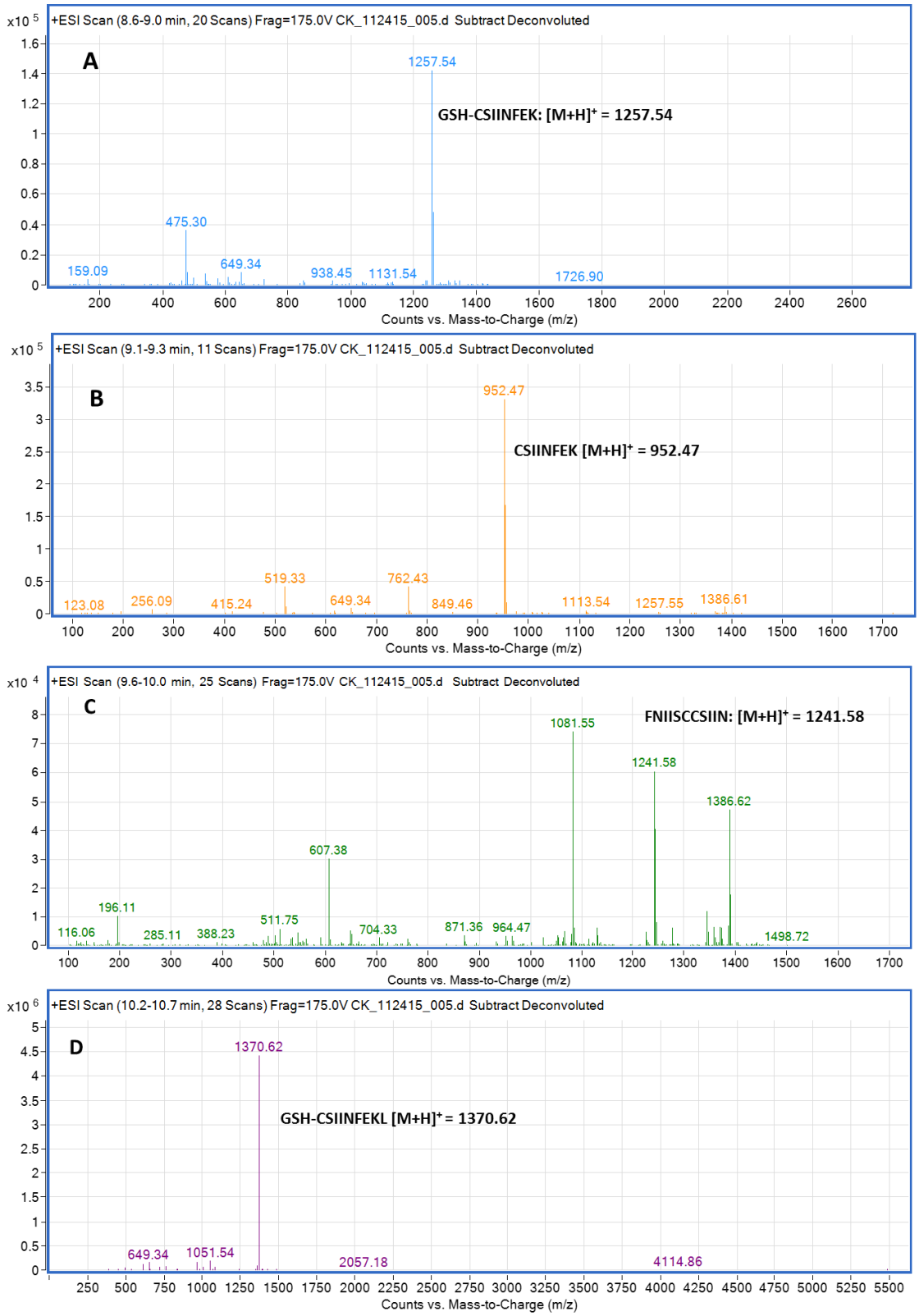

Figure-2: Mass- spectrometry analysis. (A-D) Intensity vs m/z for each species of supernatant from NP-SPDP-CSIINFEKL (48 hours)

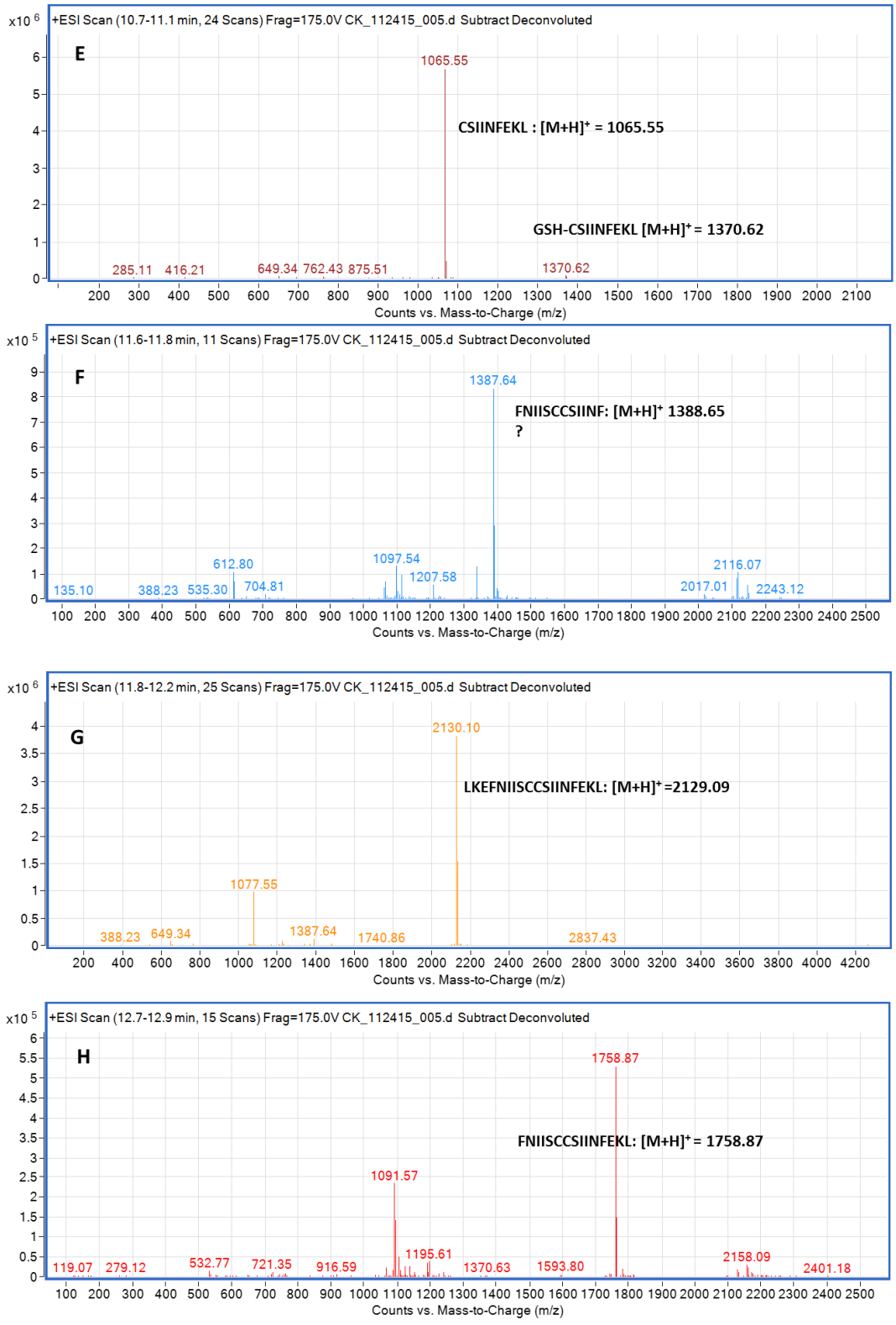

Figure-3: Mass- spectrometry analysis. (E-H) Intensity vs m/z for each species of supernatant from NP-SPDP-CSIINFEKL (48 hours)

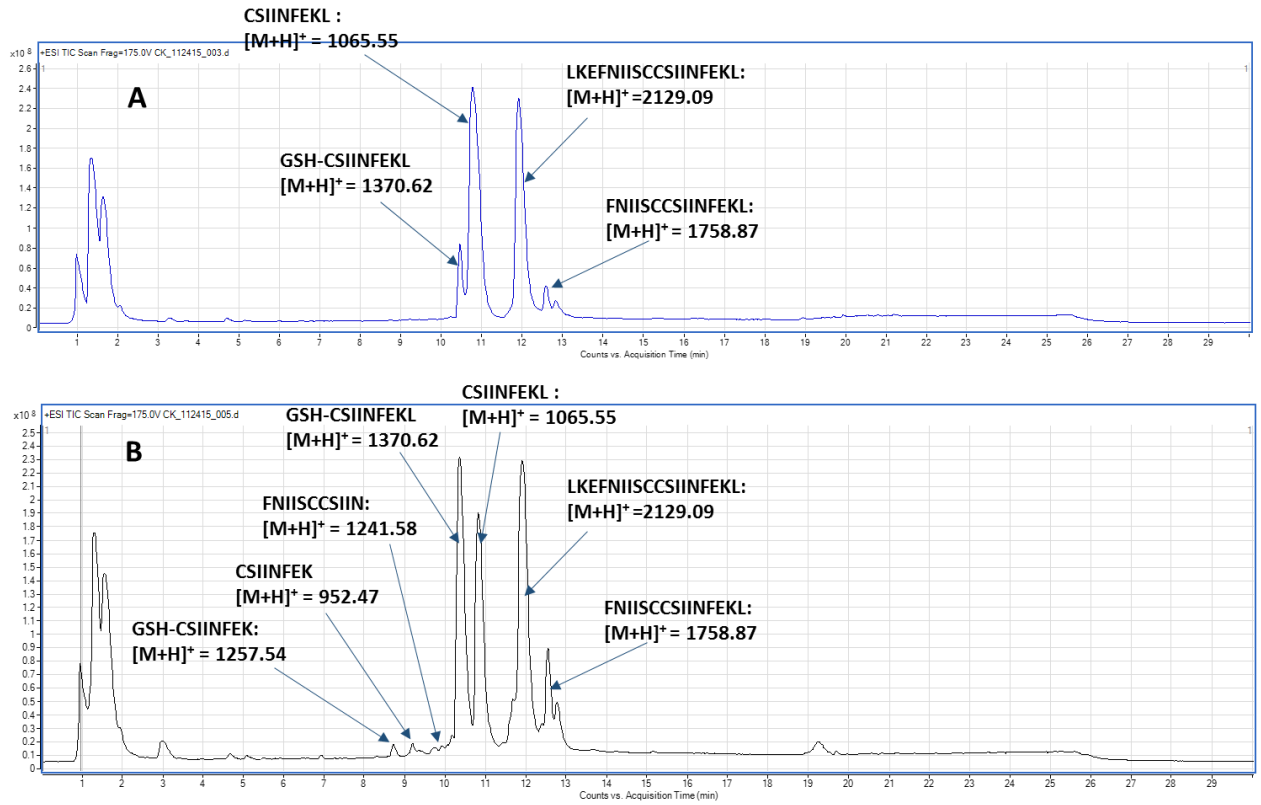

Figure-4: Total ion chromatogram (TIC) of supernatant from A) NP-SMCC-CSIINFEKL (0.5 hours) and B) NP-SMCC-CSIINFEKL (48 hours). Individual mass-spectrum of each species is shown in figure-5 (A-G)

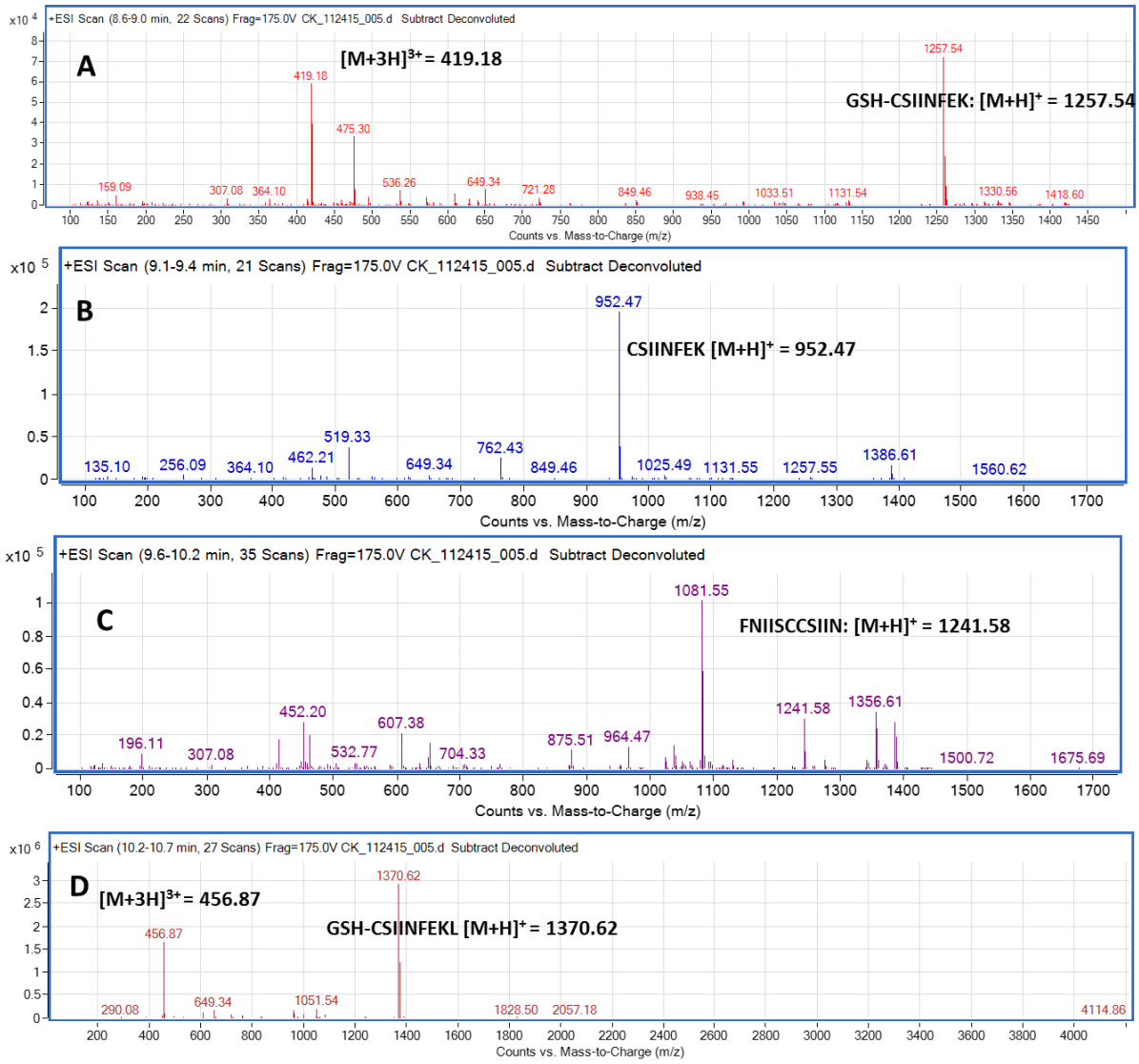

Figure-5: Mass- spectrometry analysis. (A-D) Intensity vs m/z for each species of supernatant from NP-SMCC-CSIINFEKL (48 hours)

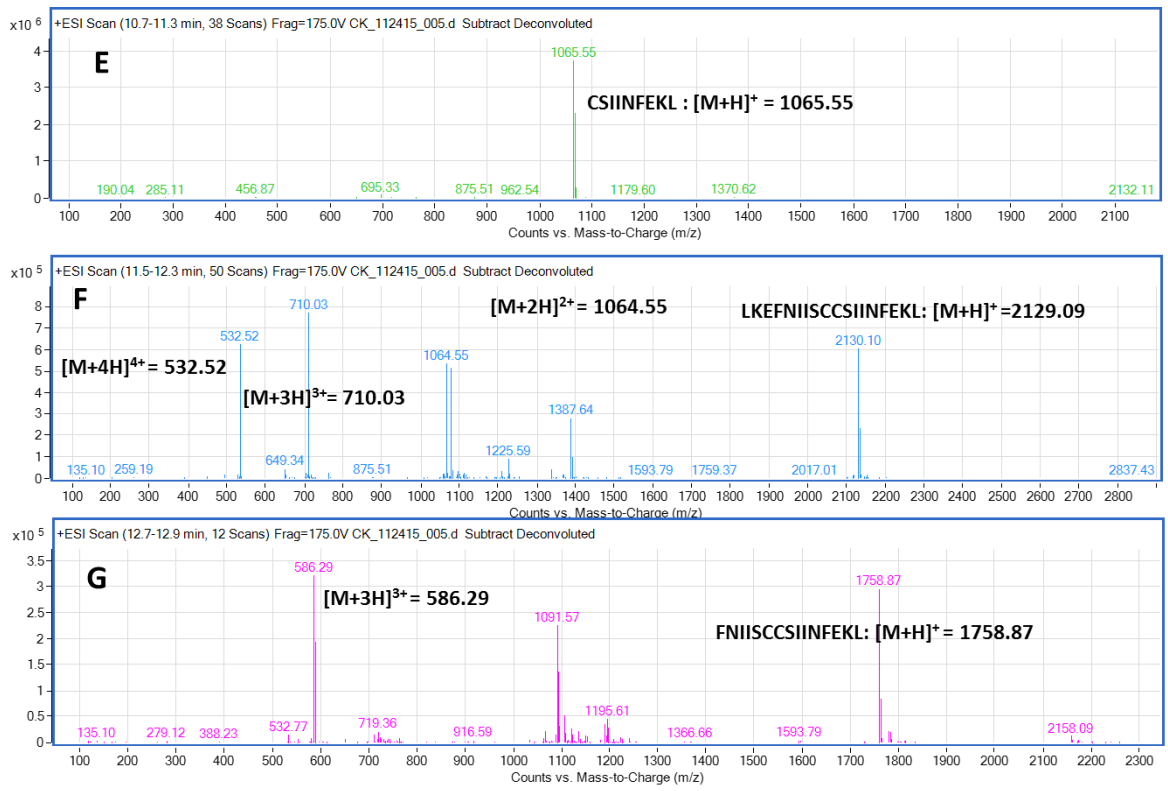

Figure-6: Mass- spectrometry analysis. (E-G) Intensity vs m/z for each species of supernatant from NP-SMCC-CSIINFEKL (48 hours)